Schizophrenia Risk Factor *Tcf4* and Gene × Environment Interaction in Mice

PhD Thesis
for the award of the degree

Doctor of Philosophy

in the Neuroscience Program
at the Georg-August-Universität Göttingen
Faculty of Biology

submitted by

Dorota Badowska

born in
Warsaw, Poland

Göttingen, 20th February 2015

Thesis committee:

Prof. Dr Moritz Rossner, Reviewer
 Division of Molecular Neurobiology, Department of Psychiatry,
 Ludwig-Maximilian-University, Munich
Prof. Dr Dr Hannelore Ehrenreich, Reviewer
 Division of Clinical Neuroscience,
 Max Planck Institute of Experimental Medicine, Göttingen
Prof. Dr André Fischer
 Department For Psychiatry and Psychotherapy, University Medical Center
 German Center for Neurodegenerative Diseases (DZNE) , Göttingen

Extended thesis committee

Prof. Dr. Michael Hörner
 Department of Cellular Neurobiology,
 European Neuroscience Institute, Göttingen
Prof. Dr. Michael Sereda
 "Molecular and Translational Neurology", Department of Neurogenetics,
 Max Planck Institute of Experimental Medicine, Göttingen
Prof. Dr Mikael Simons
 Department of Cellular Neuroscience,
 Max Planck Institute of Experimental Medicine, Göttingen

Date of Disputation: 3rd of November 2014

Contents

Acknowledgements

ACKNOWLEDGEMENTS

Abstract

Psychiatric diseases are triggered by the interaction of genetic and environmental risk factors (G×E). To model G×E in mice, we developed an approach to analysing huge behavioural data sets, which allowed us to compare mice tested in independent cohorts. In a battery of tests, we analysed and compared mice subjected to Isolation rearing (IR), Social defeat (SD) or the control condition Enriched environment (EE). By using multivariate statistics, we merged experiments measuring similar behaviours into higher-order categories (*dimension reduction*). This allowed us to create clinically relevant behavioural profiles of mice and visualise them in a single radar chart. We show that IR as a paradigm models positive symptoms of psychotic diseases, while SD models negative-like symptoms.

We used this approach to study G×E in transgenic mice overexpressing the schizophrenia risk gene *Tcf4*. They displayed deficits in fear memory and behavioural flexibility upon IR and SD, while EE rescued the phenotype. Ageing did not influence these impairments. This result points at the role of *Tcf4* in cognition. *Tcf4* overexpressing mice also displayed enhanced LTD in hippocampus as well as increased dendritic spine frequency and upregulation of proteins: CaMKII, HOMER1 and synaptobrevins in prefrontal cortex. RNA sequencing revealed deregulation of *BC1*, *Top3b* and *Mov10* involved in regulation of translation by microRNAs, and other genes, e.g. *Adora2a, Penk* and *Plxna1*.

We also tested behaviour of $Tcf4^{-/+}$ mice, which showed strong cognitive impairment specific to hippocampus-dependent spatial learning. Analysis of *Tcf4* expression in these mice revealed downregulation mainly of the isoforms that are highly expressed in the hippocampus, which is in line with the behavioural phenotype. We conclude that in mice *Tcf4* is important predominantly for cognition, which declines upon both overexpression and deficiency of the gene.

In the last project, we focused on mechanisms underlying pain insensitivity, which we observed in the IR animals. We show that IR reduces expression of pronociceptive genes *Vgf, Bdnf* and *Npyr1* in dorsal root ganglia, which may contribute to pain insensitivity. In hypothalamus, IR reduced expression of oxytocin and arginine vasopressin, potentially adding to the pain phenotype as well as to IR-induced aggressiveness.

ABSTRACT

Publications

- Dorota M Badowska, Magdalena M Brzözka, Ananya Chowdhury, Dörthe Malzahn, Moritz J Rossner. "Data calibration and reduction allows to visualize behavioural profiles of psychosocial influences in mice towards clinical domains." *Eur Arch Psychiatry Clin Neurosci*; 2014

- Dorota Badowska, Andrea Schmitt, Peter Falkai. "Connectivity and cognition in neuropsychiatric disorders with special emphasis on Alzheimers disease and Chorea Huntington." *Eur Arch Psychiatry Clin Neurosci*; 2014 Sep;264(6):465-6

PUBLICATIONS

Abbreviations

Introduction

1.1 Schizophrenia

SCHIZOPHRENIA is a highly debilitating psychiatric disease that affects around 1% of the world-wide population[1]. It drastically reduces quality of life by leading to disruption of social relationships, unemployment and homelessness[2]. It also shortens life expectancy by more than 15 years (more than bipolar disorder[3]), due to high rate of suicides ($12\times$ higher than in general population[4]), poor health care, heavy smoking, substance abuse, medication and comorbid disorders. The symptoms typically emerge in adolescence and are more severe in men than in women[5].

Schizophrenia was first identified as *dementia praecox* ("premature dementia") by Emil Krae-pelin in 1919[6]. A quarter-century later Eugen Bleuler coined the term *schizophrenia* ("split mind"). At that time the disease was mainly seen as cognitive decline and emotional dullness emerging already in young patients[6]. Later, in the 60s, Kurt Schneider drew attention to distortion of reality, which he called the *first-rank symptoms*, and proposed it as a diagnostic criterion[6].

Nowadays, according to DSM-5, the hallmarks of schizophrenia include: delusions, hallucinations, disorganized speech and behaviour, catatonia and negative symptoms and possible social dysfunctions[7]. Psychotic features occur also in schizoaffective disorder, depression or bipolar disorder, but in contrast to them, schizophrenia has no affective component[7].

Symptoms of schizophrenia are divided into three classes: positive, negative and cognitive. *Positive symptoms* represent exaggerated functions of the nervous system that do not occur in healthy people — hallucinations and delusions. *Negative symptoms* on the other hand, indicate a loss in function, e.g. reduced motivation, social withdrawal and blunted affect[5,6]. *Cognitive symptoms* include a broad spectrum of impairments[8]. Even though positive symptoms are the key diagnostic criteria, the negative symptoms and illness duration associate stronger with poor outcome[5]. Schizophrenia has a neurodevelopmental aspect[2,9]. The onset is typically in late adolescence or early adulthood[10–12], but certain behavioural abnormalities appear already during the prodromal phase, years before the first episode of psychosis[2,5].

Some of the characteristic abnormalities occur also in the healthy relatives of the patients, and are called endophenotypes. *Endophenotype* is a concept similar to the concept of biomarker, but it implies genetic underpinnings and heritability — it is a measurable behavioural, anatomical, physiological or biochemical feature of a disease[13]. Endophenotypes are often shared between several diseases and can also be reliably studied in animal models. Schizophrenia has many

endophenotypes[14], e.g. disruption of Prepulse inhibition (PPI) (a measure of sensorimotor gating), perseveration, enlarged lateral ventricles, reduced hippocampal volume, thinning of frontal gray matter, reduced P300 and enhanced P50 event-related potentials[5], hypoalgesia (see section 4.4 on page 61) and abnormal beta- and gamma-oscillations (reviewed in[15]), to name only a few.

Cognitive impairment is the core symptom of schizophrenia[16] and also the most debilitating one[2]. Even though cognitive deficits are common also in other psychiatric diseases[7], in schizophrenia they are more severe and have a broader spectrum[8,16]. The impairments affect several cognitive domains, e.g. working memory, social cognition, executive functions, attention inhibition (reviewed in[8]) and cognitive flexibility[17,18]. Such impairments, particularly of social cognition[19], lead to difficulties in finding a job and establishing social bonds and may provoke social defeat.

It is not clear what changes occur in schizophrenic brains, but different neurotransmitter systems seem to be involved. According to the dopamine hypothesis of schizophrenia, aberrant dopamine transmission is involved in positive and negative symptoms[20]. Hyperactivity in the mesolimbic pathway is thought to cause inappropriate assignment of salience to stimuli, and therefore gives raise to delusions (reviewed in[5,21]). Hypoactivity of prefrontal dopamine transmission contributes to negative symptoms[20].

Current treatment for schizophrenia is based on antypsychotic drugs (neuroleptics), which are dopamine D2 receptor antagonists[22]. They have poor efficacy and many side effects, particularly strong in first-generation (typical) antypsychotics[23]. Medication reduces positive symptoms, but fails to counteract negative and cognitive symptoms[5,22].

Aetiology of schizophrenia is not well understood, because it seems to depend on the interplay of genetic (see below) and environmental factors[5] (see section 1.3).

Genetics of schizophrenia   Heritability of schizophrenia is high — around 80%[5], but despite the strong genetic component, the disease does not follow Mendelian patterns. The reason for this is a complex polygenetic architecture where occurrence of the symptoms depends on gene $\times$ gene interactions[24] as well as other factors, e.g. epigenetics and environment[25].

Numerous Genome Wide Association Studies (GWAS) and polygenic inheritance tests have sought to map schizophrenia risk genes. Through these, researchers have identified several copy number variants (CNVs) and hundreds of common single nucleotide polymorphisms (SNPs) in different parts of the genome, confirming the polygenic character of the disease. A few of the candidate genes have been repeatedly found in several GWAS, for example: the MHC region[26–30], microRNA-137 (*MIR-137*)[28,30,31], Transcription factor 4 (*TCF4*)[26–31], Neurogranin (*NRGN*)[26–29], Neuregulin 1 (*NRG1*), Voltage-dependent L-type calcium channel subunit alpha-1C (*CACNA1C*)[28,30,31], genes repressed by Fragile X mental retardation protein (*FMRP*)[31,32], D(2) dopamine receptor (*DRD2*)[29,31], matrix metalloproteinase 16 (*MMP16*)[29,30], *NOTCH4*[26] and proteins of the ARC complex[32] (reviewed in[33]).

The SNPs identified in GWAS are common in the general population. They have low penetrance, which means they have a very small effect on the schizophrenia phenotype and explain only a small fraction of the genetic variation. This *missing heritability* probably results from various sorts of

gene × gene interactions (*epistasis*)[25], for example, *TCF4* and *CACNA1C* are targets of *MIR137*[34]. Presumably, accumulation of SNPs in the genes controlling certain biological pathways result in an overall impairment. Thus schizophrenia is postulated to be seen as a pathway disease[24].

Because schizophrenia is a polygenic disease, the type and severity of its symptoms differ between individuals. Psychosis is a continuum[35], which means that psychotic symptoms, such as hallucinations, occasionally occur also in healthy people. These psychotic-like traits in the general population are displayed as *psychoticism* — one of the three dimensions of personality, according to the P-E-N (Psychoticism-Extraversion-Neuroticism) model of personality by Eysenck[36]. Common risk alleles may increase psychoticism in an individual within the healthy range. However, if one carries many of such alleles, or in a bad combination, his/her traits may reach a pathological level, referred to as psychosis.

Genetic risks are shared between psychiatric diseases[32]. GWAS revealed a genetic overlap between schizophrenia and bipolar disorder[37], which also share clinical features, e.g. psychosis and cognitive decline[5,7] and are both treated with antipsychotic drugs[32]. Differential diagnosis is problematic. Some patients display features of both diseases and are diagnosed for an intermediate form, schizoaffective disorder[32]. Schizophrenia also has some commonalities with major depressive disorder and autism[5,7,32]. Since these genetic and clinical overlaps impede diagnosis, the Research Domain Criteria (RDoC) project was founded to develop a new diagnostic approach based on neurobiological parameters instead of observed symptoms[38]. This classification system would be organized hierarchically into five *domains* — Negative Affect, Positive Affect, Cognition, Social Processes, Arousal/Regulatory systems — each of which consists of subordinate constructs, e.g. Fear[39]. Such a revolution in the psychiatric classification system is expected to improve diagnosis and, consequently, introduce more efficient, domain-targeting treatment strategies in the patients.

1.2   TCF4 transcription factor

TCF4 (ENSG00000196628), also known as *E2-2, SEF2* and *ITF2*, encodes Transcription factor 4. Next to *MIR137*, *CACNA1C* and the MHC region[31], it is one of the most replicated GWAS schizophrenia risk genes[26–31]. *TCF4* should not be confused with *TCF7L2* (T-cell-specific transcription factor 4, ENSG00000148737), which traditionally is often referred to as "TCF4" too.

TCF4 belongs to the class I basic helix-loop-helix (bHLH) transcription factors, which are broadly expressed in various tissue types (reviewed in[40–42]). They are also called E-proteins, since they recognize palindromic CANNTG motifs known as *E-boxes* (Ephrussi-boxes)[43], via the basic region of the bHLH domain[44,45]. To gain transcriptional activity, E-proteins need to dimerize with tissue-specific class II bHLH transcription factors. The preference for different E-boxes will depend on the protein combination within a heterodimer. E-proteins can also dimerize with dominant negative HLH proteins (ID family), which lack the basic region and consequently, prevent DNA binding (reviewed in[40,46]). Thus by interacting with various tissue-specific bHLH partners or HLH repressors, E-proteins have pleiotropic functions[40,46]. Brain development is regulated by less

than 10 class II proneural proteins, which interact with ubiquitously expressed E-proteins (Fig. 1.1). While the fate of neuronal precursos and differentiation are precisely determined by the class II tissue-specific proneural factors, E-proteins seem to be interchangeable between each other[47].

Tcf4 is ubiquitously expressed with highest levels in fetal brain, cerebral cortex and spleen[48–50]. In the brain, its expression is particularly high in neocortex and hippocampus[40] and within the immune system — in dendritic cells and B lymphocytes[49]. *Tcf4* expression starts in embryonic life (Fig. 1.1) and is crucial for cell differentiation during neurodevelopment and differentiation of B and T lymphocytes[51]. Due to the developmental function *Tcf4*^{-/-} mice die after birth[47,52]. Though they display no major anatomical defects except from disrupted pontine nucleus development[47].
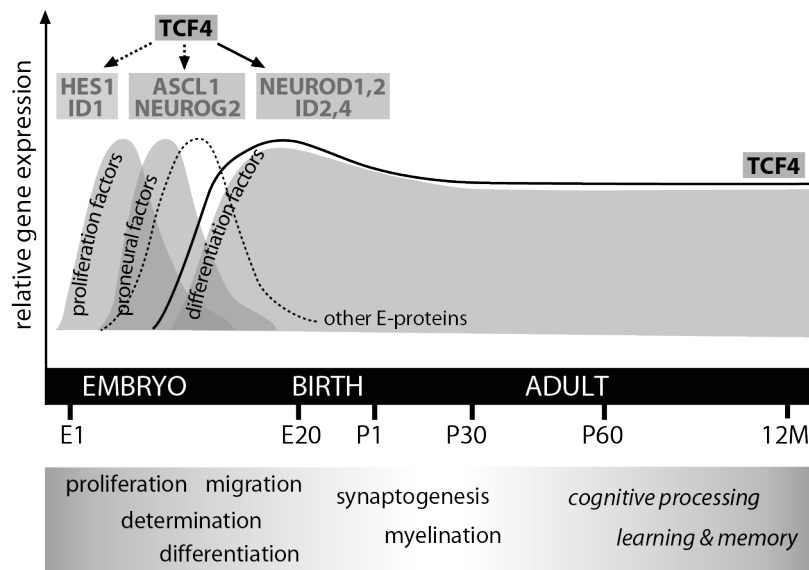
Figure 1.1: TCF4 and neurodevelopment. TCF4 expression in the central nervous system starts in embryonic life, reaches its peak around birth and remains stable during adulthood. By interacting with other bHLH proneural proteins (e.g. NEUROD family) or differentiation inhibitors (ID2 and 4), TCF4 regulates neuronal differentiation during development. Figure from Quednow *et al.* 2014[46].

TCF4 may also be involved in regulation of apoptosis. Knockdown of *TCF4* in human neuroblastoma SH-SY5Y cells led to upregulation of proapoptotic genes and downregulation of genes involved in signalling and neurodevelopment[53]. In mice *Tcf4* is a direct target of ZAC1 (Zinc finger protein regulator of Apoptosis and cell Cycle arrest 1)[54].

The *TCF4* gene is located on the reverse strand of the chromosome 18 in humans and on the forward strand in mice. In humans, the forward strand encodes additionally *MIR4529* and *RPL21P126*[55] (Fig. 1.2). The gene size is large (413.6 kb in humans and 343.5 kb in mice) and was gradually increasing during vertebrate evolution[40].

TCF4 has 48 known splice variants[56] and 18 predicted protein isoforms with distinct N-termini[48] Full-length protein has two activation domains (AD1 and AD2) that regulate transcription, and a Nuclear Localization Signal (NLS). Shorter isoforms may lack AD1 or NLS, but known isoforms contain AD2 and the N-terminally located bHLH domain[48] (Fig. 1.2).

The bHLH domain was conserved in evolution and mutations in that region cause Pitt-Hopkins syndrome (PTHS)[40] (see section 1.2.2 below). bHLH is critical for dimerization and binding
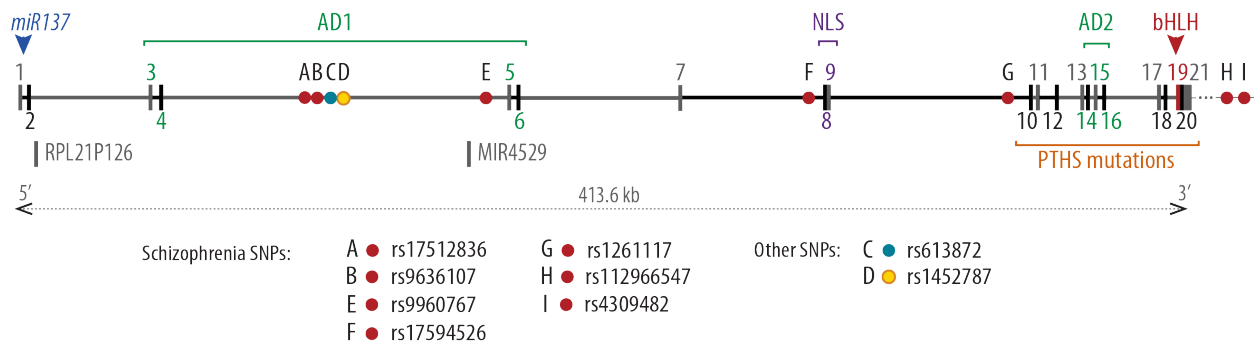
Figure 1.2: Structure of human *TCF4*. Human *TCF4* gene is 413.6 kb long and contains 21 exons (odd and even introns and exons are marked in gray and black, respectively). Two activation domains (AD1 and AD2) are encoded by exons 3–6 and exons 14–16. Exons 8–9 encode Nuclear localisation signal (NLS)[45]. The conserved basic helix-loop-helix (bHLH) region is encoded in exon 19 (red arrow). Two *miR137* binding sites (blue arrow) are located within exon 1[34]. Point mutations within the region containing exons 10–19 result in Pitt-Hopkins syndrome (PTHS) (marked in orange). Four schizophrenia risk SNPs (red dots) are located within *TCF4* introns, three of which are in the intron ENSE00003675281, the longest intron of the gene. Two more schizophrenia SNPs are downstream of the *TCF4*. Additionally, two SNPs in the intron ENSE00003675281 are associated with Fuchs's corneal dystrophy (blue dot) and sclerosing cholangitis and ulcerative colitis (yellow dot)[64,65].

E-boxes in promoters or enhancers of other genes[40]. TCF4 regulates transcription predominantly as heterodimer with class II bHLH proteins and homodimers have no known function. Proneural partners of TCF4 include NEUROD1, NEUROD2 (NDRF)[57] and NEUROD6 (NEX), while the HLH protein ID2 acts as a repressor[58]. TCF4 has many potential partners and should be considered as a hub in the network of bHLH proteins interactions[46].

Direct target genes of TCF4 are largely unknown, but it has been shown that it regulates expression of Somatostatin receptor type II (*SSTR-2*)[59] and Tyrosine hydroxylase[60].

Activity of E-proteins, including TCF4, is inhibited by Ca^{2+}/calmodulin[61,62]. Ca^{2+} levels, which indicate synaptic activity, could possibly modulate TCF4 functions by affecting its splicing, shuttling, dimerization or its partners[46]. Such regulation of TCF4 by neuronal activity might allow adaptation to environmental changes and indeed, TCF4 genotype intearcts with smoking[63].

1.2.1 *TCF4* and schizophrenia

Several schizophrenia-risk SNPs were found in introns of *TCF4* and in the intragenic region downstream of it (Fig. 1.2). Two of these polymorphisms are located in the intron ENSE00003675281 (intron 4–5) which also contains SNPs independently associated with Fuchs's corneal dystrophy and sclerosing cholangitis and ulcerative colitis[64]. Moreover, *TCF4* has also been linked to intellectual disability[31] and to bipolar disorder[66]. Thus *TCF4* is a validated risk gene for schizophrenia that may play a role in other psychiatric diseases.

The *TCF4* SNPs contribute to schizophrenia-relevant endophenotypes. Patients carrying the risk allele of rs9960767 display decreased PPI[67] and auditory P50 suppression, which is worsened in heavy smokers[63]. Risk variant of rs17512836 was associated with reduced auditory P300 amplitude[68], thus may affect attention and working memory[68]. Both SNPs are associated with

predispositions for paranoia in adolescents in general population[69]. Surprisingly, risk variants of rs9960767 in Caucasians and rs2958182 in a Chinese population correlated with worsening of verbal memory[70] or attention[71] in healthy subjects, but with improvement in the patients.

It is unclear whether these SNPs affect *TCF4* expression levels, but elevated *TCF4* mRNA was found in blood of schizophrenic patients[72] and postmortem brain tissue[73–75].

Interaction of *TCF4* with other schizophrenia risk genes is possible, since their expression patterns largely overlap[76]. In cultured non-neuronal cells, TCF4 regulates the schizophrenia and autism-related genes *CNTNAP2* and *NRXN*[77] and is regulated by *miR-137*[34] (Fig. 1.2), a microRNA involved in schizophrenia[28,30,31]. *TCF4* is also predicted to be a target of several other microRNAs associated with diseases of the central nervous system[40].

Interestingly, many murine microRNAs (*miR-137, -183, -200b, -200c* and *-429*[78,79]) are bound by *Tcf4* circular RNA (circRNA) — huge RNA molecules composed of exons. It is not clear what determines which exons are incorporated into circRNAs, but it is known that the introns neighboring the chosen exons tend to be 3 times longer than other introns. It may be interesting, concerning that the *TCF4* intron ENSE00003675281, where most of the risk SNPs are, is the longest intron of *TCF4* (over 12 kb)[56].

1.2.2   *TCF4* and the Pitt-Hopkins syndrome

The Pitt-Hopkins syndrome (PTHS) is an autosomal dominant disorder caused by haploinsufficiency of *TCF4*. It is very rare — the number of patients is estimated to be around 200–300 worldwide[41].

The hallmarks of PTHS are mental and developmental retardation, absence of speech, episodic hyperventilation and distinct facial features, e.g. strabismus, wide mouth with M-shaped Cupid's bow, fleshy lips and broad nasal bridge[42,80,81]. Patients often also display other bodily deformities, abnormal EEG, epilepsy, diminished startle response[41,42,82] and anatomical changes of the brain: thin corpus callosum, hypoplasia of the frontal lobes and small hippocampi[42]. Patients typically display autistic-like behaviours; including stereotypy, perseveration and impaired social interaction[41,80,81]; and can be easily misdiagnosed for Rett, Angelman or Mowat-Wilson syndrome[82–84]

PTHS is caused by various kinds of mutations within the *TCF4* gene. Some of them are deletions that affect the whole *TCF4* transcript or the AD2 and bHLH domains[42,45]. Nonsense mutations or small indels occur mainly in the exons 10–19, encoding AD2 and bHLH, and generate a premature stop codon or elongate the reading frame[45]. PTHS missense or elongating mutations impair TCF4 functions via protein destabilization, changing dimerization preferences or disrupting DNA-binding and transactivation activity[45]. Ultimately, all these mutations lead to TCF4 loss of function. Partial loss of function also leads to milder mental retardation without the typical PTHS features[85].

Mutations in *NRXN1* and *CNTNAP2*, potential TCF4 targets[77] and members of the neurexin superfamily, lead to PTHS-like syndromes, which have similar symptomes except from the facial features[41]. These genes are regulated by TCF4 *in vitro*[77] and possibly belong to the same pathway. In contrast to PTHS, which is an autosomal dominant disease, the PTHS-like syndromes are autosomal recessive[41].

Modelling PTHS in animals would be possible by using appropriate *Tcf4* knockouts. Different *Tcf4* knockout mouse lines are commertially available on the market (reviewed in[41]). In our project we used a mouse line from the Sanger Institute with floxed *Tcf4* exon 4 (see section 2.4 on page 17).

1.3 Gene×Environment interaction

Both genes and environment play a role in psychiatric disorders. Whether an individual will develop symptoms or not, depends on Gene × Environment interaction (G×E)[5,86]. According to the *Two-hit hypothesis*, genetic vulnerability (first hit) followed by exposure to environmental risk factors (second hit) can trigger psychotic disorders[87]. Numerous environmental factors, often of social nature[9,88], contribute to the risk of schizophrenia (reviewed in[5,9,86,87,89,90]). Some affect embryonic development, e.g. pregnancy and birth complications, maternal malnutrition, maternal immune activation or being born in winter. Other factors occur during early life: childhood adversity, childhood viral infections, cannabis consumption[86,89], migration[91,92] and urban upbringing[93–95]. The latter two come down to chronic social exclusion, isolation and defeat, which may be the essential factors for schizophrenia[5,96,97]. Social support, on the other hand, may protect from psychopathology[96].

Timing of environmental adversities can determine the type and severity of symptoms that will emerge in adulthood[90,98,99]. Schizophrenia typically has its onset during adolescence or shortly after[10–12,32], which is a time of high vulnerability, considered as the *critical period* for developing social skills and executive functions[86,100,101]. The adolescent brain undergoes intensive changes, predominantly in the frontal cortex, e.g. enhanced plasticity[101] and pronounced synapse elimination (*pruning*)[102,103].

Pruning is a natural developmental process common in many species. During healthy adolescence gray matter gets thinner in the frontal lobes (thought to result from loss of synapses), which correlates with improvement of verbal and spatial memory[101,104]. Reduction of dendritic spines[105,106] and excessive pruning in the cortex are proposed as mechanisms of cortical thinning in schizophrenia[2,101,107,108]. Interestingly, in a computational model, moderate elimination of synapses improved speech recognition, but excessive synapse loss led to hallucinations, compared to hearing "voices"[109]. Perhaps, common "pro-pruning" genes, that normally enhance cognition, in bad combinations (G×G) can exaggerate pruning and lead to psychosis[109]. Pruning is mediated predominantly by long-term depression (LTD)[101]. It selectively reduces excitatory synapses in the cortex and thereby increases inhibition/excitation ratio and refines interneuronal activity (reviewed in[101,108]). It seems that pruning proceeds in an activity-dependent manner (used connections are

reinforced, unused eliminated), which would make room for environmental and epigenetic factors to get involved in the whole process[108].

Post-weaning period is the puberty in mice (e.g. around P29 in C57Bl/6 males)[110], analogous to human adolescence. However, some differences occur — human frontal cortex and amygdala develop more extensively and human hippocampus maturates faster (in the age of 2 years, while in rodents after weaning)[90]. Puberty is a time of high vulnerability in rodents[111] and can be a useful model of the critical period in human adolescence.

Several environmental paradigms are used to model environmental risk factors for schizophrenia in animals (reviewed in[112]. Models based on pharmacological treatment, e.g. psychostimulants[113], phencyclidine (PCP)[114,115], NMDA receptor antagonists[116], have long tradition; however, these approaches usually have low clinical relevance, as they do not mimic the factors encountered by the patients. Other models include neonatal ventral hippocampal lesion[117,118] and prenatal immune activation[119]. Probably a better approach is to model risk factors commonly encountered in human adolescence, like cannabis exposure[120] and psychosocial adversities modeled by social isolation and social defeat[90] (see below).

Finally, G×E approaches have been gaining more and more attention during the last decade[121]. Several genetic mouse models of schizophrenia — e.g. *Disc1*, *Nrg1–Erbb4* mutants[90,112] and *Tcf4*-overexpressing mice[57] — have been analysed using various G×E paradigms (reviewed in[90,122–126]). In our project we focused on adolescence-related psychosocial factors, which we believe to be particularly relevant for schizophrenia, and on their interaction with *Tcf4* overexpression.

1.4 Modelling environmental factors in mice

Using rodents as disease models has several advantages compared to human studies. By testing animals of a defined genetic background in strictly controlled and standarized experimental conditions, we reduce between-subject variability. This way we can dissect even subtle influences of a given factor, e.g. mutation or environment, on the phenotype. Modeling psychiatric diseases in rodents requires performing behavioural experiments. Since animals do not speak, creating valid models is challenging, particularly in case of the the positive symptomes of psychotic diseases. What can be reliably measured in behavioural tests, is cognition and several other disease-associated endophenotypes, e.g. PPI.

Various paradigms are used to model environmental influences in laboratory conditions. To mimic environmental risk factors for schizophrenia, we subjected our mice to isolation rearing (IR) and social defeat (SD). As a control condition we used enriched environment (EE) which provides various kinds of stimulation and best resembles the natural environment of wild mice.

1.4.1 Isolation rearing (IR)

Social isolation in rodents induces a set of somatic and behavioural changes — the *isolation synrome*[127,128]. Detrimental effects of isolation have been observed also in opossum[129] and other mammalian species kept in zoological gardens in the 60s[130].

In laboratory conditions IR is achieved by housing rodents individually in a barren cages after weaning. The first reported symptoms were aggressiveness[128], nervousness during handling and tendency to bite[127], which makes these animals difficult to work with. Isolated rodents (particularly males[131]) display numerous symptoms, including learning and memory disruption[128,132,133], reduced pain sensitivity[134,135], hypersensitivity to psychostimulants[131], locomotor hyperactivity in novel environment[131,136–142] and impaired PPI[138–140,143]. IR has been proposed and as an animal model of schizophrenia in numerous studies[128,131,143].

The post-weaning period is considered as rodent puberty[110] and corresponds to the critical period of risk for psychiatric diseases in humans[144]. IR can cause irreversible changes, some of which (e.g. PPI deficits) occur only if the animals are isolated shortly after weaning[138,142,144]). and other (e.g. novelty-induced hyperactivity) are independent of developmental stage[138]. Therefore isolation rearing shortly after weaning should be distinguished from isolation housing in adulthood.

IR has three aspects: social deprivation, sensory deprivation and lack of physical activity — each of which produces different symptoms. In rats, sensory deprivation in barren cageing impairs hippocampus-dependent spatial learning in Morris water maze (MWM), while social deprivation specifically impairs reversal learning[145] and in mice pseudoisolation (animals in one cage but separated by a perforated transparent partition) induces hyperactivity in the Open Field (observed in many schizophrenia models[124]) without changes in acoustic startle response[146]. On the cellular level sensory deprivation diminishes cortical spine elimination during adolescence in mice[147].

Social isolation in humans has detrimental effects, first observed in hospitalised children in the 40s[148,149]. In adults, isolation and sensory deprivation trigger hallucinations, intrusive thoughts, confusion of dreams with reality, emotional instability and irrational fear — reported in psychological studies[150,151] and case reports, e.g. explorers, soldiers on guard duty or isolated patients[152]. Conceivably, in absence of sensory input, brain generates hallucinations as a replacement. Sensory deprivation has been proposed as a human model of schizophrenia[152], albeit criticized[150]. Long-term isolation cannot be studied for ethical reasons, but short-term (few days long) isolation in adults was shown to have temporary, yet striking, outcomes[150,152]. Prolonged isolation, particularly in the critical periods, may cause life-long impairments. The famous case of Kaspar Hauser[153] — a 19th century's German boy kept in complete isolation until the age of 17 — is an extreme example of detrimental effects of social deprivation on development of language, cognition and social skills.

Rosenzweig[152] suggested that psychosis-like symptoms upon sensory deprivation are in fact caused by *relevance deprivation* (lack of salient stimuli that would evoke a response). This state could be also induced by perceptual distortion (*incorrect understanding of perceptual experience*[154]) or sensory overload — possible alternative models of schizophrenia[152]. Schizophrenics hallucinate less in isolation[150,151], which may denote that they normally suffer from sensory overload.

1.4.2 Social defeat (SD)

Numerous evidence show that early life stress (e.g. emotional neglect, sexual abuse, violence, bullying) can trigger psychopathology in adulthood[86,155–159]. Schizophrenia risk factors: urban upbringing and migration, are associated with chronic social defeat and social exclusion, which underlies the *Social Defeat Hypothesis of Schizophrenia*[96,97]. It seems that stressors in adulthood do not contribute to the risk of schizophrenia, but the patients and their relatives are more reactive to daily hassles[156], which emphasizes the importance of the critical developmental period. Most of the stressors in Western societies are of psychosocial nature, therefore mouse models of psychosocial stress are expected to be the most relevant for psychiatric disorders.

In rodents, social defeat is one of the paradigms used to model psychosocial stress. Typically the resident-intruder paradigm is applied, which resembles bullying in humans[160]. Experimental mice are introduced to cages (territories) of more aggressive and bigger mice[120]. To assure the stress is psychosocial and not physical, experimental mice are protected by wire-mesh cages after the first attacks, but are still exposed to the aggressor. Because the procedure is repeated for 3 weeks, the stress is chronic. SD has been extensively studied in rodents and was found to cause a depressive-like phenotype[161,162], impaired cognition and PPI deficits[163]. It also affects hippocampal functioning[164] and the mesocorticolimbic dopaminergic system[165].

1.4.3 Enriched environment (EE)

Enriched environment is virtually the opposite of isolation rearing. Enrichment in laboratory conditions typically means housing rodents in groups in large cages equipped with various objects, e.g. toys, tubes and running wheels[121,166]. Such defined EE has three major aspects: *sensory* stimulation, *social* stimulation and *physical* stimulation. Sensory stimulation is required for correct functioning and connectivity of sensory cortices[167] while social stimulation allows them to develop necessary social skills. Sensory and social stimulation seem to influence different behaviours independently[145,168]. Physical activity is provided by the running wheel, which is willingly used by laboratory as well as wild mice[169,170] and enhances cognitive performance[171,172]. Similarly, sport for humans — particularly during childhood — improves cognition[172,173] and restores hippocampal function in schizophrenic patients[174].

Because of its positive effects on rodent behaviour and resemblance to the natural environment, EE is recommended as an appropriate control condition, which is better than standard housing (group housing in barren cages[166]). EE positively influences rodent brain and behaviour — increases long-term potentiation (LTP), neurogenesis, dendritic branching, vascularisation and synaptic spine density, improves cognition and exploration and reduces anxiety (reviewed in[121,167]). In numerous studies addressing G×E, EE rescued the phenotype of mouse models of various nervous system-related diseases, e.g. Fragile X syndrome, Alzheimer's disease or schizophrenia (reviewed in[121,175]) and abolished effects of juvenile stress[176,177].

1.5   Aims of the project

In this project, we focused on analysing Gene × Environment interaction in transgenic (*Tcf4*tg) mice overexpressing *Tcf4* in postnatal forebrain.

To better relate the studied mouse models to psychiatric diseases, we developed an approach to analysing complex behavioural data sets and creating clinically relevant behavioural profiles mice (published in Badowska *et al.*[178]). Initially we focused on environmental factors in wildtype (wt) mice and next, on G×E in *Tcf4*tg mice.

Previous studies by Brzózka *et al.*[57] showed that *Tcf4*tg mice display mild impairments of fear conditioning and PPI. Therefore we tested whether environment can influence the manifestation of this phenotype in these mice. Therefore we subjected them to IR and EE and analysed them in a battery of behavioural tests.

We also aimed at identifying molecular and cellular mechanisms that could underlie the behavioural phenotype. To find potential candidate genes downstream of TCF4, we analysed the transcriptome and proteome of *Tcf4*tg mice in hippocampus and prefrontal cortex (PFC). We also investigated whether *Tcf4* overexpression influences synapse morphology and electrophysiological properties of neurons.

To understand *Tcf4* function, we combined the gain-of-function approach (*Tcf4* overexpression in *Tcf4*tg mice) with the loss-of-function approach (*Tcf4* depletion). We generated a *Tcf4*$^{-/+}$ mouse line and analysed the impact of the knockout on murine behaviour.

In summary, in this project we adressed the following issues:

- Creating behavioural profiles of wildtype mice based on huge data sets

- Modelling G×E in *Tcf4*tg mice and analyses on behavioural, molecular and cellular level

- Generation and initial analysis of *Tcf4*$^{-/+}$ mice

Materials

2.1 Chemicals, reagents and laboratory supplies

Table 2.1: Chemicals and reagents.

Chemical	Supplier	Chemical	Supplier
2-Propanol	VWR	Lithium dodecyl sulfate	Sigma
Agarose	AppliChem	MES	Sigma
Bis-Tris	Sigma	Methanol	J.T.Baker
BSA (Bovine Serum Albumin)	ThermoScientific, Sigma	Non-fat milk powder	frema-Reform
Chloroform	J.T.Baker	Paraformaldehyde	Serva
dNTP 10 mM (2.5 mM each)[1] cat. no. 1969 064	Roche	Pellet Paint, cat.no. 70748-3	Millipore
DTT (Dithiothreitol) 0.1 M	PJK	SDS	Sigma
EDTA	Sigma	Serva Blue G250	Serva
Ethanol	Sigma	Sucrose	Merck
Ethidium bromide	Sigma	Tris	Roth
Glycerol	Merck	Tris base	Sigma
Glycogen		Tris-HCl	Sigma
HEPES (stock 200 mM)	Lonza	Triton X-100	Sigma
Inorganic salts	Merck, Sigma, Roth	Trizol	Roth
Lauryl sulphate	Sigma	Tween20	Merck

PhosSTOP Phosphatase Inhibitor Cocktail Tablets, cat.no. 04 906 837 001	Roche
Complete Mini Ultra EDTA free protease-inhibitor tablets, cat.no. 05892791001	Roche

Markers:

DNA ladder (100 bp, 1 kb)	Fermentas
Spectra Multicolor Broad Range Protein Ladder, cat.no. 26634	Thermo-Scientific

---

[1]diluted 1:5 with water before use, final concentration in the PCR 200 µM (50 µM each)

Table 2.2: Laboratory supplies.

Laboratory supplies	Supplier
ECL-hyperfilms	Amersham Biosciences
PVDF Membrane Hybond P	Amersham Biosciences
96-well plates for RT-qPCR	Applied Biosystems
384-well plates for RT-qPCR	Roche
NuPAGE Novex 4-12 % Bis-Tris Protein Gels, 1.0 mm, 10 well (cat.no. NP0321BOX)	Life Technologies
Kits	
Agilent RNA 6000 Nano Kit	Agilent
DC Protein Assay	Bio-Rad
ECL Plus Western-Blot Detection Reagents	Amersham Biosciences
RNeasy Mini Kit (cat.no. 74106)	Qiagen
Invisorb Spin Tissue Mini Kit (cat.no. 1032100300)	Stratec biomedical
Cloud-Clone Corp ELISA Kit (cat.no. CEA806Mu)	Uscn Life Science Inc.
Enzymes	
GoTaq DNA polymerase & 5× buffer	Sigma
RedTaq DNA polymerase & 10× buffer	
Proteinase K (10 mg/ml)	Invitrogen
SuperscriptIII Reverse Transcriptase	Invitrogen
Power SYBR Green Master Mix (2×)	Applied Biosystems
HRP-conjugated-goat secondary antibodies	Dianova

Table 2.3: Laboratory equipment and software.

Equipment	Supplier
7500 Fast Real-Time-PCR System	Applied Biosystems
LightCycler 480	Roche
2100 Bioanalyzer	Agilent
3328 Biofuge	Heraeus
Stepper pipette HandyStep® electronic	Brand
Intas Chemocam Imager ECL HR-16-3200	Intas UV-Systems
Homogenizer: Polytron PT 1200E	Polytron Hand
Arium® pro VF Water Purification System	Sartorius
SDS-PAGE Gel Electrophoresis System	Invitrogen
Eon microplate reader	BioTek
Open Field System	TSE Systems
Fear Conditioning System	TSE Systems or Ugo Basile
Prepulse Inhibition System	TSE Systems or SR-LABTM
Digital camera ProgRes C14	Jenoptik
Software	**Source**
Adobe Illustrator CS5, Adobe InDesign CS5	Adobe Design Standard CS5
Any-maze software (cat.no. 60000-FC)	Ugo Basile

Table 2.3 – *Continued from previous page*

Software	Source
DNASTAR Lasergene Core Suit 9	DNAStar
GraphPad Prism 5 for Windows ver. 5.04	`www.graphpad.com`
ImageJ	`http://imagej.nih.gov/ij/`
LaTeX (MiKTeX)	`http://miktex.org/`
Moti4, VideoMot2	TSE Systems
R	`www.r-project.org`
Universal Probe Library Assay Design Center	`www.roche-applied-science.com`
Zotero	`www.zotero.org`

2.2   Primers

Primers were designed using the Assay Design Center for Universal Probe Library by Roche (`http://lifescience.roche.com`). All oligunucleotides were produced in by the DNA Core Facility of the Max-Planck-Institute of Experimental Medicine, Göttingen, Germany. Each oligo has been given an in-house identification number (ID). Primers are listed in the Tables 3.2 and 3.6.

2.3   Buffers

Blocking buffer (western blotting) 5% non-fat milk in TBS-T or 5% BSA in TBS-T

Buffer A (synaptosome isolation) 4 mM HEPES, 0.32 M sucrose

DNA extraction buffer (1×) 0.5 % SDS, 0.1 M NaCl, 0.05 M Tris (pH 8.0), 3 mM EDTA with 0.5 mg/ml Proteinase K

MGB (1×) 67 mM Tris pH 8.8, 16.6 mM $(NH_4)_2SO_4$, 6.5 mM $MgCl_2$, 0.5% Triton-X-100

NuPAGE MES running buffer (1×) 50 mM MES, 50 mM Tris Base, 0.1% SDS, 1 mM EDTA, pH 7.3

NuPAGE sample buffer (1×) 106 mM Tris-HCl, 141 mM Tris base, 2% Lithium dodecyl sulphate, 10% Glycerol, 0.51 mM EDTA, 0.22 mM SERVA Blue G250, 0.175 mM Phenol Red, pH 8.5

NuPAGE Transfer buffer (1×) 25 mM bicine, 25m M Bis-Tris (free base), 1 mM EDTA, 0.05 mM chlorobutanol, 20% methanol pH 7.2

PBS (Phosphate buffered saline) (1×) 10% NaCl, 0.25% KCl, 0.72% Na_2HPO_4•2 H_2O, 0.25% KH_2PO_4, pH 7.2

Sucrose buffer (always freshly made) 320 mM sucrose, 10 mM Tris, 1 mM $NaHCO_3$, 1 mM $MgCl_2$, Protease-inhibitor tablets, PhosSTOP Phosphatase Inhibitor Cocktail Tablets or self-made phosphatase inhibitor coctail (4.5 mM $Na_4P_2O_7$, 5 mM NaF, 1 mM Na_3VO_4, 1 mM $ZnCl_2$)

TAE (Tris/Acetate/EDTA) (1×) 40 mM Tris-Base pH 8, 0.4 mM acetic acid, 20 μM EDTA (0.5 M; pH 8)

TBS-T buffer (1×) 50 mM Tris-Base, 150 mM NaCl, 0.01-0.1% Tween20, pH 7.4

TE buffer (1×) 10 mM Tris-HCl (pH 7.4), 1 mM EDTA

2.4   Mouse strains

C57Bl/6N wildtype mice, from Charles River (Sulzfeld, Germany) or in-house-bred, used for behavioural tests, hormone measurements, breeding and as strangers in Social Interaction test

FVB/N in-house-bred, used for breeding and as residents in SD paradigm

TMEB heterozygotic *Tcf4*tg ad wt mice on FVB/N background (see section 2.4 below)

TMEBBl6 heterozygotic *Tcf4*tg and wt mice on mixed background C57Bl/6N × FVB/N (see below). These hybrids were chosen for most of the experiments, as the most "healthy" strain (see *hybrid vigour* below).

TMEBl6_F10 heterozygotic *Tcf4*tg and wt mice on C57Bl/6N background i.e. bred to C57Bl/6N mice for 10 generations (see below)

***Tcf4*E** line MDXP EPD0103_3_A07, (C57Bl/6N background) from the Sanger Institute, carrying the EUCOMM allele *Tcf4*[tm1a(EUCOMM)Wtsi] (project ID: 26368).

***Tcf4*F** offspring of *Tcf4*E mice bred to FLIR mice (C57Bl/6N background) in order to delete the lacZ-neo cassette (Fig. 2.1). *Tcf4* function is restored in this line (see below).

***Tcf4*C** heterozygotic a whole-body *Tcf4* knockouts (C57Bl/6N background), offspring of *Tcf4*E and EIIa-Cre mice (Fig. 2.1). *Tcf4* exon 4 is lacking but the lacZ-neo cassette is maintained. The gene is disrupted in all body cells from the early development (see below).

EIIa-Cre line B6.FVB-Tg(EIIa-cre)C5379Lmgd/J from Jackson Laboratory (stock number: 003724). Cre-recombinase expression starts in all body cells before implantation in the uterine wall.

FLIR *Flp1* recombinase expressing line 129S4/SvJaeSor-*Gt(ROSA)26Sor*[tm1(FLP1)Dym]/J line from Jackson Laboratory (stock number: 003946).

TYFB mice (C57Bl/6N background) expressing EYFP under *Thy1.2* promoter[179].

Transgenic lines TMEB, TMEBBl6 and TMEBl6_F10

To explore the effect of TCF4 gain of function, we used *Tcf4*tg lines TMEB, TMEBBl6 and TMEBl6_F10, which were previously published by our group[57]. These mice overexpress full-length *Tcf4* var.1 open reading frame (2010 bp, 667 AA, 71.3 kDa) with an N-terminal Flag-tag and C-terminal double Tandem Affinity Purification tag (TAP tag) (585 bp). Therefore the construct (2595 bp, 92 kDa) constitutes of exons only and is missing introns. Overexpression is driven by *Thy1.2* promoter and occurs in projection neurons of postnatal forebrain. As reported by Brzózka *et al*, *Tcf4* mRNA levels in *Tcf4*tg mice are increased to 150% compared to their wt littermates. These mice exhibit strain-independent mild cognitive impairment and sensorimotor gating deficits[57]. Animals on mixed C57Bl/6N × FVB/N background were used in most of the experiments, as they are more "healthy" than inbred strains — they display no anatomical and behavioural abnormalities of their paternal strains and perform better in learning tasks (known as *hybrid vigour*)[180].

Tcf4 knockout mouse strains *Tcf4*E, *Tcf4*F and *Tcf4*C

Eucomm mouse line *Tcf4*E   We purchased commercially available EUCOMM *Tcf4* knockout line (*Tcf4*E) from the Sanger Institute: the EUCOMM allele *Tcf4* (see *Mouse strains* on page 16). As the knockout-first strategy [181] was applied, expression of *Tcf4* in these mice is partially reduced by a promoterless lacZ-neo cassette introduced before the exon 4. The cassette is flanked by two FRT sites and the exon 4 is flanked by two loxP sites (see section 2.4 below and Fig. 2.1 and 3.5). This mouse line can be bred to appropriate tool mouse lines and give origin to various knockout lines.

Line *Tcf4*F   To delete the LacZ-neo cassette the *Tcf4*E mice were crossed with the *Flp1* recombinase expressing mice (the FLIR strain, see section 2.4 above). The offspring line was named *Tcf4*E×FLIR (*Tcf4*F). Deletion of the cassette in restores the *Tcf4* gene function. The *Tcf4*F mice can be bred to a Cre-line of choice to generate a conditional knockout line. However, *Flp1* is not expressed in all body cells, thus the offspring knockouts show mosaic genotype. To solve this problem we plan to breed the mosaic *Tcf4*F animals to wild type mice and then select only the *Tcf4*F allele positive but *Flp1* negative offspring for further breeding.

Line *Tcf4*C — heterozygotic *Tcf4* knockout   Breeding the *Tcf4*E mice directly with the Ella-Cre line (see section 2.4 above) allowed us to generate a *Tcf4* knockout without the time consuming *Tcf4*F breeding and selection. The offspring line, named *Tcf4*E×Cre (*Tcf4*C), lacks the *Tcf4* exon 4 but maintains the lacZ-neo cassette. It is a heterozygotic whole-body knockout from an early embryonic stage.
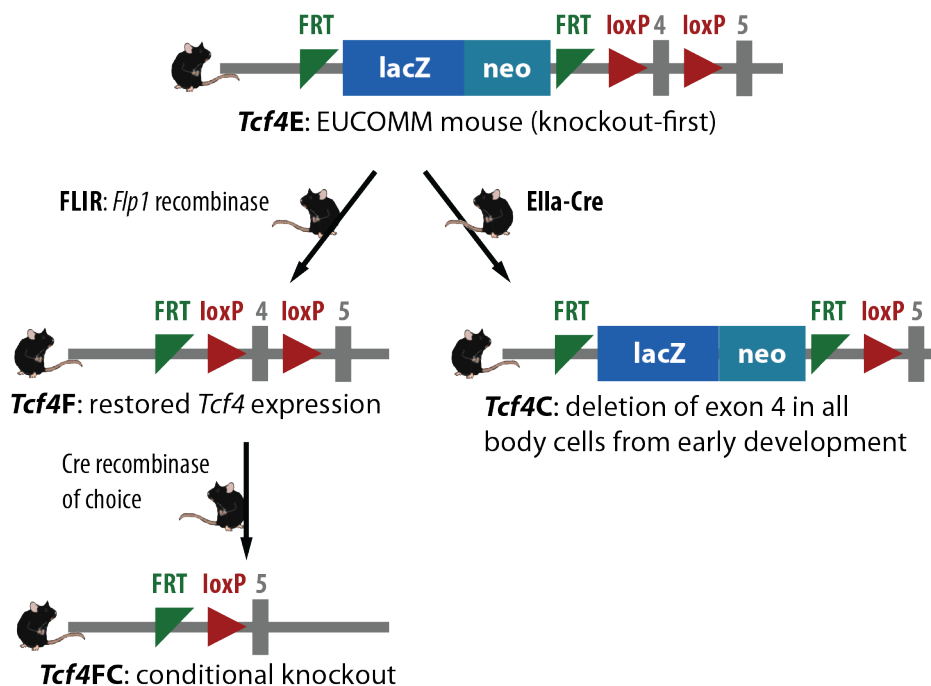
Figure 2.1: Breeding strategy of the *Tcf4* knockout mouse lines. All *Tcf4* knockout lines were derived from the commercial EUCOMM line *Tcf4*E. In this line FRT-flanked lacZ-neo cassette is introduced before the floxed exon 4 (knockout-first approach). Crossing with FLIR mice (left panel) deletes the lacZ-neo cassette and restores the gene function. The offspring (line *Tcf4*F) can be bred to appropriate Cre-line to obtain a desired conditional knockout line *Tcf4*FC. Another approach (right panel) is to breed *Tcf4*E mice directly to Ella-Cre mice, which deletes the exon 4 in all body cells from an early developmental stage, but preserves the lacZ-neo cassette.

Methods

3.1 Behavioural analyses

3.1.1 Environmental paradigms

All mice were maintained in colony rooms under standard conditions with 12 h light/dark cycle and $21\pm2\,°C$ room temperature. Food and water were provided *ad libitum*.

Isolation rearing (IR) From the age of 4 weeks animals were housed individually in Makrolon 2 cages ($26.5 \times 20.5 \times 14.5$ cm) that contained only the bedding (Fig. 3.1A,C). No tissue or other materials that could enrich the cage were provided and animals were handled only during the cage change.

Social defeat (SD) To induce psychosocial stress the resident-intruder paradigm (Fig. 3.1B) was used as described in[120]. Single-housed male FVB/N mice (Charles River, Sulzfeld, Germany) were used as residents. In brief, from the age of 4–5 weeks the experimental animals (intruders) were introduced in the cages of residents. After the first attack occurred each intruder was protected by a wire mesh cage to prevent injuries and left in the resident's cage for 1 h. The procedure was repeated daily for 3 weeks and every day intruder mice were exposed to different residents in a Latin-square manner. Between and after the stress sessions the intruders were housed individually (cages contained bedding and tissue) to prevent abolishment of stress effects by social support[163]. The FVB/N residents were kept in a separate room to avoid olfactory habituation in experimental mice.
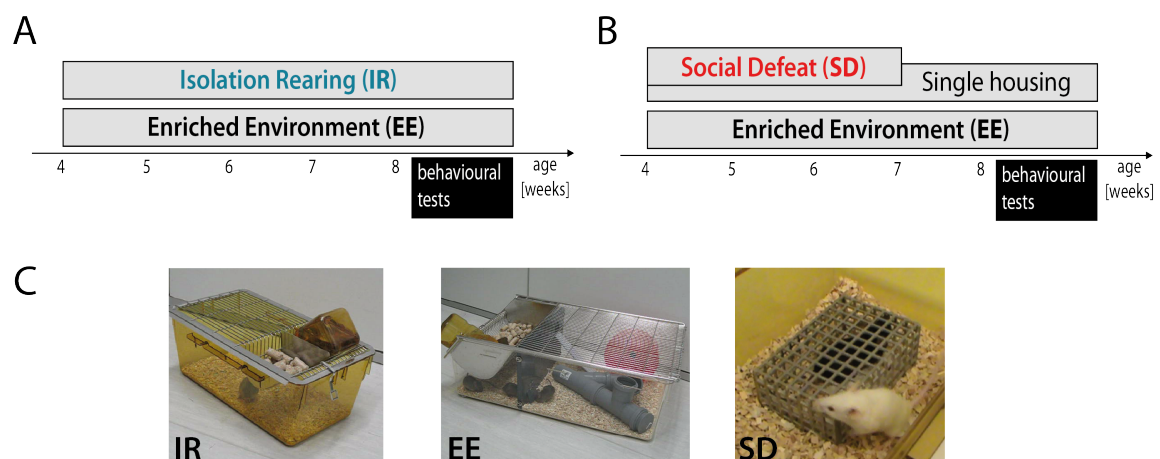
Figure 3.1: Environmental paradigms: IR, EE and SD. A) Animals were subjected to post-weaning isolation rearing (IR) or enriched environment (EE) from the age of 4 weeks remained during the testing period (from the age of 8 weeks) and after it. B) Animals were subjected to social defeat (SD) (daily for 3 weeks) from the age of 4–5 weeks. The control group was housed in EE. C) Photographs present isolation rearing (left), social defeat (middle) and enriched environment (right).

Enriched environment (EE) From the age of 4 weeks animals were group-housed (usually 5–8 mice per cage) in Makrolon 4 cages ($60 \times 38 \times 20$ cm). Cages were divided into two compartments: bigger compartment containing a running wheel and tunnels made of PCV pipe fittings and smaller compartment providing access to food pellets and drinking water. Animals could freely move between the compartments by climbing a ladder or passing through a one-way gate (Fig. 3.1A,C).

3.1.2 Behavioural tests

Most of the experiments were described in our publication[178]. All tests were performed during the light phase. The experiments were approved by the appropriate ethics committee of Lower Saxony and have been performed according to the ethical standards of the Declaration of Helsinki (1964) and its later amendments. The experimental chambers and mazes were washed with 70% ethanol before and after each use, unless stated differently.

Open field (OF) and Hole board (HB) Animals were placed into a grey box ($45 \times 45 \times 55$ cm) and allowed to explore the surrounding for 10 min. In the OF test, time moving, covered distance, rearing and time in the centre were quantified using an infrared monitoring system and the Moti4 software (TSE Systems, Bad Homburg, Germany).

The HB experiment was performed in the same boxes, but with a floor insert containing 16 symmetrically deployed holes (2 cm diameter). During the 10 min long test, the number of nose pokes into the holes and total time of hole exploration were measured automatically by the Moti4 software.

Light-dark preference (LD) The experiment was performed in a chamber divided into two compartments: black-walled "dark" chamber and transparent "light" chamber, both connected by a door-like opening. Mice were placed into the light chamber, with their heads facing the wall opposing the gate. The test lasted 5 min from the first entry into the dark chamber. The latency to enter the dark chamber and the total time spent there were measured manually.

Elevated plus maze (EPM) The EPM setup was built in a shape of a "plus" sign with two opposing open and two closed arms (30×5 cm arms, walls 15 cm high) and raised 50 cm above the floor. Each animal was placed at the crossing of the arms. The time spent in the open and closed arms were manually measured for 5 min.

Tail suspension test (TST) Mice were suspended upside-down and attached to a fixed rod by an adhesive tape by the tip of the tail. Fighting time, which reflects the escape motivation of the mice, was manually scored for each mouse for 6 min.

Y-maze Mice were inserted into a gray plastic maze in the shape of "Y" with arms identical and symmetric to each other. Animals were allowed to explore the maze for 10 min. The number of arm explorations (*choices*) and number of alternations were scored. Alternation was defined as a sequence of thee arms explorations without visiting the same arms twice.

Social interaction We used the *Crawley test of sociability*[182] to analyse social behaviour. The test box consisted of three compartments separated by transparent plexi walls with entrances. In the acquisition phase (5 min) the experimental animal was placed in the middle, empty compartment and the entrances to other compartments were blocked. Next, in the *sociability* phase, an unfamiliar mouse (*stranger 1*) was introduced to one of the compartments and covered by a wire-mesh cage. And empty wire mesh cage was placed in the opposite compartment. The experimental mouse was allowed to explore all compartments for 10 min.

In the last phase (*social memory*) another unfamiliar mouse (*stranger 2*) was placed in the previously empty wire-mesh cage and the experimental animal was allowed to explore the box for 10 min. Experiments were recorded by a camera placed above the test box and the time spent in each of the side compartments was then manually measured. Sociability and memory indexes were calculated according to the formula:

$$ \text{sociability index} = \frac{t_{s1}}{t_{s1} + t_e} + 50 \qquad \text{memory index} = \frac{t_{s2}}{t_{s1} + t_{s2}} + 50 $$

where t_{s1} and t_{s2} are times spent in the compartments with stranger 1 and stranger 2 and t_e is the time in the compartment with the empty wire-mesh cage.

All stranger mice were C57Bl/6N males younger than the experimental mice. To avoid any repulsive stress or anxiety signals from the strangers, before the experiment they were habituated to the wire-mesh cages several times and during the experiment different pairs of strangers were used in consecutive sessions, to let the mice recover.

Prepulse inhibition (PPI) Diminished PPI is an endophenotype of schizophrenia[14], therefore we measured it also in our animals. The experiment was performed as described in works by Brzózka *et al.*[57,183]. Two different commercial PPI systems were used: 4-station PPI system from TSE Systems (Bad Homburg, Germany) for the *Tcf4*tgIR-EE-young cohort and The SR-LAB[TM] Startle Response System (San Diego Instruments) for the *Tcf4*C#1 cohort. Animals were habituated to experimental cages for few days before the experiment.

TSE Systems. The instrument contained 4 soundproof stations with sensors recording vertical movements of the floor. In each station a metal grid cage of dimensions $90 \times 40 \times 40$ mm would restrict animals locomotory movements and during the whole experiment 65 dB white noise was played from speakers on both sides of the grid cage. Animals were placed one by one into the stations and after 2 min habituation baseline recording was done for 1 min. Then six 40 ms long 120 dB sound were played to stabilize the startle response and diminish the impact of within-session habituation. The intensity of *startle responses* to acoustic stimuli were recorded for 100 ms, starting from the onset of the stimulus. Next, in the PPI test, we measured response to non-startling 20 ms-long prepulses of 70, 75 or 80 dB and 40 ms-long 120 dB startling stimuli played 100 ms later. The prepulses were presented in pseudorandom order with 8–22 s long intervals between the trails. The *amplitude of startle response* was calculated as the difference between the intensity of the strongest recorded startle and intensity of startle directly before pulse onset. Means of maximal amplitudes (expressed in arbitrary units, AUs) were calculated separately for startle pulses with or without a prepulse. PPI was calculated as % of startle response, according to the formula:

$$ \text{PPI} = \frac{100 - SA_{p+p-}}{SA_{p-}} \times 100[\%] $$

where SA_{p+p-} stands for amplitude of startle response and SA_{p-} is startle amplitude after pulse only.

SR-LAB[TM] The protocol was as described above. The measurement was performed according to the manufacturer's instructions with the use of two cabinets (type: ABS) and enclosures for mice (type: Small).

Fear conditioning (FC) The test was performed as described in[57,183]. Commercial fear conditioning systems were used: TSE Systems (Bad Homburg, Germany) for the *Tcf4*tg vs. wt cohorts and Ugo Basile (Siena, Italy) for the *Tcf4*C cohort. The paradigm is presented in Fig. 3.2.
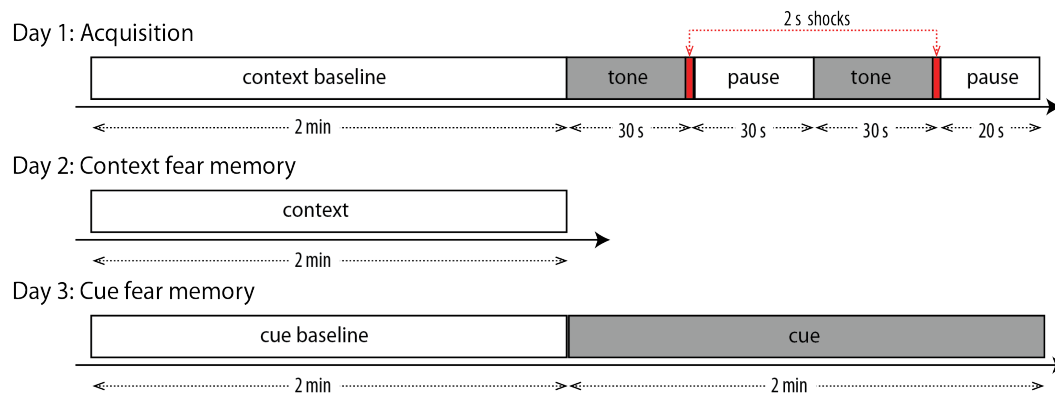
Figure 3.2: Fear conditioning paradigm. Day 1) Mice were tested in the *context* chamber. Baseline freezing was assessed for 2 min, after which animals were subjected to two 30 s long tones (*cues*) paired with 2 s footshocks. **Day 2)** Frezing was measured in the context chamber for 2 min to assess context fear memory. **Day 3)** Baseline freezing was measured in a novel chamber. Next cue was played for 30 s and freezing was measured to assess cue fear memory.

TSE Systems. Foot shocks were applied in the *context* chamber ($36 \times 20 \times 20$ cm), using an electric metal grid made of stainless rods (4 mm in diameter, spaced 6 mm apart). To prevent conditioning to external sounds, background noise was played in both chambers during all phases of the experiment. On day 1 animals were placed in the context chamber and baseline levels of freezing were manually scored for 2 min every 5 s. Next, an auditory stimulus (*cue*) of 10 kHz and 75 dB was played from a speaker for 30 s and immediately afterwards an electric shock of 0.4 mA was applied for 2 s. After 30 s pause, the tone–shock pairing was repeated once. On day 2 mice were placed in the same *context* chamber and freezing was scored for 2 min to assess contextual memory. On day 3 animals were tested in a novel box (grey, triangle-shaped chamber, washed with water). Cue baseline freezing was measured for 2 min. For the next 2 min, the freezing levels were determined in the presence of the sound (*cue*) of the same intensity as during conditioning. To assess remote fear memory context and cue procedures (day 2 and 3 respectively) were repeated one month later.

Ugo Basile System no. 46000. The procedure was performed like in the TSE Systems, but with following modifications: i) freezing was recorded by an infra-red CCD camera (47400-025) and measured automatically by the Any-maze software (cat.no. 60000-FC); ii) shocks were applied in the Ugo Basile 46003 Mouse Boxes (inside dimensions: $17 \times 17 \times 25$(h) cm with the vertical stripe patterns on the walls; iii) for cue memory Mouse Boxes were replaced by a transparent Plexiglas cylinders (diameter 19.5 cm, height 25 cm).

Morris water maze (MWM) The paradigm[184] is presented in Fig. 3.3. The test was performed as described in[57,183], in a white pool (diameter 120 cm) filled with water dyed with white paint. White platform (diameter 10 cm) was located in one of the target quadrants (TQs), 1 cm under the water surface. To allow navigation, a single cue was placed on the wall. The animals' position, time, distance, route and speed of swimming were tracked using TSE VideoMot-Systems. The test consisted of several phases and different behavioural qualities were tested in each phase.

Learning curves. For several consecutive days mice had four swimming trials per day, each time at the different pole of the pool (the order of the poles was different every day). Animals were tested in batches of 4–5 mice, so the trials were separated by intervals of around 5 min. During each trial (max. 90 s long) animals were supposed to find for the hidden platform and remain on it for 10 s. If a mouse failed to find the platform, it was gently guided to it and
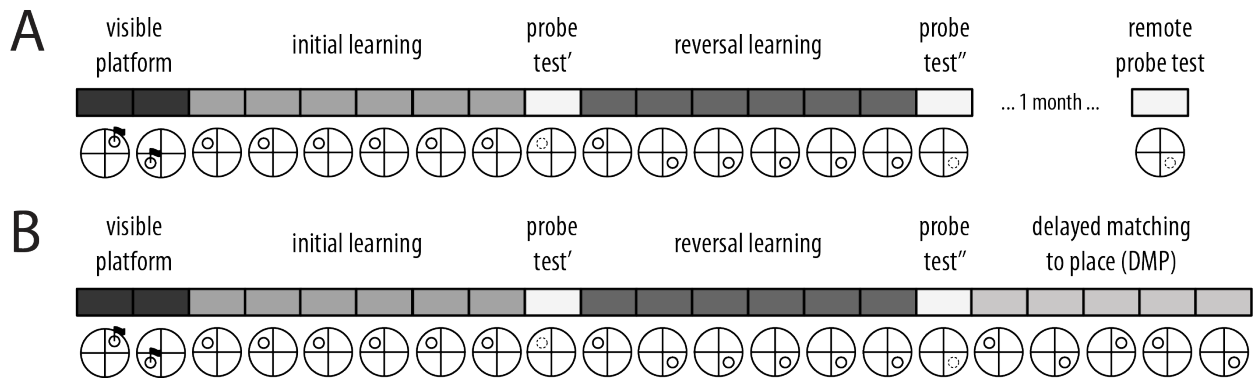
Figure 3.3: Morris water maze paradigm. Mice were inserted to the maze for several consecutive days; each day is represented by a box. **A)** The experiment consisted of distinct phases: I) Visible platform (2 days, 4 trials per day) – mice learn to find a platform marked by a flag. II) Initial learning (6 days, 4 trials per day) – mice search for the platform hidden under the water. III) Probe test' (1 day, 1 trial) – the platform is removed and the time they spend in target quadrant (TQ) is measured. IV) Reversal learning (6 days, 4 trial per day) – the hidden platform is moved to a different position. V) Probe trial" (1 day, 1 trial) – like probe test'. VI) Remote probe test (1 day, 1 trial) – probe test" repeated after 1 month to assess long-term memory. **B)** In another version of the paradigm probe test" was followed by delayed matching to place (DMP) (5 days, 4 trials per day) in which the platform was located in different position every day.

allowed to sit for 10 s. The time and distance needed to reach the platform were measured. The means of all four trials were used to draw the learning curves. The test was composed of an initial acquisition phase - *visible platform* (2 days) - , an *initial learning* - hidden platform (6 days) - where the animals had to navigate based on the position of the cue, showing spatial learning abilities, and a *reversal learning* phase (6 days) where the platform was moved to the opposite quadrant to asses rigidity and perseveration. In the modified version of the experiment (Fig. 3.3B) five additional days of *delayed matching to place (DMP)*[185] were included to test perseveration in a more challenging task (platform in a different location every day).

Memory recall was assessed in *probe tests* (1 day) in which the platform was removed and mice were allowed to swim in the pool for 90 s in a single trial. The time and distance spent in TQ were recorded. Probe tests were performed after *initial* and *reversal learning* and a remote probe test 1 month later (remote test not done if DMP was included).

Hot plate (HP) Thermal pain sensitivity was assessed by putting mice on a hot plate preheated to 52 °C. The latency until licking the hind paws or jumping was measured. Afterwards animals were immediately removed from the hot plate and put on a metal top to cool down their paws.

Pain threshold Pain sensitivity to electric shocks was measured in the TSE System that was used for Fear conditioning. Animals were placed on the shock grid and a series of 2 s electric shocks of different intensities (0.1–0.7 mA) was applied. The shock intensities were presented in a randomized order and with randomized intervals between them. The animals were observed and the lowest shock intensities that induced reaction (jumping, vocalizing) were noted.

Statistical analyses of behavioural profiles

All behavioural data were initially analysed using t-tests, Mann-Whitney tests, t-tests with Wesch correction or Two-way ANOVA, when appropriate. For MWM RM Two-way ANOVA was applied. Next, the raw data were used to create behavioural profiles (see section 3.1.4 on page 23).

3.1.3 Behavioural cohorts

wtIR 28 male C57Bl/6N mice (Charles River, Suzfeld, Germany) housed in IR (n=15) or EE (n=13) from the age of 4 weeks and subjected to behavioural testing from the age of 8 weeks. Order of tests: OF, HB, LD, TST, EPM, HP, Y-Maze, FC

wtSD 29 in-house-bred male C57Bl/6N mice at the age 4-5 weeks were subjected to either EE (n=14) or SD (n=15) for 3 weeks and then subjected to behavioural testing. All experimental procedures for this cohort were performed by Ananya Chowdhury during her lab rotation under my supervision.
Order of tests: OF, LD, HB, EPM, TST, Social Interaction, Radial Arm Water Maze, Social Avoidance, FC, HP.

***Tcf4*tgIR-EE-young** or *Tcf4*tg *Young* cohort. 59 male *Tcf4*tg and wt mice on C57Bl/6N × FVB/N background were housed in IR or EE from the age of 4 weeks and tested from the age of 8 weeks. The cohort consisted of 16 wt IR, 15 *Tcf4*tg IR, 16 wt EE and 12 *Tcf4*tg EE animals. Testing was performed in cooperation with Dr Magdalena M. Brzózka[1].
Order of tests: LD, OF, HB, Y-maze, PPI, Social Interaction, TST, FC, HP, MWM, pain threshold.

***Tcf4*tgIR-EE-aged** or *Ageing* cohort. 59 male *Tcf4*tg and wt mice on C57Bl/6N × FVB/N background were housed in IR or EE from the age of 4 weeks and tested from the age of 12 months. The cohort consisted of 14 wt IR, 16 *Tcf4*tg IR, 13 wt EE and 16 *Tcf4*tg EE animals.
Order of tests: LD, EPM, OF, HB, Y-maze, Social Interaction, TST, Grip strength, FC, MWM, remote FC, HP.

***Tcf4*C# 1** 30 male mice (14 wt, 16 *Tcf4*C) on C57Bl/6N background were housed in IR from 4 weeks of age and tested from the age of 10–13 weeks. The animals were not the same age – difference between the oldest and the youngest animals was 3 weeks – but there was no age bias between the genotypes. Based on our experience with *Tcf4*tg mice, IR was chosen to enhance the potential phenotype of the knockouts.
Order of tests: LD, EPM, OF, HB, Y-maze, Social Interaction, TST, FC, MWM (variant with DMP), PPI, remote FC, HP.

3.1.4 Behavioural profiling of mice

Our approach was described in details in our article *Data calibration and reduction allows to visualize behavioural profiles of psychosocial influences in mice towards clinical domains*[178]. The data were analysed in collaboration with Dr. Dörthe Malzahn (Department of Genetic Epidemiology, University Medical Center, Georg-August University, 37099 Göttingen, Germany). Analyses were done in R software version 2.15.2 using R-package nlme and R-functions *gls* and *anova*. Graphs were generated using R-package *plotrix*, exported as .eps files and edited in Adobe Illustrator CS5. The procedure below is described for comparison of two wt cohorts: IR vs. EE-1 and SD vs. EE-2 (see "Behavioural cohorts" on page 23). The analysis involved several steps (see Fig. 3.4):

---

[1]Dept. Neurogenetics, Max Planck Institute of Experimental Medicine, Göttingen, Germany

1. **Directionality** Different behavioural parameters, called *measures*, are expressed in different units (i.d. seconds, meters, indexes etc.). To allow comparisons, each of the 14 measures was given an arbitrary sign, such that higher values indicate improved performance and lower values indicate impairments (Fig. 3.4 panel 2). All raw data were multiplied by 1 or -1 according to the assigned directionality. The signs of all measures are presented in Tab. 3.1 (column *Dir.*).

2. **Data calibration** Experimental groups were calibrated to appropriate controls (i.e. IR group to EE-1 and *Tcf4*tg to wt) using z-transformation. After this procedure the means of control groups were set as zero and the values of experimental groups were relative to the controls (Fig. 3.4 panel 3).

3. **Reduction to traits** The measures of the same behaviours were merged into single sum scores called *traits*, e.g. *exploration time* and *nose pokes* in HB were compressed to *HB-exploration* (Fig. 3.4 panel 4). Consequently, we reduced the number of dimensions from 14 measures to 11 domains.

4. **Reduction to domains** Traits reflecting similar behaviours were analysed together as single domains by using multivariate statistics (Fig. 3.4 panel 5), e.g. *OF-time in the centre*, *Dark preference* and *EPM-anxiety* were analysed collectively as *Anxiety*. In the wt IR–SD study, we reduced the number of dimensions to 6 domains. To analyse bigger data sets, i.e. *Tcf4*tg and *Tcf4*C mice, the reductions were made even further into Superdomains and Symptom classes (see Table 3.1), which could be compared to clinical symptom classes of psychiatric patients.

5. **Visualisation of behavioural profiles** Calibrated data from different levels of reduction can be visualised in a single figure by plotting them in a radar chart. Thin black line indicates EE, which is set to zero and coloured lines indicate experimental groups in reference to EE — here IR in blue and SD in red. Such plots can be then overlaid to compare their profiles and the strength of alterations (Fig. 3.4 panel 6 and Fig. 4.9).

6. **Severity scores** To compare the overall level of impairment between experimental groups, we calculated *severity scores*, which were average squared treatment effects that were calculated on the trait level, but can be also calculated on other levels. Higher scores indicate greater difference from the reference group (improvement or impairment).

Statistical comparisons by 1-way ANOVA were done in a hierarchical order — first on the domain level and then, if significant, on lower levels. This approach reduced the loss of statistical power caused by correction for multiple testing.
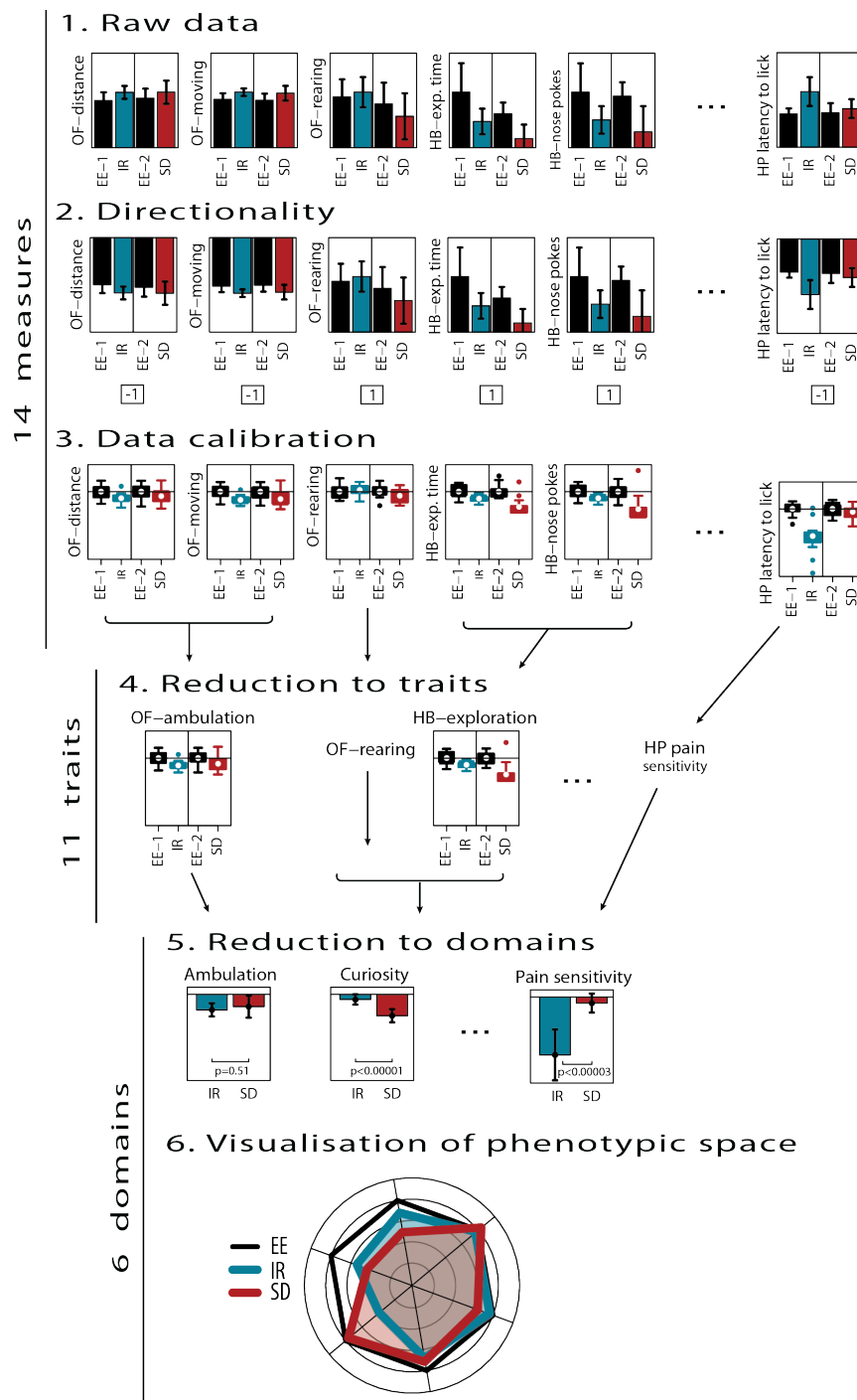
Figure 3.4: Creating behavioural profiles of mice. Panel 1: Two cohorts were analysed. In cohort 1 IR (blue) was referred to EE-1 control (black); in cohort 2: SD (red) was referred to EE-2 (black). Raw data had different units and scales, partially due to experimenter effects. Bar graphs represent mean with standard deviation. **Panel 2**: Raw data were assigned directionality such that higher values indicate improved performance. **Panel 3**: Data were calibrated within cohorts by z-transformation with EE controls set as zero. Boxplots represent means, interquartiles and range of data. **Panels 4 and 5**: Calibrated data were reduced (merged) to traits and domains by summarizing measures into single sum scores (measures to traits) or by multivariate statistics (traits to domains). **Panel 6**: Behavioural profiles of calibrated effect sizes (deviances from EE: black line) were plotted in radar charts. IR (blue) or SD (red) deviations from the black line towards the middle of the chart indicate impairments. **Abbreviations:** isolation rearing (IR), social defeat (SD), enriched environment (EE), Open field (OF), Hole board (HB), Hot plate (HP). Figure adapted from Badowska *et al*[178].

Table 3.1: Directionality and dimension reduction. To analyse huge behavioural data sets, we applied the strategy of synchronizing data and grouping them into hierarchically organized dimensions (*Traits, Domains, Superdomains* and *Symptom classes*) based on similarity of measured behaviours. In the first step all behavioural parameters (*Measures*) were given arbitrary directionality 1 or −1 (column *Dir.*), which determined that higher values of the raw data would always mean better performance in a given test. Measures of the same behaviours (e.g. time moving and distance) were merged into *Traits* and then grouped into hierarchical categories: *Domains, Superdomains* and *Symptom classes*. The last category refers to the three symptoms classes of psychotic patients[5].

Abbreviations: Fear conditioning (FC), Morris water maze (MWM), Open field (OF), Light-dark preference (LD), Elevated plus maze (EPM), Hole board (HB), Tail suspension test (TST), Hot plate (HP)

Superdomain	Domain	Trait	Measure	Dir.
Symptom class: COGNITIVE				
Fear memory	Context memory	Context memory	FC: context	1
		Remote context memory	FC: remote context	1
	Cue memory	Cue memory	FC: cue	1
		Remote cue memory	FC: remote cue	1
	Social fear memory	Remote social fear memory	remote social avoidance	-1
		Social fear memory	social avoidance	-1
Spatial learning and memory	Memory recall	MWM-recall	MWM: probe test'	1
		MWM-remote recall	MWM: probe test"	1
	Perseveration	MWM-reversal learning	MWM: reversal learning (latency)	-1
			MWM: reversal learning (distance)	-1
	Spatial learning	MWM: initial learning	MWM: initial learning (latency)	-1
			MWM: initial learning (distance)	-1
		MWM-visible platform	MWM: visible platform (latency)	-1
			MWM: visible platform (distance)	-1
Working memory		Y-maze-alternations	Y-maze: altenations	1
Symptom class: NEGATIVE				
Anxiety		Thigmotaxis	OF: time in centre	1
		Dark preference	LD: time in dark	-1
		EPM-anxiety	EPM: time in open arms	1
			EPM: time in closed arms	-1
Curiosity		Curiosity	OF: rearing	1
		HB-exploration	HB: exploration time	1
			HB: nose pokes	1
Motivation		LD-latency	LD: latency to enter dark	-1
		TST-motivation	TST: fighting time	1
Pain sensitivity		HP-pain sensitivity	HP: latency to lick	-1
Symptom class: POSITIVE				
Hyperactivity	Ambulation	Y-maze-choices	Y-maze: choices	1
		HB-ambulation	HB: time moving	-1
		LD-ambulation	LD: crossings	-1
		OF-ambulation	OF: time moving	-1
			OF: distance	-1
	Speed	OF-speed	OF: speed	-1
		MWM-speed	MWM: speed	-1

3.2 Molecular analyses

3.2.1 Genotyping

Animals were genotyped by polymerase chain reaction (PCR) with tail DNA used as template.

MGB tail prep Tails were incubated overnight in the MGB buffer with Proteinase K at 55 °C with shaking. Next day the samples were incubated 20–30 min at 90 °C and diluted 1:1 with water.

Chlorophorm extraction Tails were incubated in 400 μl of extraction buffer and 20 μl 0.5 mg/ml Proteinase K 40 min at 56 °C. Next, 75 μl of 8 M potassium acetate and 400 μl of chlorophorm were added. Samples were mixed and centrifuged 10 min at 13000 rpm, at room temperature. 200 μl of the upper phase was transferred to a fresh tube with 400 μl cold 100% ethanol. Tubes were inverted 10 times and centrifuged 10 min at 13000 rpm, at room temperature. Supernatant was removed and DNA pellets were air dried and resuspended in 200 μl TE buffer.

1 μl of the tail DNA extract was used for 20 μl PCR. Genotyping reactions (Table 3.2), were performed using the programs presented in Table 3.4 and the master mixes in Table 3.3. PCR products were loaded on 1.5–2% agarose gels in TAE buffer and separated by electrophoresis. DNA was visualised with ethidium bromide (around 1 μg/ml in the gel) or 1× GelRed in the samples, under UV light. Representative gel pictures (GelRed) are shown in Fig. 3.6. Genotyping primer sequences are listed in Table 3.2.
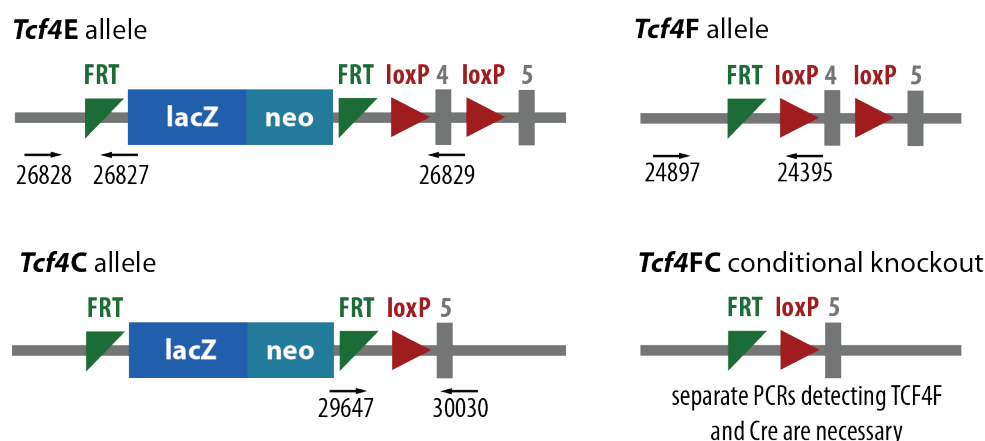
Figure 3.5: Genotyping strategy of the *Tcf4* knockout mouse lines Animals were genotyped by PCR using DNA from tail biopsies. The primer IDs and locations are indicated in the pictures.

Table 3.2: Genotyping primers. Genotyping of alleles marked with (*) require chlorophorm DNA isolation. For others, MGB protocol was used. Column *Prog.* indicates which PCR program from Tab. 3.4 is appropriate.

Allele	fwd	fwd 5'– 3' sequence	rev	rev 5'– 3' sequence	Band [bp]	Prog.
EllaCre	4192	CAGGGTGTTATAAGCAATCCC	4193	CCTGGAAAATGCTTCTGTCCG	550	60 °C
Sry	28741	GTGAGAGGCACAAGTTGGC	28742	CTCTGTGTAGGATCTTCAATC	147	SRY
TAP tag	4873	TCATAGCCGTCTCAGCAGCCAACCGC	4872	CATCGTGTTGCGCAAGAGCCGCGG	140	TAP tag
*Tcf4*C	29647	TCAGCCATATCACATCTGTAGAGG	30030	AAATGACTTCCCGCCAGAC	497	60 °C
*Tcf4*F*	24897	AGGCGCATAACGATACCACGAT	24395	GAACCAGGCACAGGGCTAC	464	60 °C
*Tcf4*E	26828	CCGATGACAGTGATGATGGT	26827	TCGTGGTATCGTTATGCGCC	172	TCF4
Tcf4 wt*	26828	CCGATGACAGTGATGATGGT	26829	AAGTTAAGCTGAAGTAAATACCCACA	300	TCF4
TYFB	4858	CGCTGAACTTGTGGCCGTTTACG	4859	TCTGAGTGGCAAAGGACCTTAGG	300	TYFB

Table 3.3: PCR master-mixes

TAP tag	
gDNA	1 µl
primer 4872	0.1 µl
primer 4873	0.1 µl
5×buffer	4 µl
dNT	2 µl
GoTaq	0.1 µl
H$_2$O	10.5 µl
	20 µl

SRY	
gDNA	1 µl
primer 28741	1 µl
primer 28742	1 µl
5×buffer	4 µl
dNT	2 µl
GoTaq	0.1 µl
H$_2$O	10.9 µl
	20 µl

TCF4C	
gDNA	1 µl
primer 29647	1 µl
primer 30030	1 µl
5×buffer	4 µl
dNT	2 µl
GoTaq	0.1 µl
H$_2$O	10.9 µl
	20 µl

TCF4F	
gDNA	1 µl
primer 24897	0.1 µl
primer 24395	0.1 µl
5×buffer	4 µl
dNT	2 µl
GoTaq	0.1 µl
H$_2$O	10.9 µl
	20 µl

TCF4	
gDNA	1 µl
primer 26827	1 µl
primer 26828	0.5 µl
primer 26829	0.5 µl
5×buffer	4 µl
dNT	2 µl
GoTaq	0.1 µl
H$_2$O	10.9 µl
	20 µl

TYFB	
gDNA	1 µl
primer 4858	0.5 µl
primer 4859	0.5 µl
10×buffer	4 µl
dNT	2 µl
REDTaq	0.1 µl
H$_2$O	12.7 µl
	20 µl

Table 3.4: Standard PCR programs

TAP tag PCR program		
95 °C	3 min	
68 °C	30 s	
72 °C	60 s	36×
95 °C	30 s	
68 °C	1 min	
72 °C	10 min	
10 °C	pause	

SRY PCR program		
95 °C	3 min	
60 °C	30 s	
72 °C	60 s	36×
95 °C	30 s	
68 °C	1 min	
72 °C	10 min	
10 °C	pause	

60 °C PCR program		
95 °C	3 min	
60 °C	30 s	
72 °C	60 s	36×
95 °C	30 s	
68 °C	1 min	
72 °C	10 min	
10 °C	pause	

TCF4 PCR program		
94 °C	5 min	
94 °C	30 s	
58 °C	30 s	34×
72 °C	45 s	
72 °C	5 min	
10 °C	pause	

TYFB PCR program		
94 °C	3 min	
94 °C	30 s	
60 °C	30 s	36×
72 °C	60 s	
72 °C	10 min	
10 °C	pause	
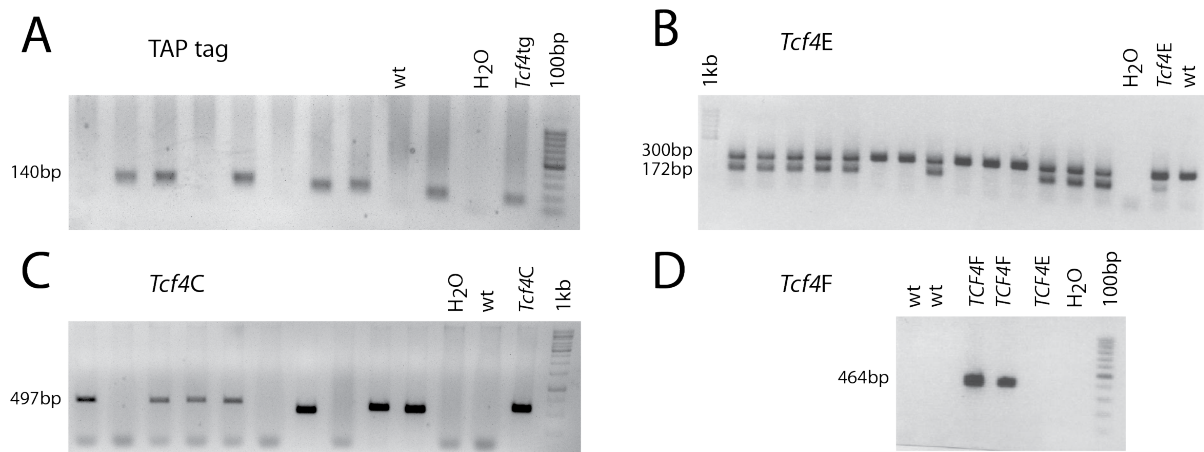
Figure 3.6: Genotyping PCR electrophoresis. Products of genotyping PCRs were separated by electrophoresis in agarose gels and visualised using ethidium bromide or GelRed under UV light. Photographs show representative genotyping gels for: **A)** TAP tag, **B)** *Tcf4*E (172 bp) and wt allele (300 bp), **C)** *Tcf4*C allele, **D)** *Tcf4*F allele.

3.2.2 Tissue isolation and processing

All animal studies have been approved by the appropriate ethics committee of Lower Saxony and were performed in line with the ethical standards in Declaration of Helsinki (1964) and its later amendments. Animals were anesthetised with chloroform and sacrificed by cervical dislocation, unless stated differently. Brain tissues were isolated, frozen on dry ice and stored at $-80\,^{\circ}$C.

Blood treatment and hormone measurements

Blood samples were collected by cardiac puncture from chlorophorm-anesthetised mice.

Serum Blood samples were stored overnight at $4\,^{\circ}$C to coagulate. The next day they were centrifuged 20 min at $1000\times$g at $4\,^{\circ}$C. The supernatant – serum – was transferred to fresh tubes, stored at $4\,^{\circ}$C overnight and used for ELISA.

Plasma Blood was transferred to tubes containing $12\,\mu$l of $50\,$mg/ml EDTA, mixed and centrifuged 15 min in 3000 rpm at $4\,^{\circ}$C. Supernatant was kept on ice until measurement on the same day.

Corticosterone, adrenaline and noradrenaline Mass spectrometric measurements in plasma were performed by Dr rer.nat Frank Streit[2].

β-endorphin Cloud-Clone Corp ELISA Kit (cat.no. CEA806Mu) was used to measure β-endorphin in serum of IR (n=5) and EE (n=6) mice. The test was performed according to the manufacturers instructions. Serum samples were measured in triplicates and standard curve in quadruplicates. Absorbance was detected at the wave length $450\,$nm in BioTek Eon microplate reader with correction for volume differences. The standard curved and β-endorphin concentrations were calculated using BioTek software.

---

[2]Dept. Clinical Chemistry of Göttingen Medical University Clinic (UMG Klinikum), Robert-Koch-Straße 40, 37075 Göttingen

Tissue lysates

To isolate proteins and nucleic acids, tissue samples were homogenized in fresh sucrose buffer (250–300 μl per sample) using the Polytron Hand homogenizer. 100 μl of the lysate was transferred to a tube containing 600 μl RLT buffer (Qiagen), mixed and kept at room temperature until they were stored at −80 °C for RNA analysis. The rest of the lysate, used for protein analysis, was kept on ice. Unless transmembrane proteins were analysed, the protein lysates were centrifuged 5 min at 13000 rpm and 4 °C. Supernatant was transferred to fresh tubes. Protein concentration was measured in 1:5 dilutions in sucrose buffer, using the Biorad kit. BSA dilutions in sucrose buffer were used as a standard curve. Proteins were then appropriately diluted with water to obtain equal concentrations between the samples. Finally the diluted proteins were mixed with 4×NuPage loading buffer and 10×DTT and incubated 10 min at 70 °C. Undiluted proteins were stored at −80 °C and proteins in sample buffer were stored at −20 °C.

3.2.3 RNA analysis

RT-qPCR

The procedure of reverse transcription quantivative polymerase chain reaction (RT-qPCR) involved: 1) tissue homogenization (see section 3.2.2 above); 2) RNA purification; 3) RNA precipitation (optional); 4) complementary DNA (cDNA) synthesis; 5) quantitative PCR.

RNA purification RNA was purified with the RNeasy kit (Qiagen). All steps were performed at room temperature and filtered tips were used during the whole procedure. Samples stored in RLT buffer were thawed at 37 °C , mixed with 700 μl of 70% ethanol and immediately loaded on the columns provided in the kit. Columns were centrifuged at 1 min at 13000 rpm and the flow through as discarded. Next, 500 μl of RW1 buffer was loaded and centrifugation was repeated. Then 500 μl of RPE buffer was loaded, and columns were centrifuged — this step was repeated once. The flow through was discarded and columns were centrifuged again 2 min at 13000 rpm to dry. Finally the columns were inserted into fresh tubes, 50–100 μl of RNAse-free water was loaded and columns were centrifuged 1 min at 13000 rpm. To increase the yield the flow-through was reloaded and on the column and centrifugation was repeated. From that step RNA samples were kept on ice and stored at −80 °C. Concentration and quality of RNA was measured in 2100 Bioanalyzer (Agilent) using Agilent RNA 6000 Nano Kit. Only good quality samples (RIN=8 or higher) were included in further experiments.

In case of dorsal root ganglions (DRGs), a fat-rich tissue, RNA was obtained by homogenization in 1ml Trizol at room temperature, adding 200 μl chlorophorm, vortexing 15 s, incubating 3 min at room temperature and centrifuging 15 min at 13000 rpm and 4 °C. 400–500 μl of the upper, aqueous phase was transferred to 600 μl of 70% ethanol, vortexed 15 s and loaded on RNeasy Mini Kit columns (Qiagen). Next series of RW1 and RPE washes were done as described earlier. RNA was eluted in 60 μl water.

RNA precipitation Desired amount of RNA (e.g. 1 μg) was adjusted with water to the volume of 50 μl . 2 μl of Pellet Paint (Millipore, cat.no. 70748-3) was added to the sample and votexed. Next 25 μl of 7.5 M ammonium acetate was added and vortexed, followed by mixing the sample with 180 of ethanol. Samples were centrifuged 15 min at 13000 rpm. Supernatant was removed, pellet was washed with 70% ethanol and air dried. RNA was resuspended in 4 μl of water for generation of cDNA or in 2 μl of freshly diluted 2 pmol/ μl T7-B-Mix primer for Illumina sequencing. Samples were kept 10 min on ice to dissolve.

cDNA synthesis cDNA was synthesized using SuperScript III First-Strand Synthesis System for RT-PCR (Invitrogen, cat.no. 18080-051). 400–600 ng RNA was used for each 10.5 μl reaction. 4 μl of RNA was transferred into a PCR tube containing 1 μl of 0.6 pmol/μl dT-mix primer (ID 9578) and 1 μl of 120 pmol/μl N9 random primer (ID 4542) and the mix was incubated 10 min at 70 °C. Next, the tubes were put on ice and to each reaction 2 μl of 5×1st strand buffer, 1 μl 0.1 M DTT, 0.5 μl deoxynucleotides (dNTPs) (10 mM each) and 1 μl of superscript III reverse transcriptase (200 U/μl) were added. The tubes were incubated in the thermocycler 10 min at 25 °C , 45 min at 50 °C and 45 min at 55 °C. Afterwards cDNA was diluted with water and immediately used for qPCR or stored at −80 °C.

RT-qPCR The master mix and standard RT-qPCR program are shown in Tab. 3.5. 4 μl cDNA (typically 1:80 or 1:100 dilution in water) was used as a template. Samples were amplified in triplicates or quadruplicates and detected in LightCycler 480 (384-well plates) or 7500 Fast Real-Time-PCR System (96-well plates). *Ct* values and melting curves were obtained using the software provided. Data were normalized to housekeeping genes (*Cyc1* and *Rpl13*) and expressed in reference to the mean of wt samples (or mean of wt exons 1–2 in case of comparing different *Tcf4* exons to each other). It was done according to the formula:

$$\varepsilon = \frac{1}{E^{\Delta Ct}} \qquad\qquad \varepsilon' = \frac{\varepsilon}{\bar{\varepsilon}_{\text{wt}}}$$

where ε is expression normalized to mean of housekeepers, ε' is expression relative to wt, $\bar{\varepsilon}_{\text{wt}}$ is the mean normalized expression in wt group, E is the efficiency of qPCR reaction and ΔCt is the difference between Ct of a replicate and mean Ct of housekeepers for this sample-10. Efficiency was determined to compare different *Tcf4* exons. To determine efficiency, qPCR reactions were run with 5 serial logarithmic cDNA dilutions measured in triplicates on a single plate. The slope of the E curve was calculated in Excell2010 using a formula:

$$E = 10^{\frac{-1}{a}}$$

where E is the efficiency and a is the slope of the efficiency curve. Obtained E values and primer sequences are shown in Table 3.6. In other cases a typical E value 1.96 was used.

Table 3.5: Standard RT-qPCR

(a)	
Stardard RT-qPCR program	
50 °C	2 min
95 °C	10 min
95 °C	15 s
60 °C	1 min

40× (applies to the 95 °C 15 s and 60 °C 1 min steps)

(b)	
Master mix	
cDNA	4 μl
primer fwd	0.1 μl
primer rev	0.1 μl
2×SYBR	5 μl
H$_2$O	1 μl
	10 μl

Table 3.6: Primers used for RT-qPCR. In-house IDs are indicated columns *fwd ID* and *rev ID* for forwards and reverse primers respectively. Efficiency of qPCR reactions is indicated in the column *E*. Primers for genes marked with a star (*) were designed without intron spanning. Genes marked in bold are the housekeepers used for reference.

Gene	fwd ID	fwd 5'– 3' sequence	rev ID	rev 5'– 3' sequence	*E*
Actb	11280	ACGGCCAGGTCATCACTATTG	11281	AGGAAGGCTGGAAAAGAGCC	
Adora2a	18619	GGTCCTCACGCAGAGTTCC	18620	TCACCAAGCCATTGTACCG	
Atp5b	10568	GGCACAATGCAGGAAAGG	10569	TCAGCAGGCACATAGATAGCC	
*Avp**	33703	CTACGCTCTCCGCTTGTTTC	33704	GGGCAGTTCTGGAAGTAGCA	
Bc1	31920	GTTGGGGATTTAGCTCAGTGG	31921	AGGTTGTGTGTGCCAGTTACC	
Bdnf	10659	AATGGGAGGGGTAGATTTCTG	10661	CGCTTTATCAACCAGAATGGA	
Cyc1	10572	CAGAGCATGACCATCGAAAA	10573	CACTTATGCCGCTTCATGG	
Fos	8879	GAATGGTGAAGACCGTGTCA	8892	TCTTCCTCTTCAGGAGATAGCTG	
Npyr1	28528	TCACAGGCTGTCTTACACGACT	28529	TTTCTCCTTTTCAAGCGAATG	
*Oxt**	33701	CACCTACAGCGGATCTCAGAC	33702	CGAGGTCAGAGCCAGTAAGC	
P2ry1	33707	GCAGTCCAGTCTTTGGCTAGA	33708	AGTTTCAACCTTTCCATACCACA	
Penk	21048	CCCAGGCGACATCAATTT	21049	TCTCCCAGATTTTGAAAGAAGG	
Plxna1	33753	CTCAGATGTGCGCCATACC	33754	TTAATCACATTCACCCAGAAGC	
Rpl13	10574	ATCCTCCACCCTATGACAA	10575	GCCCCAGGTAAGCAAACTT	
Tcf4 ex1-2	33456	CATATTTGTGGCCATTGAAGG	25642	GTCCCTAAGGCAGCCATTC	1.95
Tcf4 ex5-6	31143	GGATCTTGGGTCACATGACAA	31144	GCAACCCTGAACGTTTTCTC	1.93
Tcf4 ex7-9	33466	GTATTCAAGCAATAATGCCCG	33467	GGCGAGTCCCTGTTGTAGTC	1.92
Tcf4 ex9-10	3205	CCTAGCTCCTTCTTCATGCA	3200	GCTGATTCATCCCGCTGGAG	1.98
Tcf4 ex15-16	3207	CAGGGTACGGAACTAGTCTT	3202	GAGAGAATGGCTGCCTCTCA	1.76
Tcf4 ex18-19	8756	CTGGAGCAGCAAGTTCGAG	8757	TTCTCTTCCTCCCTTCTTTTCA	2
Top3b	33751	GGTCGCTTTTCCAACGAG	33752	AGACCAGAACAGCAGCAAT	
Vgf	33705	CGACCCTCCTCTCCACCT	33706	CCCAACCCCTGGATCAGTA	

Illumina sequencing

Preparation of RNA samples for Illumina sequencing was done according to the protocol described in [186] and performed by Dr Elena Ciirdaeva[3]. In brief, double-stranded cDNA was synthesized and used for antisense RNA (aRNA) generation. Based on aRNA, another round of cDNA amplification was performed and Illumina adaptors were added by PCR. Such prepared sample library were sent to the Max-Planck Genome Centre in Cologne, Germany and single-end sequencing was performed in Illumina Sequencer HiSeq2500 (type TruSeq RNA) with Phix control and 20 000 000 required reads. All sequencing data analyses were carried out by Nirmal Kannaiyan[4]. Reads were barcode sorted, quality analyzed and mapped to to UCSC Mm10 reference genome using Tophat1 [187], which allows for split mapping against splice junctions. Expression abundance estimates and differential gene expression analysis were computed using Cufflinks [188]. Gene set enrichment analysis (GSEA) [189,190] was performed using the gene expression values using the GO gene sets. This pipeline of analysis was performed using a local installation of GenePattern genome analysis platform [191]. Gene set size filters were set to minimum of 5 and maximum of 500 and false discovery rate (FDR) was set to 25%.

---

[3]Dept. Neurogenetics, Max-Planck-Institute of Experimental Medicine, Göttingen, Germany

[4]Department of Psychiatry and Psychotherapy, Ludwig Maximilian University of Munich, Germany

3.2.4 Synaptosome isolation and proteome analysis

Synaptosomes were isolated according to a modified protocol from Gray & Whittaker[192,193] in cooperation with Dr Magdalena M. Brzózka[5] and Dr Christoph Biesemann[6]. All centrifugation steps were done at 4 °C and samples were kept on ice between steps. 4 weeks old male TMEBBl6 mice (*Tcf4*tg n=4, wt n=4) were sacrificed and PFC (600–900 mg) was isolated, washed with ice-cold PBS and homogenized 10 times by 12–15 up and down strokes in 900 μl of ice-cold buffer A suplemented with phosphatase inhibitor coctails I and II (Sigma, 1 μl per 100 μl buffer). Left PFC was pooled within genotypes in 900 μl buffer A and right PFC was treated individually for each animal. Homogenate was centrifuged at 3200 rpm for 10 min. Supernatant (S1-nuclei) was transferred to a different tube using a 200 μl pipette with a cut tip and kept on ice. Pellet (P1-cell debris) was resuspended in 800 μl of buffer A (without phosphatase inhibitors) and centrifuged at 3200 rpm for 10 min. Supernatant S1' was combined with S1 and 100 μl S1 was saved for further analysis. Pellet (P1) was resuspended in 800 μl buffer A and 100 μl was saved for further analysis. The supernatant S1 was centrifuged at 11500 rpm for 15 min and 100 μl of supernatant (S2) was saved. Pellet (P2) was carefully resuspended with a pipette in 1 ml of homogenization buffer (0.32 M sucrose) and pipetted on top of a discontinuous sucrose density gradient (from bottom: 4 ml 1.2 M, 4 ml 1 M and 3 ml 0.8 M) and centrifuged in and Ultracentrifuge with rotor Sv40Ti 2 h at 25000 rpm. The synaptosomal fraction, obtained from 1.2–1 M interphase, was diluted 1:1 in water (water added drop by drop with mixing) and centrifuged 20 min at 30000 rpm with rotor TLA 100.3 in polyallometer centrifuging tubes 13 × 51 mm. The pellet (S4, synaptosomes) was resuspended in 10 μl water for proteomic or in 50 μl for western blotting and stored at −20 °C.

Proteome analysis of cytosolic fractions (S1) and synaptosomes (S4) and the western blots were performed in collaboration with Dr Daniel Martins-de-Souza[7], according to his established protocol[194]. In brief: samples (100 μg total protein) underwent isotope-coded protein labeling (ICPL)[195] and 50 μg proteins were prefractionated by on a 12% SDS-PAGE minigel. Shotgun mass spectrometry was performed and proteins were identified using an in-house version of MASCOT Distiller 2.2.3 software (Matrix Sciences, London, UK) and searched against a decoy Uniprot mouse protein database (release 2012_06). Proteins were considered as differentially expressed when they had more than 2 × fold change or 1.5–2 × when quantified by minimum 5 peptides. Then, proteins were divided to classes based on Human Protein Reference Database `http://www.hprd.org`[196].
Western blot analysis was done using 10 μl of protein extracts run individually on 12% SDS-PAGE minigels and transferred on PVDF membranes. Proteins were detected using primary antibodies against CamKII, VAMP1, VAMP2 and HOMER1 (SySy) followed by anti-c-MYC-peroxidase antibody (GE Healthcare, Uppsala, Sweden), incubated with ECL solutions and scanned in a Gel Doc[TM] XR+ System (BioRad).

3.2.5 Western blotting

Samples (prepared as in section 3.2.2 on page 30) and the protein ladder were loaded on a NuPAGE Novex 4–12% Bis-Tris Protein Gels and run in the MES buffer at constant voltage 200 V. Next, the proteins were transferred on a PVDF membrane in the NuPAGE transfer buffer at 30 V for 2.5–3.5 h. Afterwards the membrane was rinsed with TBS-T, blocked in 5% milk in TBS-T for

---

[5]Dept. Neurogenetics, Max Planck Institute of Experimental Medicine, Göttingen, Germany

[6]Dept. Molecular Neurobiology, Max Planck Institute of Experimental Medicine, Göttingen, Germany

[7]Department of Psychiatry, Ludwig Maximilians Universität, Munich, Germany

30 min and incubated with the primary antibody overnight at 4 °C. The next day the membrane was washed 3–5 times with TBS-T (5–10 min each wash), incubated for 1 h at room temperature with the secondary antibody, washed 5–6 times with TBS-T. Membranes were incubated 30 s with ECL solutions and imaged in the Intas developer.

3.3 Morphological analyses

3.3.1 Electron microscopy

Sample preparation Samples were prepared by Torben Ruhwedel[8]. Mice were anaesthetized with avertin (SigmaAldrich,) and perfused with 15 ml of Hanks balanced salt solution (HBSS, PAA laboratories, Pasching, Austria) and then by fixative as described in[197] using a Heidolph PD5201 Peristaltic Pump. The brain tissue was dissected and 200 μm coronal sections were cut with a Leica VT1200S Vibratom (Leica Microsystems, Wetzlar). The medial orbitofrontal cortex (MO), anterior cingulate cortex (ACC) and cortex transversal areas (Fig. 4.3A–C) were punched out of the section by using a 2 mm Harris Uni-core Punch. After postfixation with 2% OsO_4 (Science Services, Munich, Germany) and dehydration with ethanol and propylenoxid (automated system EMTP Leica Microsystems, Wetzlar) samples were embedded in Epon (Serva) and cut in the microtome (Ultracut S, Leica). Semi-thin (500 nm) and ultra-thin (50 nm) sections were prepared using diamond knifes (Histo 45°and Ultra 45°, Diatome Biel CH). Semi-thin sections were collected onto a glass slide and dried on a 60 °C hot plate to verify the area of interest by using a Leica Dialux 20 light-microscope. Ultra-thin sections were placed on 100 mesh hexagonal copper Grids (Gilder Grids Ltd. Grantham UK) coated with "Formvar" (Plano Wetzlar) and stained with Uranylacetat (SPI-Chem West Chester,USA) and Lead citrate (Merck, Darmstadt)(REYNOLDS, 1963). Ultra-thin sections were analyzed using a Zeiss EM900 Elektron-Microscop (Zeiss, Oberkochen, Germany) with the 3000×, 12000× and 30000× magnification. Digital pictures were taken by the wide-angle dual speed 2K-CCD-Camera (TRS, Moorenweis, Germany). Photos of of the transverse cortical sections were taken by Bogusława Sadowska.

Image analysis Pictures of MO and ACC regions were taken under 12000 × and 30000 × magnifications. Total number of synapses, perforated synapses and mitochondria was counted within 20 randomly taken images under 12000 × magnification. The synapse structure was analysed under 30000 × magnification with 50 synapses per animal. The average length and width of the active zones, number of synaptic vesicles per synapse and the synaptic vesicle cluster density (number of vesicles divided by the area they occupy) were calculated separately for symmetric and asymmetric synapses. Additionally the average distance of the vesicles from the active zone was measured using the Concentric Circles plugin for ImageJ software: 5 differently sized circles with the centre in the middle of the active zone were overlaid on the synapse images. Circles divided the synapse area into 5 zones, each 100 nm wide. Zone 6 is the area outside of the biggest circle, more than 500 nm away from the active zone. The number of vesicles in each zone was counted for each synapse and the averages were calculated. 30000 × pictures were analysed for 6 wt animals and 4 *Tcf4*tg animals and 12000 × pictures were analysed for n=6 per group.

---

[8]Electron Microscopy facility, Max Planck Institute of Experimental Medicine, Göttingen, Germany

3.3.2 High-resolution microscopy via STED nanoscopy

The stimulated emission depletion (STED) nanoscopy experiment was performed in collaboration with Dr Payam Dibay[9]. To analyse spine morphology, TMEB mice were bred to TYFB mice that express EYFP in postnatal forebrain under *Thy1.2* promoter[179,198]. TMEBBl6×TYFB mice were aesthetised by intraperitoneal injections of pentobarbital (120 mg per kg body weight) and Buprenorphine (2 µg) and perfused with 4 % PFA in 0.1 M phosphate buffer (pH 7.4). After an overnight postifxation in 4 % PFA at 4 °C, the brains cut on Vibratome into 70 µm sections. Images of spine morphology were taken in ACC using a home-built STED microscope. Recording of image stacks x-y-z (18 µm × 18 µm × 3 µm) was performed with a STED resolution around 60 nm and pixel dwell time of 10 µs. Images of dendrites parallel to the slice surface were processed using the "Simple Neurite Tracer" function of ImageJ or Fiji software.

TMEBBl6×TYFB male mice were analysed at the age of 4 weeks (wt n=5, *Tcf4*tg n=7; 19 dendrites per mouse) and 12 weeks housed under control condition (wt n=4, *Tcf4*tg n=4; 15 dendrites per mouse) or subjected to social defeat (wt n=7, *Tcf4*tg n=11; 12 dendrites per mouse).

3.4 Electrophysiology

LTP and LTD in hippocampus *Tcf4*tg and wt TMEBBl6 animals were sacrificed at the age of 4–5 weeks and LTP and LTD were measured in transverse hippocampal slices. Schaffer collateral afferents were stimulated and field excitatory postsynaptic potentialss (fEPSPs) were measured in the stratum radiatum of CA1 with a GABA inhibitor. e-LTP was induced by 1 s of high frequency stimulation and LTD by applying low frequency stimulation for 15 min. fEPSP slopes were expressed relative to normalized baseline. For Input-output curves mean fEPSPs from three consecutive responses were used. The data were analysed using t-test. The experiment was performed in collaboration with Dr Jeong Seop Rhee[10].

---

[9]Dept. Neurogenetics, Max Planck Institute of Experimental Medicine, Göttingen, Germany
[10]Dept. Molecular Neurobiology, Max Planck Institute of Experimental Medicine, Göttingen, Germany

Results

To assess *Tcf4* functions in adult murine brain, we combined gain-of-function (*Tcf4* overexpression in *Tcf4*tg mice) and loss-of-function approach (*Tcf4* knockout line *Tcf4*C). To exclude the developmental aspect of *Tcf4* function, we analysed *Tcf4*tg mice that overexpress *Tcf4* in neurons of postnatal brain, under *Thy1.2* promoter[57]. Due to the big gene size (343.5 kb), the mice overexpressed not the full *Tcf4*, but a tagged open reading frame. In all experiments with *Tcf4*tg mice, we used animals on C57 × FVB background, since hybrid strains are considered as healthier than inbred strains[180]. We performed analyses on molecular, cellular as well as behavioural level. The knockout strain was generated from the *Tcf4* Eucomm line *Tcf4*E on C57 background. Therefore all analysed *Tcf4*C animals were on C57 background. In all experiments described below, we used *Tcf4*tg or *Tcf4*C male mice. Unless stated differently, in molecular and cellular experiments, we analysed them at the age of 4 weeks, because the postweaning period is a critical developmental window in rodents[144]. Behavioural experiments were performed on older animals.

4.1 Molecular and cellular analyses in *Tcf4*tg mice

4.1.1 Electrophysiology: enhanced LTD in *Tcf4*tg mice

Since *Tcf4*tg mice exhibit cognitive deficits[57], we tested they show any alterations in synaptic plasticity. To do this, we performed electrophysiological recordings in collaboration with Dr Jeong Seop Rhee[1]. We used 4–5 weeks old animals. Early phase LTP (e-LTP) and LTD were measured in hippocampal slices, in the CA1 region upon stimulation of Schaffer collaterals (28 *Tcf4*tg and 32 wt animals were used for the e-LTP experiment and 24 *Tcf4*tg and 15 wt were used for the LTD experiment). Overall e-LTP was unaltered, but during the first 15 min after stimulation it tended to be higher in the *Tcf4*tg mice (Fig. 4.1A). LTD was significantly enhanced in the *Tcf4*tg animals (p<0.001)(Fig. 4.1B). Finally, we checked the input/output curves, which were comparable between the genotypes (Fig. 4.1C). This suggests that *Tcf4* overexpression did not change basal receptor levels in the hippocampal synapses.

---

[1]Dept. Molecular Neurobiology, Max Planck Institute of Experimental Medicine, Göttingen, Germany
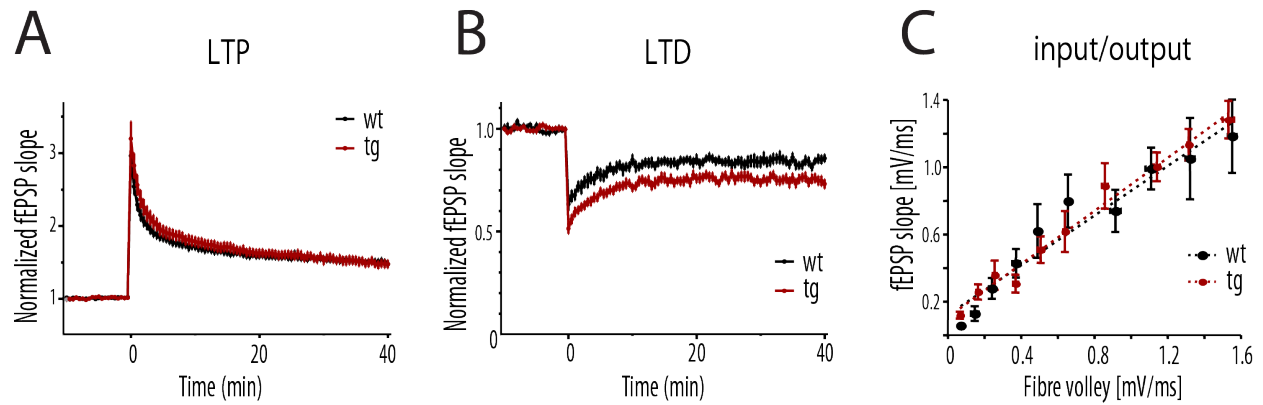
Figure 4.1: LTP and LTD in hippocampal CA1 of *Tcf4*tg mice. A) Early phase LTP (first 40 min after stimulation of Schaffer collateral) was unchanged in *Tcf4*tg mice (*Tcf4*tg n=28, wt n=32). However, during the first 15 min *Tcf4*tg mice showed an increase of LTP. **B)** LTD was enhanced in *Tcf4*tg mice compared to wt (p<0.001)(*Tcf4*tg n=24, wt n=15). **C)** The input/output curves are unaltered in *Tcf4*tg mice. **Abbreviations:** long-term potentiation (LTP), long-term depression (LTD), field excitatory postsynaptic potentials (fEPSP)

4.1.2 STED: increased spine frequency in *Tcf4*tg mice

Spine morphology, frequency and density were analysed with STED microscopy in PFC of 4 weeks old *Tcf4*tg and wt male mice. Frequency of five types of spines were assessed: filipodium/stripe, stubby/stump, mushroom/racket, cup/sickle and branch. *Tcf4*tg mice displayed no obvious changes in spine morphology (Fig.4.2A), but increased overall number (p=0.0055, two-way ANOVA) and frequency (p=0.0303, Mann-Whitney test) of spines (Fig.4.2B,G). However, no alterations in spine morphology and frequency were observed in 12 weeks old *Tcf4*tg mice neither in control condition nor after social defeat (Fig.4.2C–F).

4.1.3 Electron microscopy: unchanged synapse morphology in *Tcf4*tg mice

To confirm the increased number of spines observed in STED microscopy (see: section refsec:spines-results) and myelin alterations in RNA sequencing (RNAseq), we analysed 4 weeks old *Tcf4*tg (n=5) and wt (n=5) male mice with the use of electron microscopy. We looked at several parameters: number of excitatory synapses, percentage of perforated synapses, average length and width of active zones, number of synaptic vesicles (SVs) per synapse, synaptic vesicle cluster density, number of mitochondria, number of myelinated axons and myelin thickness (Fig. 4.3). Hippocampal knockdown of *mir137*, an upstream regulator of *Tcf4*[34], increases distances of SVs from the active zone (personal communication with Sandra Siegert[2]). Therefore, we analysed the SVs distances in *Tcf4*tg mice, by using the *concentric circles* function in ImageJ software. We observed no significant difference in any of the parameters (Fig. 4.4).

---

[2]Dept. of Brain and Cognitive Sciences, Massachusetts Institute of Technology, Cambridge, UK
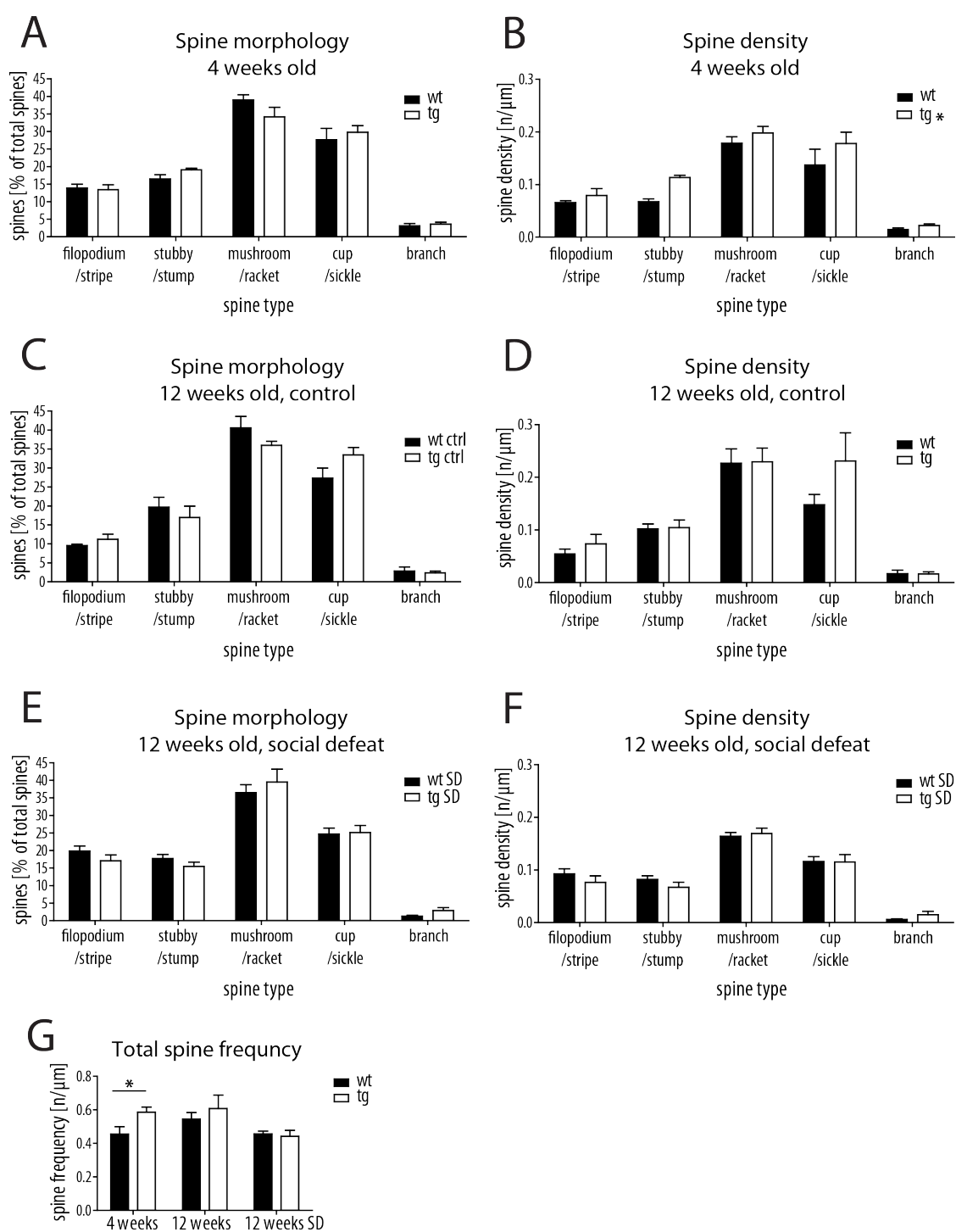
Figure 4.2: Spine analysis in *Tcf4*tg mice. Spine density (mean spine number per dendrite) and morphology in PFC were analysed using STED microscopy in collaboration with Dr. Payam Dibaj. Animals at the age of 4 weeks (wt n=5, *Tcf4*tg n=7) and 12 weeks under control (wt n=4, *Tcf4*tg n=4) or social defeat conditions (wt n=7, *Tcf4*tg n=11) were used. **A)** Spine morphology at 4 weeks. **B)** Spine density at 4 weeks was increased in *Tcf4*tg mice (p=0.0055, two-way ANOVA). **C)** Spine morphology at 12 weeks in control mice. **D)** Spine density at 12 weeks in control mice. **E)** Spine morphology at 12 weeks. **F)** Spine density 12 weeks after SD stress. **G)** Total spine frequency was increased in *Tcf4*tg mice at the age of 4 weeks (p=0.0303, Mann-Whitney test) but not at 12 weeks neither in control nor in SD stress group.
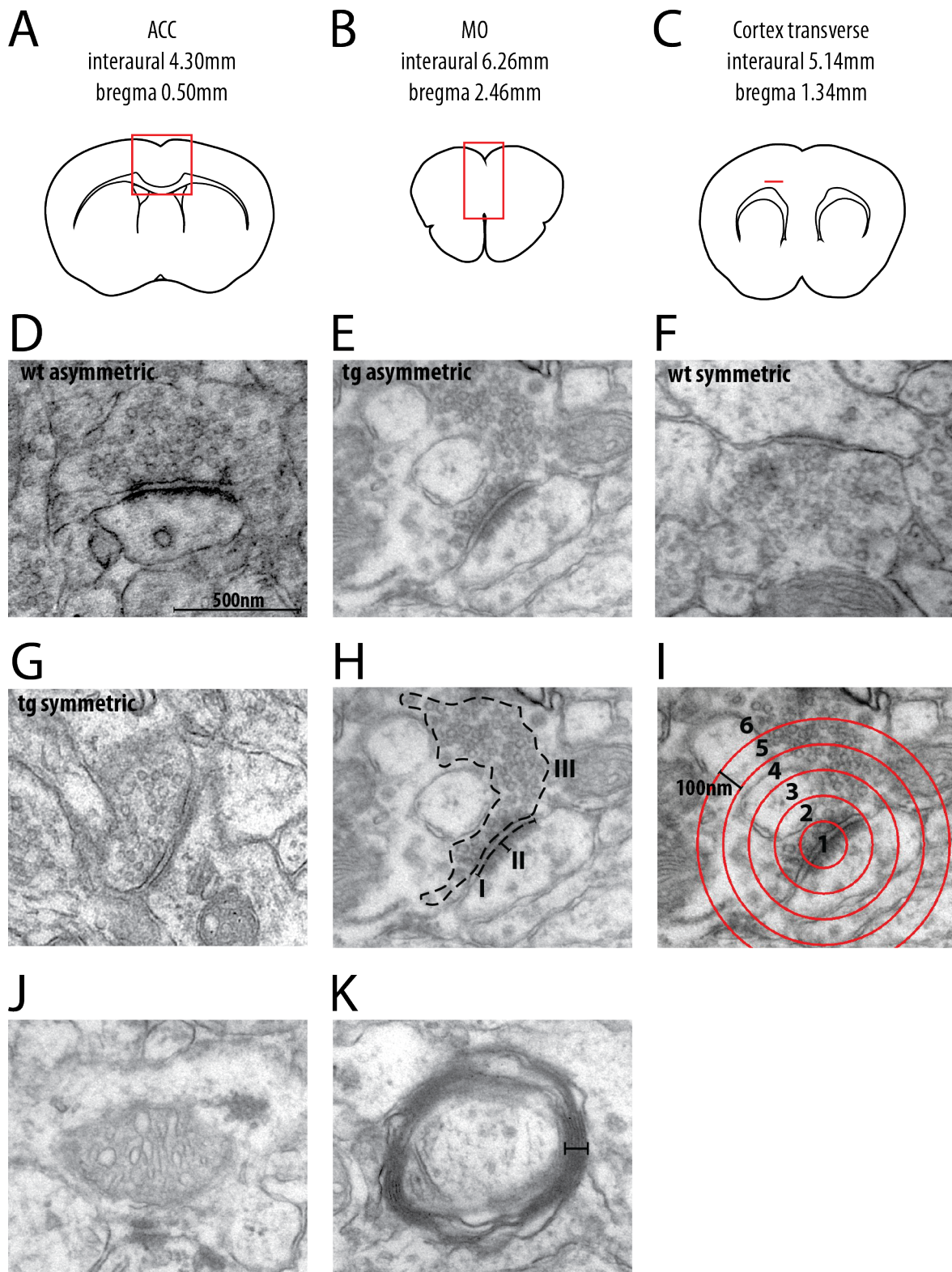
Figure 4.3: Electron microscopy. Synapse morphology in *Tcf4*tg mice was examined in: **A)** anterior cingulate cortex (ACC) and **B)** medial orbitofrontal cortex (MO). **C)** Myelin abundance was analysed in cortical transverse sections. **D–E)** Exemplary asymmetric synapses in a wt (n=5) and *Tcf4*tg animals (n=5). **F–G)** Exemplary symmetric synapses in a wt and *Tcf4*tg animal. **H)** The length (I) and width (II) of synaptic active zone and area occupied by synaptic vesicles (III) were measured. **I)** Distances of synaptic vesicles from the active zone were measured by counting numbers of synaptic vesicles in each of the 6 zones marked by the red concentric circles. **J)** Numbers of mitochondria were counted in ACC and MO. Picture shows an exemplary mitochondrion. **K)** Myelin thickness was measured in the cortical transverse region.
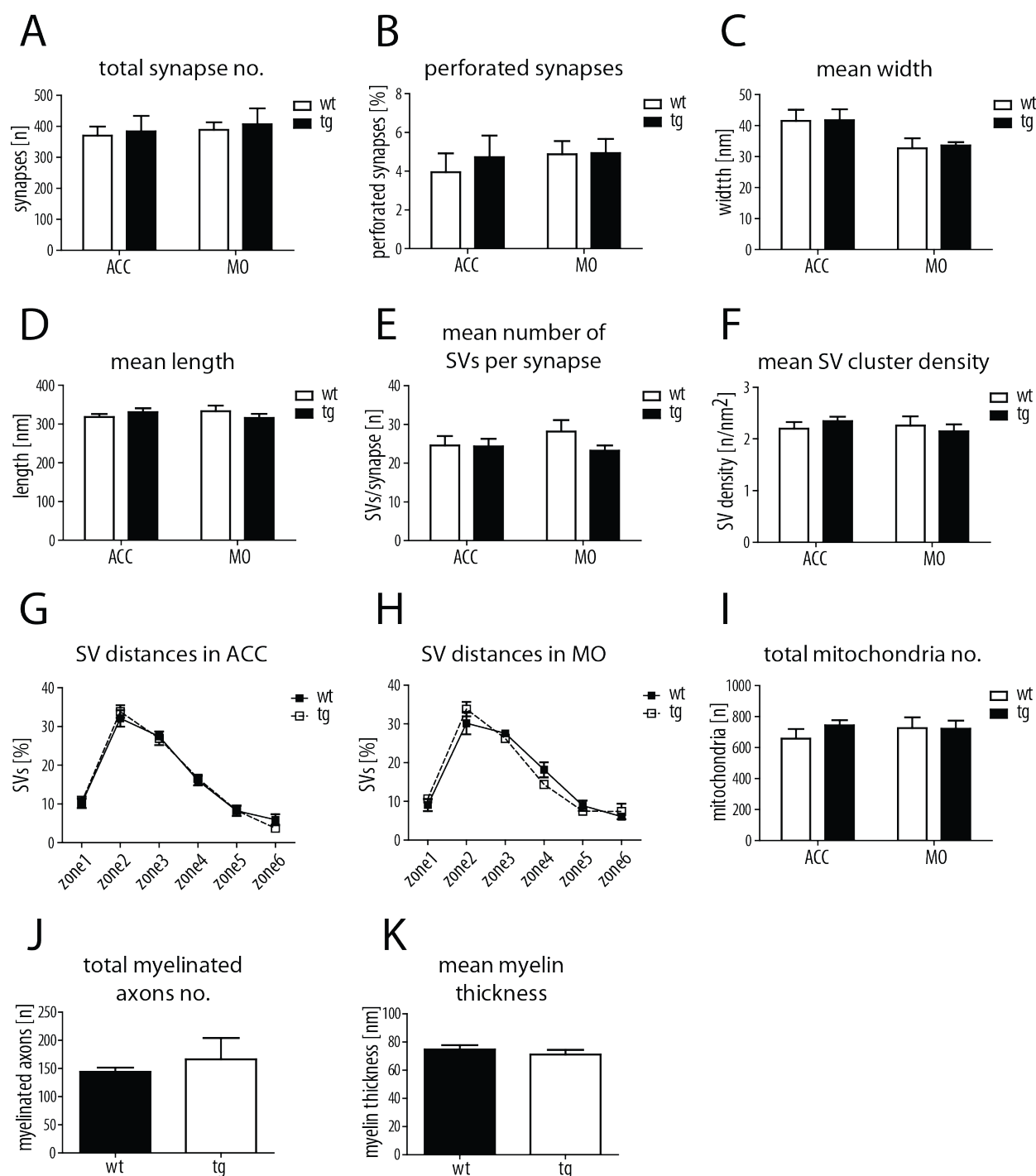
Figure 4.4: Synapse morphology in *Tcf4*tg mice. A) Total number of synapses within 20 random pictures. **B)** Percent of perforated synapses within all counted synapses. Because the numbers of symmetric synapses were too low, further analysis was done only on asymmetric synapses. **C)** Mean width **D)** and length of the active zones. **E)** Mean number of synaptic vesicles (SVs) per synapse. **F)** Mean SVs cluster density. **G)** Mean distances of SVs from the active zone in anterior cingulate cortex (ACC) and in **H)** medial orbitofrontal cortex (MO). Zones 1–5 represent distances within 100–500 nm from the active zone; zone 6 contains all SVs that are more than 500 nm away from the active zone. **I)** Total number of mitochondria counted within 20 random pictures. **J)** Total number of myelinated axons in the transversal coronal section within 20 random pictures. **K)** Mean myelin thickness in transverse coronal sections.

4.1.4 RNA sequencing in *Tcf4*tg mice

We performed RNAseq of total mRNA isolated from PFC and hippocampal tissue of *Tcf4*tg and wt mice at the age of 4 weeks. The samples contained both male and female mice with a gender bias, therefore sex-related genes *Xist* (inactive X specific transcripts), *Uty* (ubiquitously transcribed tetratricopeptide repeat gene, Y chromosome), *Ddx3y* (DEAD (Asp-Glu-Ala-Asp) box polypeptide 3, Y-linked) and *Eif2s3y* (eukaryotic translation initiation factor 2, subunit 3, structural gene Y-linked) were not considered as interesting.

In PFC of *Tcf4*tg mice only few genes were upregulated (Table 4.1), e.g. *Mov10* (Moloney Leukemia Virus 10, Homolog (Mouse)), and we observed more genes that were downregulated, including *Adora2a* (Adenosine receptor 2A), *Penk* (Proenkephalin), *Tac1* (Tachykinin 1), *Pde10a* (Phosphodiesterase 10a) and *Drd1a* (Dopamin receptor 1A), *Foxp2* (Forkhead box protein P2) and *Mag* (Myelin-associated glycoprotein).

Analysis of the hippocampal transcriptome (Table 4.2) revealed upregulation of *Top3b* (topoisomerase (DNA) III beta), *Bc1* (brain cytoplasmic RNA 1) and *Plxna1* (Plexin-A1) while *Ttr* (transthyretin) and *Mov10* (Moloney Leukemia Virus 10, Homolog (Mouse)) were downregulated.

Table 4.1: RNAseq: Genes deregulated in PFC of *Tcf4*tg mice. In 4 weeks old *Tcf4*tg mice, *Mov10* was upregulated and *Adora2a*, *Penk*, *Tac1*, *Pde10a* and *Drd1a* were among the most downregulated genes.

Gene	log2 fold change)	p-value	q-value
upregulated			
Uty	2.356857478	0.001467616	1
Ddx3y	1.723449998	0.003841885	1
Eif2s3y	0.760359651	0.01139759	1
Zfp825	0.505726137	0.119585625	1
Smc1b	0.505127544	0.552853233	1
Mov10	0.455759192	0.122597818	1
downregulated			
Erdr1	-0.453932657	0.08753336	1
Sez6	-0.457338401	0.003414727	1
Nnat	-0.457694739	0.003194241	1
Tbc1d16	-0.461461299	0.000807181	0.994823224
Gm606	-0.465440907	0.00038319	0.708402521
Pkn2	-0.468443581	0.006862101	1
Unc13c	-0.468956547	0.047570356	1
Spock3	-0.469166189	0.011697411	1
Mag	-0.472136197	0.011366762	1
Nrsn2	-0.480792086	0.000790263	0.994823224
Kcna5	-0.486999425	0.000235968	0.484704209
Rxrg	-0.490025564	0.013795055	1
Slc32a1	-0.491767384	0.001923278	1
Eif2s3x	-0.519751609	0.000494012	0.761067362
Gad2	-0.525564658	0.031027759	1

Continued on next page

Table 4.1 – *Continued from previous page*

Gene	log2 fold change)	p-value	q-value
Foxp2	-0.536091408	0.010973279	1
Musk	-0.536407446	3.15E-05	0.13148404
Tmem158	-0.546487678	0.004270464	1
Habp2	-0.56130833	0.007219107	1
Inf2	-0.566855678	0.006885522	1
Dgkb	-0.567402036	0.000772139	0.994823224
Htr2c	-0.580735425	0.003939147	1
Rarb	-0.583095508	9.75E-05	0.257547479
Slc25a17	-0.593233112	0.023893995	1
Gnal	-0.624961572	8.63E-07	0.006980159
Rgs2	-0.631042192	1.13E-06	0.006980159
Ddx1	-0.634459242	0.03789148	1
Nexn	-0.635960819	0.001689473	1
Comp	-0.675562054	0.000156554	0.361777556
Pde1b	-0.680827771	0.00610263	1
Rasd2	-0.723349409	0.00223994	1
Pou3f4	-0.746025845	4.42E-05	0.136221867
Klhl13	-0.780688718	3.56E-05	0.13148404
Rasgrp2	-0.855435392	0.001321307	1
Tmem90a	-0.898297515	0.000909174	1
Gng7	-0.992907322	2.49E-07	0.004598419
Tsix	-1.02551036	0.002900251	1
Drd1a	-1.050470631	0.012557658	1
Pde10a	-1.1368682	0.002083819	1
Gpr88	-1.305308987	0.00547236	1
Ppp1r1b	-1.329720023	0.002964721	1
Six3	-1.429692733	0.004368645	1
Tac1	-1.450904913	0.010563382	1
Penk	-1.513621123	0.011187743	1
Adora2a	-1.806484974	0.010113878	1
Xist	-1.97678391	0.000487009	0.761067362

Table 4.2: RNAseq: Genes deregulated in hippocampus of *Tcf4*tg mice. In 4 weeks old *Tcf4*tg mice *Top3b*, *Bc1* and *Plxna1* were among the top upregulated genes and *Ttr* and *Mov10* were downregulated.

Gene	log2 fold change)	p-value	q-value
upregulated			
Uty	2.442874226	0.001315171	1
Ddx3y	1.724531248	0.005048596	1
Eif2s3y	0.792626035	0.011974287	1
Ptpru	0.649270556	0.123836496	1
Hba-a1	0.610615334	0.435888831	1
Slc16a2	0.587998895	0.117722223	1

Continued on next page

Table 4.2 – *Continued from previous page*

Gene	log2 fold change)	p-value	q-value
Hba-a2	0.559955061	0.456840867	1
Beta-s	0.514627276	0.45416861	1
Top3b	0.505075697	0.004112155	1
Bc1	0.499641295	0.002435527	1
Plxna1	0.464333382	0.001436315	1
Hbb-b1	0.452633697	0.477009567	1
Gabra2	0.447062357	0.560010346	1
downregulated			
Mtbp	-0.472120572	0.290811705	1
Sla	-0.474072765	0.000776867	1
Lama2	-0.477137387	0.418796431	1
Hells	-0.492922504	0.02587771	1
Snx9	-0.501069661	0.014061808	1
Tshz3	-0.508746358	0.00319265	1
Vmn2r37	-0.510533543	0.11145069	1
Ptgds	-0.52422796	0.177935037	1
Kremen1	-0.544589284	0.026354096	1
Peg12	-0.550935688	0.052007167	1
Cda	-0.560754252	0.000880105	1
Ttr	-0.587735293	0.342253302	1
Mov10	-0.610776663	0.053019467	1
Zfp414	-0.621446643	0.021644652	1
Ddx51	-0.629219058	1.97E-06	0.036421
Ccdc75	-0.636729247	0.055702478	1
Ppp2r2b	-0.687181646	0.037507286	1
Zfp825	-0.722028253	0.039964472	1
Acaca	-0.725513955	0.030772285	1
Lin7b	-0.77422458	0.041785881	1
Tsix	-0.82256129	0.022262926	1
Zfp248	-0.920663422	0.005238188	1
Slc25a17	-0.955280143	0.000343368	1
1700020D05Rik	-1.010106539	0.047582604	1
Xist	-1.961134529	0.00124231	1

RT-qPCR of candidate genes in *Tcf4*tg mice

To validate the RNAseq results we used an independent cohort of 4 weeks old *Tcf4*tg and wt male mice (n=3 per group). The cDNAs were prepared by Dr Magdalena Brzózka[3] and Nirmal Kannayian[4]. The experiment failed to validate the candidate genes found in sequencing of PFC

---

[3]Department of Psychiatry and Psychotherapy, Ludwig Maximilian University of Munich, Germany
[4]Department of Psychiatry and Psychotherapy, Ludwig Maximilian University of Munich, Germany

and hippocampus (Fig. 4.5A–B). This may be due to the low number of animals or possibly, the RNAseq results were affected by the gender bias, therefore couldn't be replicated in the sex-matched sample used for validation.

Comparison of different housekeeping genes revealed that *Actb* tended to be higher expressed in *Tcf4*tg mice in both PFC and hippocampus. This may be in line with upregulation of cytoskeletal and actin-related proteins in proteomic analysis (see: section 4.1.5).
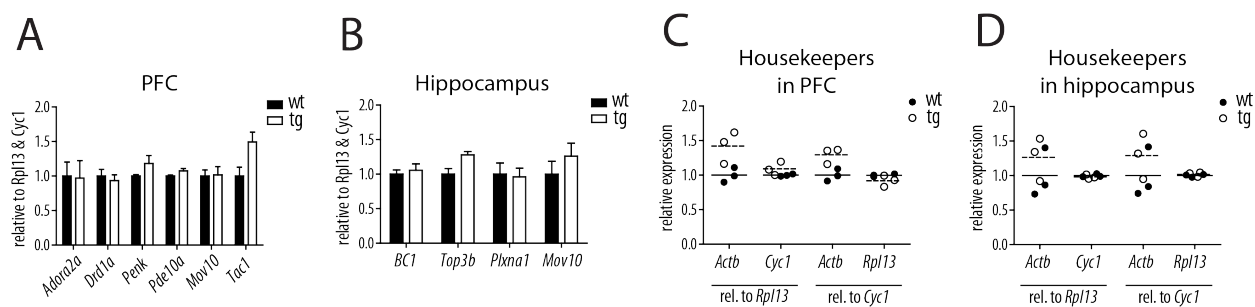
Figure 4.5: RT-qPCR with the RNAseq candidates in *Tcf4*tg mice. Candidate genes from RNAseq were measured by RT-qPCR in 4 weeks old male *Tcf4*tg and wt mice (n=3 per group) in **A)** PFC and **B)** in hippocampus. The experiment failed to confirm deregulation of any of the analysed genes. **C–D)** *Rpl13* and *Cyc1* were used as reference genes. *Actb* was excluded, due to its higher levels in *Tcf4*tg animals.

4.1.5   Proteome analysis in *Tcf4*tg mice

The experiment was performed in collaboration with western blots were performed in cooperation with Dr Magdalena Brzózka[5] and Dr Daniel Martins-de-Souza[6] We analysed protein composition of synaptosomes (containing pre- and postsynapses) and cytosol in PFC of 4 weeks old *Tcf4*tg and wt mice. Several proteins associated with cellular signalling, protein or energy metabolism, transport and cell growth were differentially expressed. In cytosolic fraction of *Tcf4*tg mice, we observed an upregulation of β-tubulins, yet downregulation of cytoskeletal associated proteins. Ribosomal proteins and GTPases were consistently downregulated (see: Table 4.3) and two vesicle-associated membrane proteins, VAMP1 (Synaptobrevin 1) and VAMP2 (Synaptobrevin 2), were upregulated in transgenes 4.72 and 2.69 fold respectively. In synaptosomes, proteins involved in signalling, oxidoreductases, ribosomal subunits, Ser/Thr kinases and GTPases were mainly upregulated (see: Table 4.4 in the Appendix on page 49). Among them we found a postsynaptic density scaffolding protein HOMER1, vesicle-associated VAMP2 (Synaptobrevin 2) and CaMK II alpha (calcium/calmodulin-dependent protein kinase II alpha subunit) upregulated $7.63 \times$, $2.16 \times$ and $1.96 \times$ respectively.

CaMK II alpha, HOMER1, VAMP1 and VAMP2 were validated by western blotting in pooled protein synaptosome or cytosolic protein fractions, as presented in Fig. 4.6. Whole blots are shown in the Appendix in Fig. 7 on page 107.

---

[5]Department of Psychiatry and Psychotherapy, Ludwig Maximilian University of Munich, Germany
[6]Department of Psychiatry, Ludwig Maximilians Universität, Munich, Germany

Table 4.3: Proteomics in cytosol. The "fold change" column shows the ratio of tg to wt (values above 1 indicate upregulation, below 1 downregulation). Upregulated proteins are marked in bold.

Gene	tg/wt	no. pept.	Description	Localisation	Biological process	Molecular class	Molecular function
upregulated							
SNAP91	**3.4977**	**3**	**synaptosomal-associated protein, 91kDa homolog (mouse)**	**Plasma Membrane**	**Cell communication & Signaling**	**Adapter molecule**	**Receptor signaling complex scaffold activity**
EHD3	0.2513	3	EH-domain containing 3	Cytoplasm	Cell communication & Signaling	Cytoskeletal associated protein	Cytoskeletal protein binding
AGAP2	0.2980	2	ArfGAP with GTPase domain, ankyrin repeat and PH domain 2	Nucleus	Cell communication & Signaling	GTPase	GTPase activity
RAC1	0.6192	18	ras-related C3 botulinum toxin substrate 1 (rho family, small GTP binding protein Rac1)	Plasma Membrane	Cell communication & Signaling	GTPase	GTPase activity
RAC3	0.5184	18	ras-related C3 botulinum toxin substrate 3 (rho family, small GTP binding protein Rac3)	Cytoplasm	Cell communication & Signaling	GTPase	GTPase activity
RAP1B	0.3846	7	RAP1B, member of RAS oncogene family	Cytoplasm	Cell communication & Signaling	GTPase	GTPase activity
RAB11B	**1.7120**	**6**	**RAB11B, member RAS oncogene family**	**Cytoplasm**	**Cell communication & Signaling**	**GTPase activating protein**	**GTPase activator activity**
BRSK1	**5.9067**	**7**	**BR serine/threonine kinase 1**	**Cytoplasm**	**Cell communication & Signaling**	**Serine/threonine kinase**	**Protein serine/threonine kinase activity**
CAP2	0.6238	3	CAP, adenylate cyclase-associated protein, 2 (yeast)	Plasma Membrane	Cell communication & Signaling	Unclassified	Molecular function unknown
DAB2IP	**4.2230**	**4**	**DAB2 interacting protein**	**Plasma Membrane**	**Cell communication & Signaling**	**Unclassified**	**Molecular function unknown**
Srcin1	0.3778	6	p130Cas-associated protein OS=Mus musculus GN=P140 PE=1 SV=2	unknown	Cell communication & Signaling	Unclassified	Molecular function unknown
ABI1	0.4274	2	abl-interactor 1	Cytoplasm	Cell growth & maintenance	Adapter molecule	Binding
CDH13	0.4002	2	cadherin 13, H-cadherin (heart)	Plasma Membrane	Cell growth & maintenance	Adhesion molecule	Cell adhesion molecule activity
DSC3	**3.6364**	**2**	**desmocollin 3**	**Plasma Membrane**	**Cell growth & maintenance**	**Adhesion molecule**	**Cell adhesion molecule activity**
ACTN2	0.6361	5	actinin, alpha 2	Nucleus	Cell growth & maintenance	Cytoskeletal associated protein	Cytoskeletal protein binding
ANK2	0.5249	6	ankyrin 2, neuronal	Plasma Membrane	Cell growth & maintenance	Cytoskeletal associated protein	Cytoskeletal protein binding
ARPC4	**2.1580**	**26**	**actin related protein 2/3 complex, subunit 4, 20kDa**	**unknown**	**Cell growth & maintenance**	**Cytoskeletal associated protein**	**Cytoskeletal protein binding**
MAP1B	0.3141	5	microtubule-associated protein 1B	Cytoplasm	Cell growth & maintenance	Cytoskeletal associated protein	Cytoskeletal protein binding
INA	0.6382	9	internexin neuronal intermediate filament protein, alpha	Cytoplasm	Cell growth & maintenance	Cytoskeletal protein	Structural constituent of cytoskeleton
TUBB	**1.5743**	**17**	**tubulin, beta class I**	**Cytoplasm**	**Cell growth & maintenance**	**Cytoskeletal protein**	**Structural constituent of cytoskeleton**
CRYM	0.2895	2	crystallin, mu	Cytoplasm	Cell growth & maintenance	Enzyme: Deaminase	Hormone binding
MOG	0.1139	4	myelin oligodendrocyte glycoprotein	Extracellular Space	Cell growth & maintenance	Immunoglobulin	Antigen binding
CDK10	0.0682	2	cyclin-dependent kinase 10	Nucleus	Cell growth & maintenance	Serine/threonine kinase	Protein serine/threonine kinase activity
ANLN	**3.8715**	**2**	**anillin, actin binding protein**	**Cytoplasm**	**Cell growth & maintenance**	**Structural protein**	**Structural molecule activity**
CLTC	0.4565	46	clathrin, heavy chain (Hc)	Plasma Membrane	Cell growth & maintenance	Structural protein	Structural molecule activity
Tubb4a	**1.5385**	**9**	**Tubulin beta-4 chain OS=Mus musculus GN=Tubb4 PE=1 SV=3**	**unknown**	**Cell growth & maintenance**	**Structural protein**	**Structural molecule activity**
COTL1	0.1780	2	coactosin-like 1 (Dictyostelium)	Cytoplasm	Cell growth & maintenance	Unclassified	Molecular function unknown
ACLY	0.3295	4	ATP citrate lyase	Cytoplasm	Energy Metabolism	ATPase	ATPase activity
ATP6V1D	**1.5375**	**5**	**ATPase, H+ transporting, lysosomal 34kDa, V1 subunit D**	**Cytoplasm**	**Energy Metabolism**	**ATPase**	**ATPase activity**
PSAT1	0.4838	2	phosphoserine aminotransferase 1	Cytoplasm	Energy Metabolism	Enzyme: Aminotransferase	Transaminase activity
GNPDA1	**3.9417**	**2**	**glucosamine-6-phosphate deaminase 1**	**Cytoplasm**	**Energy Metabolism**	**Enzyme: Deaminase**	**Deaminase activity**
Gsta4	0.2165	2	glutathione S-transferase, alpha 4	Cytoplasm	Energy Metabolism	Enzyme: Glutathione transferase	Glutathione transferase activity
AHCYL1	**4.6447**	**3**	**adenosylhomocysteinase-like 1**	**Cytoplasm**	**Energy Metabolism**	**Enzyme: Hydrolase**	**Hydrolase activity**
AHCYL2	**6.8120**	**2**	**adenosylhomocysteinase-like 2**	**unknown**	**Energy Metabolism**	**Enzyme: Lyase**	**Molecular function unknown**
PYGM	0.4640	2	phosphorylase, glycogen, muscle	Cytoplasm	Energy Metabolism	Enzyme: Phosphorylase	Phosphorylase activity
CHST7	**23.9751**	**3**	**carbohydrate (N-acetylglucosamine 6-O) sulfo-transferase 7**	**Cytoplasm**	**Energy Metabolism**	**Enzyme: Sulphotransferase**	**Sulfotransferase activity**
HSPD1	0.3861	3	heat shock 60kDa protein 1 (chaperonin)	Cytoplasm	Protein metabolism	Heat shock protein	Heat shock protein activity
RPL24	0.2988	3	ribosomal protein L24	Cytoplasm	Protein metabolism	Ribosomal subunit	Structural constituent of ribosome

Table 4.3 – *Continued from previous page*

Gene	tg/wt	no. pept.	Description	Localisation	Biological process	Molecular class	Molecular function
RPL28	0.2680	3	ribosomal protein L28	Cytoplasm	Protein metabolism	Ribosomal subunit	Structural constituent of ribosome
RPS3A	0.5441	6	ribosomal protein S3A	Cytoplasm	Protein metabolism	Ribosomal subunit	Structural constituent of ribosome
RPS7	0.4024	3	ribosomal protein S7	Cytoplasm	Protein metabolism	Ribosomal subunit	Structural constituent of ribosome
RPS8	0.4535	2	ribosomal protein S8	Cytoplasm	Protein metabolism	Ribosomal subunit	Structural constituent of ribosome
PABPC1	0.3050	2	poly(A) binding protein, cytoplasmic 1	Cytoplasm	Reg of nucleic acid metabolism	RNA binding protein	RNA binding
STAT3	**23.6911**	**2**	**signal transducer and activator of transcription 3 (acute-phase response factor)**	**Nucleus**	**Reg of nucleic acid metabolism**	**Transcription factor**	**Transcription factor activity**
SUB1	0.2507	2	SUB1 homolog (S. cerevisiae)	Nucleus	Reg of nucleic acid metabolism	Transcription factor	Transcription factor activity
CTBP1	**5.5096**	**2**	**C-terminal binding protein 1**	**Nucleus**	**Reg of nucleic acid metabolism**	**Transcription regulatory protein**	**Transcription regulator activity**
PHB2	0.6353	4	prohibitin 2	Cytoplasm	Reg of nucleic acid metabolism	Transcription regulatory protein	Transcription regulator activity
RPH3A	0.4859	8	rabphilin 3A homolog (mouse)	Plasma Membrane	Transport	Membrane transport protein	Auxiliary transport protein activity
VAMP1	**4.7214**	**9**	**vesicle-associated membrane protein 1 (synaptobrevin 1)**	**Plasma Membrane**	**Transport**	**Membrane transport protein**	**Auxiliary transport protein activity**
VAMP2	**2.6961**	**12**	**vesicle-associated membrane protein 2 (synaptobrevin 2)**	**Plasma Membrane**	**Transport**	**Membrane transport protein**	**Auxiliary transport protein activity**
SLC25A4	**1.5195**	**35**	**solute carrier family 25 (mitochondrial carrier; adenine nucleotide translocator), member 4**	**Cytoplasm**	**Transport**	**Transport/cargo protein**	**Transporter activity**
NAPB	**3.6088**	**2**	**N-ethylmaleimide-sensitive factor attachment protein, beta**	**Cytoplasm**	**Transport**	**Unclassified**	**Molecular function unknown**
SDF2	**3.2819**	**3**	**stromal cell-derived factor 2**	**Extracellular Space**	**Unknown**	**Secreted polypeptide**	**Molecular function unknown**
CHCHD3	0.3076	2	coiled-coil-helix-coiled-coil-helix domain containing 3	Cytoplasm	Unknown	Unclassified	Molecular function unknown
DLGAP1	**1.5101**	**4**	**discs, large (Drosophila) homolog-associated protein 1**	**Plasma Membrane**	**Unknown**	**Unclassified**	**Molecular function unknown**
Emc2	0.0637	2	Tetratricopeptide repeat protein 35 OS=Mus musculus GN=Ttc35 PE=2 SV=1	unknown	Unknown	Unclassified	Molecular function unknown
Emc7	0.3128	2	UPF0480 protein C15orf24 homolog OS=Mus musculus GN=ORF3 PE=2 SV=1	unknown	Unknown	Unclassified	Molecular function unknown
FMNL2	0.0066	6	formin-like 2	Cytoplasm	Unknown	Unclassified	Molecular function unknown
IQCH	0.4075	5	IQ motif containing H	unknown	Unknown	Unclassified	Molecular function unknown
Mblac2	**2.1000**	**2**	**Beta-lactamase-like protein FLJ75971 homolog OS=Mus musculus PE=2 SV=1**	**unknown**	**Unknown**	**Unclassified**	**Molecular function unknown**
NEGR1	0.1173	2	neuronal growth regulator 1	Extracellular Space	Unknown	Unclassified	Molecular function unknown
PHYHIP	0.4708	2	phytanoyl-CoA 2-hydroxylase interacting protein	unknown	Unknown	Unclassified	Molecular function unknown
TCP11L2	**9.6993**	**2**	**t-complex 11 (mouse)-like 2**	**unknown**	**Unknown**	**Unclassified**	**Molecular function unknown**
WDR7	**21.7344**	**2**	**WD repeat domain 7**	**unknown**	**Unknown**	**Unclassified**	**Molecular function unknown**
ZFAT	**4.0161**	**2**	**zinc finger and AT hook domain containing**	**Nucleus**	**Unknown**	**Unclassified**	**Molecular function unknown**

Table 4.4: Proteomics in synaptosomes. The "fold change" column shows the ratio of tg to wt (values above 1 indicate upregulation, below 1 downregulation). Upregulated proteins are marked in bold.

Gene	tg/wt	no. pept.	Description	Localisation	Biological process	Molecular class	Molecular function
upregulated							
SNAP91	0.2694	2	Synaptosomal associated protein, 91 kD	Plasma Membrane	Cell communication & Signaling	Adapter molecule	Receptor signaling complex scaffold activity
PACSIN1	**2.281**	**10**	**Protein kinase C and casein kinase substrate in neurons 1**	**Cytoplasm**	**Cell communication & Signaling**	**Adapter molecule**	**Receptor signaling complex scaffold activity**
HOMER1	**7.631**	**3**	**Homer 1**	**Plasma Membrane**	**Cell communication & Signaling**	**Adapter molecule**	**Receptor signaling complex scaffold activity**
NCAM1	**1.657**	**8**	**Neural cell adhesion molecule 1**	**Plasma Membrane**	**Cell communication & Signaling**	**Adhesion molecule**	**Cell adhesion molecule activity**
CALM1	0.3983	2	Calmodulin	Cytoplasm	Cell communication & Signaling	Calcium binding protein	Calcium ion binding
HPCA	**5.687**	**2**	**Hippocalcin**	**Cytoplasm**	**Cell communication & Signaling**	**Calcium binding protein**	**Calcium ion binding**
NCALD	**5.687**	**4**	**Neurocalcin delta**	**Cytoplasm**	**Cell communication & Signaling**	**Calcium binding protein**	**Calcium ion binding**

Table 4.4 – *Continued from previous page*

| Gene	tg/wt	no. pept.	Description	Localisation	Biological process	Molecular class	Molecular function
SEPT_7	**1.606**	**7**	**Cell division cycle 10**	**Cytoplasm**	**Cell communication & Signaling**	**Cell cycle control protein**	**Protein binding**
SIRPA	**1.585**	**4**	**SIRP alpha 1**	**Plasma Membrane**	**Cell communication & Signaling**	**Cell surface receptor**	**Receptor activity**
MACF1	**3.648**	**4**	**Macrophin 1**	**Cytoplasm**	**Cell communication & Signaling**	**Cytoskeletal associated protein**	**Cytoskeletal protein binding**
GNB2	**1.57**	**12**	**Guanine nucleotide binding protein beta polypeptide 2**	**Plasma Membrane**	**Cell communication & Signaling**	**G protein**	**GTPase activity**
GNB1	**1.848**	**19**	**Guanine nucleotide binding protein, beta 1**	**Plasma Membrane**	**Cell communication & Signaling**	**G protein**	**GTPase activity**
RALA	**1.503**	**5**	**Ras related protein Ral A**	**Cytoplasm**	**Cell communication & Signaling**	**GTPase**	**GTPase activity**
RAC1	**1.77**	**5**	**Ras related C3 botulinum toxin substrate 1**	**Plasma Membrane**	**Cell communication & Signaling**	**GTPase**	**GTPase activity**
KRAS	**2.327**	**2**	**KRAS**	**Cytoplasm**	**Cell communication & Signaling**	**GTPase**	**GTPase activity**
RAB5A	**2.806**	**2**	**Ras related protein Rab 5A**	**Cytoplasm**	**Cell communication & Signaling**	**GTPase**	**GTPase activity**
RAB5C	**2.806**	**2**	**Ras associated protein Rab5C**	**Cytoplasm**	**Cell communication & Signaling**	**GTPase**	**GTPase activity**
RAP1A	**3.183**	**2**	**Ras related protein 1A**	**Cytoplasm**	**Cell communication & Signaling**	**GTPase**	**GTPase activity**
DIRAS2	**4.082**	**2**	**DIRAS2**	**Plasma Membrane**	**Cell communication & Signaling**	**GTPase**	**GTPase activity**
CDC42	**4.229**	**2**	**CDC42**	**Cytoplasm**	**Cell communication & Signaling**	**GTPase**	**GTPase activity**
ARHGAP20	0.09033	6	ARHGAP20	Cytoplasm	Cell communication & Signaling	GTPase activating protein	GTPase activator activity
PRKAR2A	**1.651**	**3**	**Protein kinase, cAMP dependent, regulatory type II, alpha**	**Cytoplasm**	**Cell communication & Signaling**	**Serine/threonine kinase**	**Protein serine/threonine kinase activity**
Camk2b	**1.912**	**22**	**CaM kinase II beta subunit**	**Cytoplasm**	**Cell communication & Signaling**	**Serine/threonine kinase**	**Protein serine/threonine kinase activity**
CAMK2A	**1.958**	**46**	**CaMK II alpha subunit**	**Cytoplasm**	**Cell communication & Signaling**	**Serine/threonine kinase**	**Protein serine/threonine kinase activity**
CAMK2G	**2.242**	**26**	**CaM kinase II gamma subunit**	**Cytoplasm**	**Cell communication & Signaling**	**Serine/threonine kinase**	**Protein serine/threonine kinase activity**
CDK5	**3.661**	**2**	**Cyclin dependent kinase 5**	**Nucleus**	**Cell communication & Signaling**	**Serine/threonine kinase**	**Protein serine/threonine kinase activity**
PPP2R1A	**1.591**	**12**	**Protein phosphatase 2, regulatory subunit A , alpha isoform**	**Cytoplasm**	**Cell communication & Signaling**	**Serine/threonine phosphatase**	**Protein serine/threonine phosphatase activity**
MTCH2	0.3465	2	Mitochondrial carrier homolog 2	Cytoplasm	Cell communication & Signaling	Unclassified	Molecular function unknown
SRCIN1	**2.184**	**5**	**SNIP**	**Cytoplasm**	**Cell communication & Signaling**	**Unclassified**	**Molecular function unknown**
CTTN	0.4145	2	Cortactin	Plasma Membrane	Cell growth & maintenance	Cytoskeletal associated protein	Cytoskeletal protein binding
TUBB2A	**1.529**	**32**	**Tubulin beta-2A chain**	**Cytoplasm**	**Cell growth & maintenance**	**Cytoskeletal associated protein**	**Cytoskeletal protein binding**
COL5A2	0.1811	2	Collagen, type V, alpha 2	Extracellular Space	Cell growth & maintenance	Extracellular matrix protein	Extracellular matrix structural constituent
CLTC	0.6502	24	Clathrin, heavy polypeptide	Plasma Membrane	Cell growth & maintenance	Structural protein	Structural molecule activity
ABAT	0.2476	3	Gamma Aminobutyrate Transaminase	Cytoplasm	Energy Metabolism	Enzyme: Aminotransferase	Transaminase activity
GLUL	**1.597**	**21**	**Glutamate ammonia ligase**	**Cytoplasm**	**Energy Metabolism**	**Enzyme: Aminotransferase**	**Transaminase activity**
GOT1	**1.826**	**7**	**Glutamate oxaloacetate transaminase-1**	**Cytoplasm**	**Energy Metabolism**	**Enzyme: Aminotransferase**	**Transaminase activity**
MDH2	**1.572**	**16**	**Malate dehydrogenase mitochondrial**	**Cytoplasm**	**Energy Metabolism**	**Enzyme: Dehydrogenase**	**Catalytic activity**
PDHA1	**2.403**	**10**	**Pyruvate dehydrogenase complex, E1-alpha polypeptide 1**	**Cytoplasm**	**Energy Metabolism**	**Enzyme: Dehydrogenase**	**Catalytic activity**
ENO2	**1.775**	**17**	**Enolase 2**	**Cytoplasm**	**Energy Metabolism**	**Enzyme: Hydratase**	**Catalytic activity**
TPI1	**2.008**	**5**	**Triosephosphate isomerase 1**	**Cytoplasm**	**Energy Metabolism**	**Enzyme: Isomerase**	**Isomerase activity**
MGLL	**2.143**	**2**	**Monoglyceride lipase**	**Plasma Membrane**	**Energy Metabolism**	**Enzyme: Lipase**	**Lipase activity**
NDUFB5	**1.562**	**3**	**NADH dehydrogenase 1 beta subcomplex, 5**	**Cytoplasm**	**Energy Metabolism**	**Enzyme: Oxidoreductase**	**Oxidoreductase activity**
NDUFS7	**1.567**	**6**	**NADH ubiquinone oxidoreductase Fe S protein 7**	**Cytoplasm**	**Energy Metabolism**	**Enzyme: Oxidoreductase**	**Oxidoreductase activity**
CBR1	**1.835**	**6**	**Carbonyl reductase 1**	**Cytoplasm**	**Energy Metabolism**	**Enzyme: Oxidoreductase**	**Oxidoreductase activity**
NDUFA6	**2.562**	**3**	**NADH dehydrogenase 1 alpha subcomplex, 6**	**Cytoplasm**	**Energy Metabolism**	**Enzyme: Oxidoreductase**	**Oxidoreductase activity**
PFKP	0.32	2	Phosphofructokinase platelet type	Cytoplasm	Energy Metabolism	Enzyme: Phosphotransferase	Catalytic activity

Continued on next page

Table 4.4 – *Continued from previous page*

Gene	tg/wt	no. pept.	Description	Localisation	Biological process	Molecular class	Molecular function
CKB	**1.64**	**16**	**Creatine kinase brain type**	**Cytoplasm**	**Energy Metabolism**	**Enzyme: Phospho-transferase**	**Catalytic activity**
PGK1	**1.861**	**7**	**Phosphoglycerate kinase 1**	**Cytoplasm**	**Energy Metabolism**	**Enzyme: Phospho-transferase**	**Catalytic activity**
Pkm	**2.05**	**18**	**Pyruvate kinase 3**	**Cytoplasm**	**Energy Metabolism**	**Enzyme: Phospho-transferase**	**Kinase activity**
CYB5R3	**5.219**	**2**	**Cytochrome-b5 reductase**	**Cytoplasm**	**Energy Metabolism**	**Enzyme: Reductase**	**Catalytic activity**
SLC25A5	0.6446	11	Solute carrier family 25 (mitoc carrier, translocator), member 5	Cytoplasm	Energy Metabolism	Integral membrane protein	ATP binding
COX6C	0.257	2	Cytochrome c oxidase, subunit VIc	Cytoplasm	Energy Metabolism	Regulatory/other subunit	Oxidoreductase activity
ATP6V1A	**1.55**	**19**	**ATP6V1A1**	**Cytoplasm**	**Energy Metabolism**	**Transport/cargo protein**	**Transporter activity**
CADM3	**1.57**	**4**	**Immunoglobulin superfamily member 4B**	**Plasma Membrane**	**Immune response**	**Immunoglobulin**	**Antigen binding**
HSPA12A	0.2763	2	Heat shock 70kDa protein 12A	unknown	Protein metabolism	Heat shock protein	Heat shock protein activity
Rps9	**1.598**	**3**	**Ribosomal protein S9**	**Cytoplasm**	**Protein metabolism**	**Ribosomal subunit**	**Structural constituent of ribosome**
RPS5	**3.276**	**2**	**Ribosomal protein S5**	**Cytoplasm**	**Protein metabolism**	**Ribosomal subunit**	**Structural constituent of ribosome**
RPL9	**6.266**	**2**	**Ribosomal protein L9**	**Cytoplasm**	**Protein metabolism**	**Ribosomal subunit**	**Structural constituent of ribosome**
EIF4H	0.4628	6	Williams Beuren syndrome chromosome region 1	Cytoplasm	Protein metabolism	Translation regulatory protein	Translation regulator activity
UBA1	0.2935	2	Ubiquitin activating enzyme 1	Cytoplasm	Protein metabolism	Ubiquitin proteasome system protein	Ubiquitin-specific protease activity
UBB	**2.065**	**6**	**Polyubiquitin-B**	**Cytoplasm**	**Protein metabolism**	**Ubiquitin proteasome system protein**	**Ubiquitin-specific protease activity**
UBE2D3	**2.117**	**2**	**Ubiquitin conjugating enzyme E2D 3**	**unknown**	**Protein metabolism**	**Ubiquitin proteasome system protein**	**Ubiquitin-specific protease activity**
PA2G4	**2.04**	**4**	**PA2G4**	**Nucleus**	**Reg of nucleic acid metabolism**	**Transcription regulatory protein**	**Transcription regulator activity**
NAV3	0.3103	2	Neuron navigator 3	Nucleus	Reg of nucleic acid metabolism	Unclassified	Molecular function unknown
ATP1B2	**3.874**	**2**	**ATP1B2**	**Plasma Membrane**	**Transport**	**ATPase**	**ATPase activity**
VAMP3	**2.162**	**11**	**Cellubrevin**	**Plasma Membrane**	**Transport**	**Integral membrane protein**	**Protein binding**
ATP6V0A1	**1.637**	**4**	**ATPase H+ transporting lysosomal noncatalytic accessory protein 1A**	**Cytoplasm**	**Transport**	**Ion channel**	**Ion channel activity**
KCTD12	**4.098**	**2**	**Potassium channel tetramerisation domain**	**Plasma Membrane**	**Transport**	**Ion channel**	**Ion channel activity**
VAMP2	**2.162**	**11**	**Synaptobrevin 2**	**Plasma Membrane**	**Transport**	**Membrane transport protein**	**Auxiliary transport protein activity**
SYN1	**1.658**	**24**	**Synapsin I**	**Plasma Membrane**	**Transport**	**Transport/cargo protein**	**Transporter activity**
CACNA1H	0.0306	6	Calcium channel voltage dependent T type alpha 1H subunit	Plasma Membrane	Transport	Voltage gated channel	Voltage-gated ion channel activity
CACNA1F	**11.19**	**2**	**Calcium channel, voltage dependent, alpha 1F subunit**	**Plasma Membrane**	**Transport**	**Voltage gated channel**	**Voltage-gated ion channel activity**
SFXN3	0.5243	5	Sideroflexin 3	Cytoplasm	Unknown	Integral membrane protein	Molecular function unknown
SAMD4A	0.0716	2	Sterile alpha motif domain containing 4	unknown	Unknown	Unclassified	Molecular function unknown
	0.1471	4	DC12 protein	unknown	Unknown	Unclassified	Molecular function unknown
DLGAP3	**2.908**	**2**	**Discs, large homolog-associated protein 3**	**Cytoplasm**	**Unknown**	**Unclassified**	**Molecular function unknown**
OCIAD2	**4.491**	**2**	**OCIA domain containing 2**	**Cytoplasm**	**Unknown**	**Unclassified**	**Molecular function unknown**
NEGR1	**4.985**	**3**	**Neuronal growth regulator 1**	**Extracellular Space**	**Unknown**	**Unclassified**	**Molecular function unknown**
LRRC57	**11.59**	**2**	**Leucine rich repeat containing 57**	**unknown**	**Unknown**	**Unclassified**	**Molecular function unknown**
FMNL2	**17.4**	**6**	**Formin like 2**	**Cytoplasm**	**Unknown**	**Unclassified**	**Molecular function unknown**
IFFO1	**25.74**	**2**	**HOM-TES-103 tumor antigen-like**	**unknown**	**Unknown**	**Unclassified**	**Molecular function unknown**
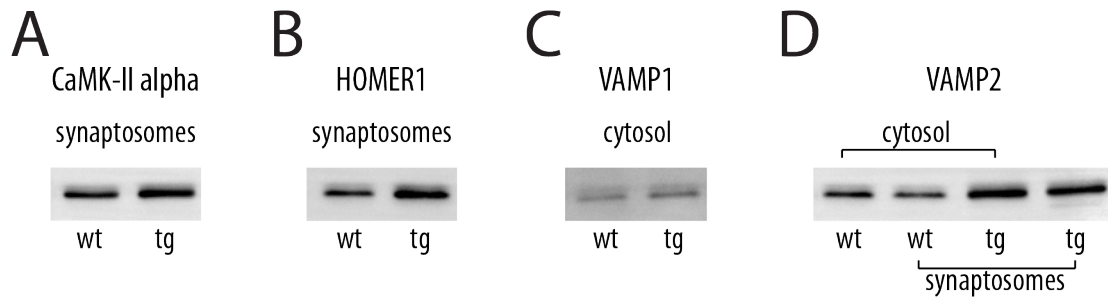
Figure 4.6: Validation of proteomics candidates by western blotting. Western blots were performed on pooled samples from 4 weeks old *Tcf4*tg and wt mice. **A)** CaMK II alpha in synaptosomes. **B)** HOMER1 in synaptosomes. **C)** VAMP1 in cytosolic fraction. **D)** VAMP2 in cytosolic fraction and synaptosomes. Whole blots are presented in the Appendix in Fig. 7 on page 107.
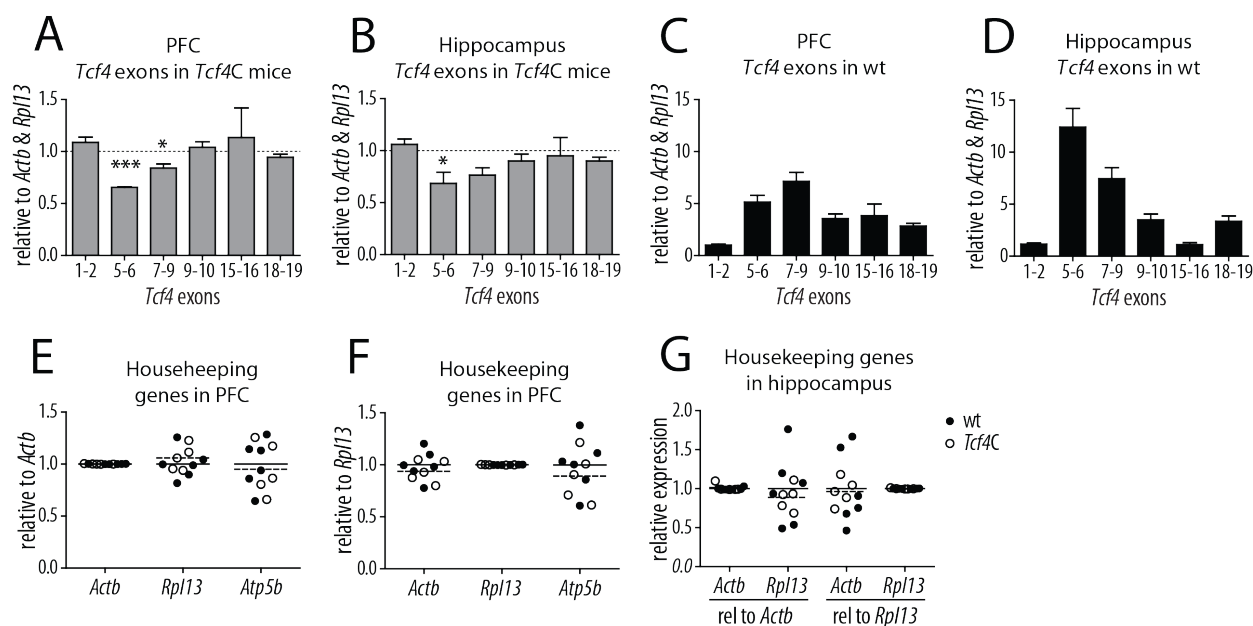
4.2   Analyses in *Tcf4*C knockout mice

We generated heterozygotic *Tcf4* knockout mice *Tcf4*C. They breed well and show no major developmental impairments nor increased mortality. However, this may be different in homozygotic animals. We have not studied them, but the Sanger Institute has reported partial lethality at postnatal day 14 in homozygotic *Tcf4* knockout-first Eucomm mice (*Tcf4*E) and several morphological deviations (craniofacial abnormalities, decreased body length and weight, reduced grip strength and abnormal morphology of pelvis and joints) in homozygotic *Tcf4*E females[199]. Thus, increased mortality should be expected in *Tcf4*C homozygotes. The phenotype may be even more severe, considering that the knockout in *Tcf4*C should be more effective than in the *Tcf4*E line.

4.2.1   *Tcf4* expression in *Tcf4*C mice

To validate *Tcf4*C as a knockout line, we measured *Tcf4* RNA levels in PFC and hippocampus of *Tcf4*C (n=5) and wt animals (n=6), using RT-qPCR. *Tcf4* transcripts were detected with six primer pairs targeting different exons in different regions of *Tcf4*. They were designed in a way that would allow distinguish different *Tcf4* isoforms, based on Ensembl.org[200]. Levels of exons 1–2 in *Tcf4*C mice were comparable to wt. Exons 5–6, located directly downstream of the deleted exon 4, were clearly reduced in both PFC (p<0.0001, t-test) and hippocampus (p=0.0277, t-test). The consecutive exons were gradually increasing — exons 7–9 showed less pronounced decrease in PFC (p=0.0174, t-test) and a tendency in hippocampus (Fig. 4.7A,B).

Additionally, we compared the abundance of different exons in wt mice. After adjustment for different qPCR efficiencies, we observed different patterns of *Tcf4* exons expression in PFC and hippocampus. In PFC, the most abundant were exons 7–9 (Fig. 4.7C) while in hippocampus, exons 5–6 were expressed at highest levels (Fig. 4.7D). Direct comparison of hippocampus and PFC was impossible due to differences in expression of the housekeeping genes. *Atp5b*, also considered as a reference gene, was excluded due to incompatibility with the other two (Fig. 4.7F,G).

Figure 4.7: *Tcf4*C **expression in** *Tcf4*C **knockout mice. A)** *Tcf4* exons expression in PFC of *Tcf4*C mice (n=5), normalized to wt. Exons 5–6 (p<0.0001, t-test) and 7–9 (p=0.0174) show decreased levels. **B)** *Tcf4* exons expression in hippocampus of *Tcf4*C mice (n=5), normalized to wt. Exons 5–6 are reduced (p=0.0277, t-test). **C)** *Tcf4* exon expression in PFC of wt animals (n=6), normalized to exons 1–2. Exons 7–9 show highest expression. **D)** *Tcf4* exon composition in hippocampus of wt animals (n=6), normalized to exons 1–2. Exons 5–6 show highest expression. **E)** Housekeeping genes in PFC normalized to *Actb*. **F)** Housekeeping genes in PFC normalized to *Rpl13*. **G)** Housekeeping genes in hippocampus normalized to *Actb* and *Rpl13*.

4.2.2 Morphometrics in *Tcf4*C mice

Since PTHS patients display abnormal facial features[42], we checked whether the *Tcf4*C mice display any alterations in facial and body features. As presented in Fig. 4.8A, we measured body length, head length, width and height and the distance between the eyes. Analysis showed no significant differences in any of the parameters nor in their ratios (Fig. 4.8B-E). We also monitored
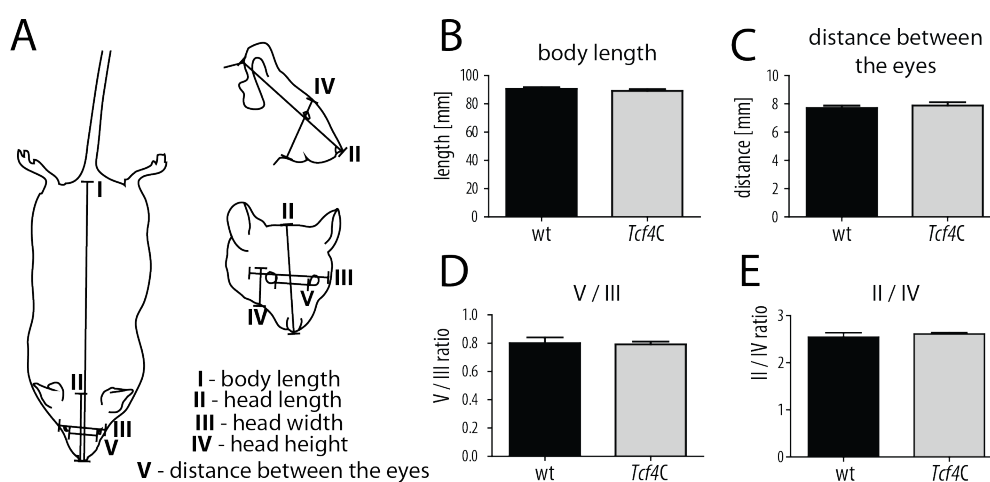
Figure 4.8: *Tcf4*C **mouse morphometrics. A)** Measured dimensions. **B-E)** No morphological differences between the genotypes were found. **B)** Body length. **C)** The distance between the eyes. **D)** The distance between the eyes / head width ratio. **E)** Head width / head height ration. Bars represent means with SEM.

body weight, which was mildly reduced in the *Tcf4*C animals at the age of 4 (t-test, p=0.0125) but not at 14 weeks (Fig. 5A, Appendix A, page 103).

4.3   Behavioural profiling of mice

To better understand Gene × Environment interaction, we began with studying the influence of environment on behaviour, by comparing wt mice subjected to IR or SD. To do this we established an approach to analysing huge behavioural data sets that cover various aspects of murine behaviour measured in different tests and in independent mouse cohorts. The method is described in details in our article *Data calibration and reduction allows to visualize behavioural profiles of psychosocial influences in mice towards clinical domains*[178].

IR and SD were tested in two independent cohorts and by different experimenters. To analyse them, we normalized IR and SD to their control groups, which were identical in both cohorts (EE-1 and EE-2 respectively). To compare different behavioural measures to each other, we gave them arbitrarily assigned *directionality*. We merged measures reflecting the same behaviours into single traits, which we then fused into behavioural domains by using multivariate statistics. Finally, we visualised the data as behavioural profiles in single graphs (Fig. 4.9) and we calculated Severity scores, that reflect the degree of deviation form the EE control. Detailed methods description and full data tables are presented in our publication[178] (attached in Appendix D).

4.3.1   Different effects of Isolation rearing and Social defeat in wt mice

Both IR and SD had prominent impact on the behaviour. In many aspects they were similar, but showed also some differencies. Isolated animals displayed locomotor hyperactivity in novel environment in OF, reduced exploratory behaviour in HB, increased latency to enter the dark compartment in LD, reduced pain sensitivity and freezing in cue FC. The last result should be taken with caution, as it may reflect pain insensitivity instead of cognitive impairment (Fig. 4.9A). On the domain level IR had significant influence on novelty-induced locomotor activity (Ambulation), Pain sensitivity, Motivation and Fear memory (Fig. 4.9B).

SD group showed pronounced reducions of exploration in HB and of fighting time in TST as well as prolonged latencies to enter the dark compartment in LD. Both context and cue FC were impaired, but pain sensitivity was normal (Fig. 4.9C). Thus Fear memory, Motivation and Curiosity are the domains, that undergo greatest changes upon SD (Fig. 4.9D).

Both IR and SD have detrimental impact on latencies in LD, cue FC and exploratory behaviour in HB (Fig. 4.9E), but SD affects the latter two significantly more than IR (marked as black, encircled stars). SD has also a stronger influence on context FC and motivation in TST. On the other hand IR, in contrast to SD, affects pain sensitivity in HP and ambulation in OF. This is also visible on the domain level (Fig. 4.9F) — SD has strong detrimental effects on Fear memory, Motivation and Curiosity, while IR impairs Fear memory and Motivation milder, but has pronounced effects on Pain sensitivity and Ambulation. The meaning of prolonged latency to exit the bright
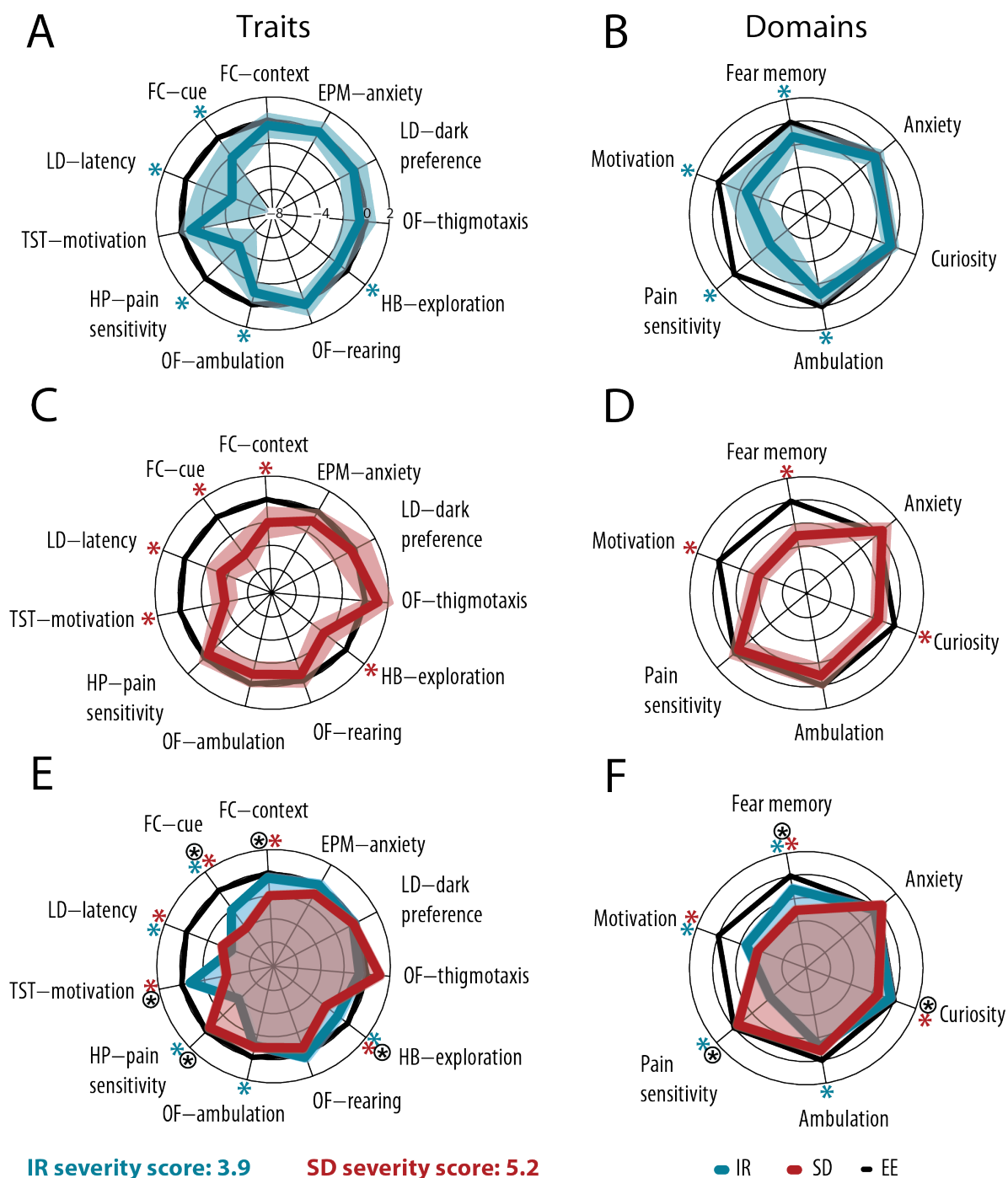
Figure 4.9: Behavioural profiles of wildtype IR and SD mice. Radar charts present behavioural profiles on trait (left) and domain level (right). IR (blue line) and SD means (red lines) are relative EE controls (black lines) set as zero. Deviations towards the centre of the graph (values below zero) mean worsened the performance. Shading in graphs A–D represents 99.17% CI, while in E–F represent plot areas. Stars mark significant differences of IR (blue) and SD (red) from the controls. IR profiles are depicted on **A)** train level and **B)** domain level. Analogously, SD profiles are presented on **C)** trait and **D)** domain level. Overlaid figures on **E)** trait and **F)** domain level allow visual comparison of IR and SD profiles and impairment severity. Black encircled stars show significant differences between them. Overall degree of behavioural alterations is expressed plot area sizes (smaller areas indicate stronger impairments) and severity score calculated on trait level (higher score indicates greater changes). **Abbreviations**: isolation rearing (IR), social defeat (SD), enriched environment (EE), confidence interval (CI) Fear conditioning (FC), Elevated plus maze (EPM), Light-dark preference (LD), Open field (OF), Hole board (HB), Hot plate (HP), Tail suspension test (TST). Figure adapted from Badowska *et al.*[178].

compartment and enter the dark one is not clear, but it may have similar origin as prolonged latencies to emerge from a small enclosure[201]. It may reflect unfocused activity due to excessive ambulation[137] or initial immobility[201] possibly caused by neophobia or reduced motivation.

Both IR and SD have significant impact on five traits each, but SD appears to induce greater changes in overall behaviour. To compare it, we calculated Severity scores on the trait level (Fig. 4.9E). SD displayed higher score (5.2 with 95% CI [3.9, 6.4]) than IR (3.9 with 95% CI [1.7, 6.1]), which suggests that SD affected behaviour stronger than IR. However, this difference has not reached significance level.

Stress hormones upon social defeat   To confirm that SD induces stress in mice, we measured stress hormones in blood plasma immediately after a single SD session and in non-stressed EE mice. We measured corticosterone, noradrenaline (associated with activity) and adrenaline — the best marker of distress[202] — in plasma by mass spectrometry. Stress increased corticosterone levels ($p=0.0079$, Mann Whitney test) (Fig. 4.10A). As expected[202], noradrenaline levels remained stable (Fig. 4.10B) and adrenaline showed a tendency for an increase upon stress (Fig. 4.10C).
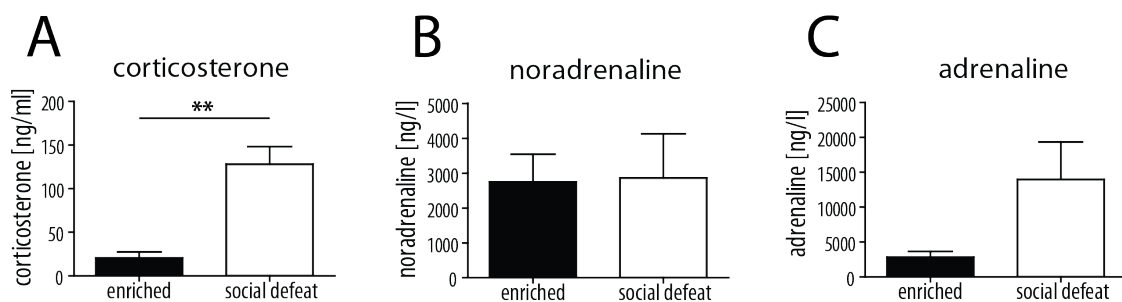

Figure 4.10: Stress hormones are increased in blood after acute SD. Stress hormones were monitored in blood plasma after acute SD stress (n=5) and in EE mice (n=5). **A)** Coritcosterone was increased upon SD compared to EE ($p=0.0079$, Mann Whitney test). **B)** Noradrenalie levels were unchanged by SD. **C)** SD mice showed a tendency for increased adrenaline ($p=0.1508$, Mann-Whitney test).

4.3.2   Gene $\times$ Environment interaction in *Tcf4*tg mice

In a battery of tests, we analysed behaviour of *Tcf4*tg and wt mice in IR or EE. We used two cohorts: tested form the age of 8 weeks (*Tcf4tgIR-EE-young* or *Young*), or at 1 year of age (*Tcf4tgIR-EE-aged* or *Ageing*) to check if ageing contributes to the behavioural deficits.

Gene $\times$ Environment interaction in *Tcf4*tg mice

Behavioural analysis of the *Tcf4*tg vs. wt cohorts revealed cognitive impairments of *Tcf4*tg mice which were manifested only upon IR. In the *Young* cohort, we observed housing-dependent impairments of cue FC (Fig. 4.11B) in *Tcf4*tg mice both 48 h and 1 month after foot shock acquisition. We also observed a tendency for impaired initial learning in MWM (Fig. 4.11C) and a very pronounced impairment of reversal learning in *Tcf4*tg animals housed in IR (Fig. 4.11D). Memory recall in probe tests was not altered by the *Tcf4* overexpression (Fig. 4.11E).
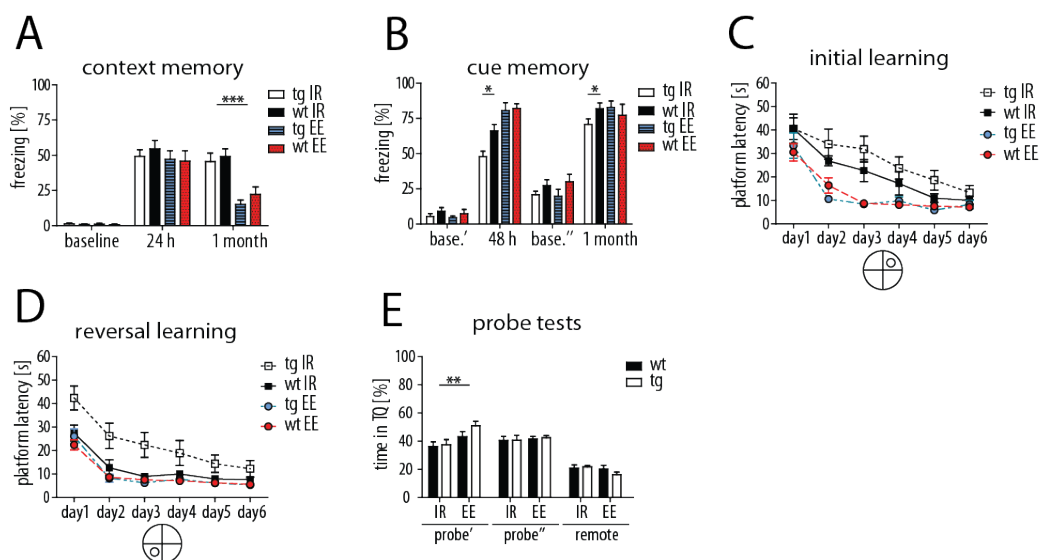
Figure 4.11: Cognition in *Tcf4*tg mice upon IR and EE. A) Context FC: Genotype has no effect on context memory, but EE reduces freezing 1 month after shock (p<0.0001). **B)** Cue FC: In IR *Tcf4*tg mice showed reduced cue memory 48 h (p<0.05, Bonferroni) and 1 month after the shock (p=0.0381, t-test). **G–J)** MWM, mean latencies to reach the platform. **C)** Initial learning: EE mice learned faster than IR mice (p=0.0001, RM ANOVA). **D)** Reversal learning: *Tcf4*tg mice performed worse than wt in IR, but not in EE: genotype (p=0.024, RM ANOVA), housing (p=0.0001, RM ANOVA) and their interaction effects (p=0.038, RM ANOVA). **E)** Probe tests. IR mice spent less time in TQ than EE mice (p=0.0051) in the probe test after initial learning, but not after reversal learning and 1 month later. **Abbreviations**: Fear conditioning (FC), Morris water maze (MWM), target quadrant (TQ).
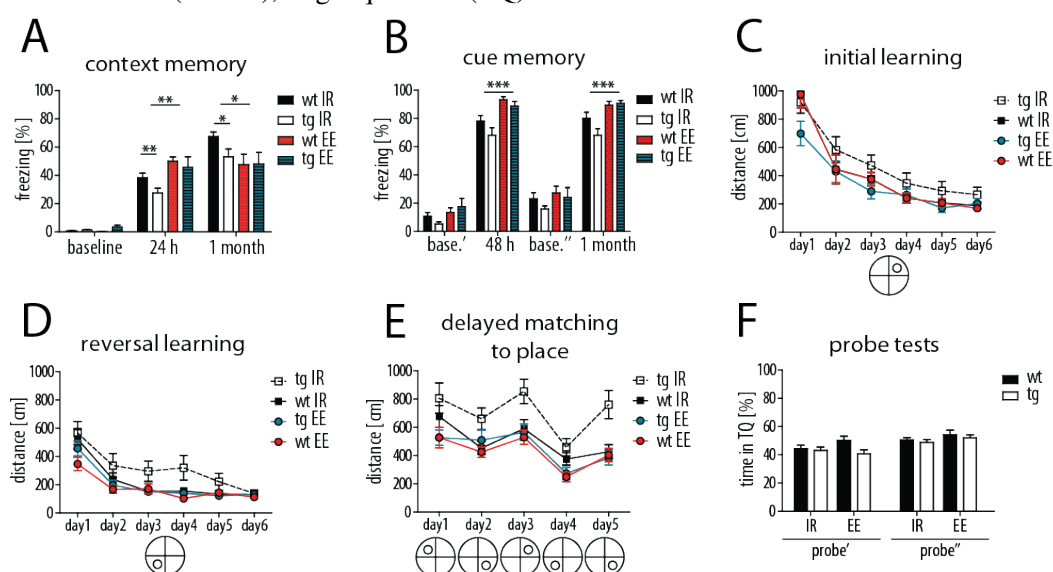
Figure 4.12: Cognition in aged *Tcf4*tg mice upon IR and EE. A) Context FC: 24 h after shock, freezing was reduced by IR (p=0.001) and *Tcf4*tg-IR mice froze less than wt-IR mice (p=0.0273, Mann Whitney test)which we also saw one month later (p=0.0333, t-test with Welch's correction and housing effect p=0.0485). **B)** Cue FC was impaired by IR 48 h (p<0.0001) and one month after the shock (p<0.0001). **C–F)** WM, mean total distances were analysed, due to speed differences between IR and EE. **C)** Initial learning. **D)** Reversal learning was mildly impaired in *Tcf4*tg-IR mice with housing (p=0.009, RM ANOVA) and genotype effects (p=0.057, RM ANOVA). **E)** In DMP, housing (p<0.0001, RM ANOVA), genotype (p=0.002, RM ANOVA) and G×E interaction (p=0.013, RM ANOVA) influenced performance of mice. **F)** In the first probe test (after initial learning) *Tcf4*tg mice performed worse (p=0.0454) but not in the second test (after reversal). Tests were analysed using two-way ANOVA, unless stated differently. **Abbreviations**: Fear conditioning (FC), Morris water maze (MWM), delayed matching to place (DMP).

In the *Ageing* cohort, *Tcf4*tg mice showed cognitive deficits only when housed in IR but not when housed in EE (Fig. 4.12). Freezing in context FC (Fig. 4.12A) was reduced in *Tcf4*tg mice only when housed in IR. In cue FC we observed a similar tendency; however, the difference between *Tcf4*tg and wt mice in IR was not significant (Fig. 4.12B). In MWM initial learning was unaffected (Fig. 4.12C), but worsened performance was observed in isolated *Tcf4*tg mice in reversal learning (Fig. 4.12D) and delayed matching to place (DMP) (Fig. 4.12E). Time spent in target quadrant (TQ) was the same in all groups (Fig. 4.12F).

Replication of findings in IR

In the G×E cohort we replicated several observations concerning wildtype IR behaviour (see: Appendix A): prolonged latency to enter dark (Fig. 1B), increased ambulation in OF (Fig. 1F,G), reduced exploration in HB (Fig. 1K), reduced fighting in TST (Fig. 2G) and pain insensitivity (Fig. 1J,K). Apart from that, we detected some abnormalities of IR mice that have not been tested in the wt cohort: increased running in OF and swimming speed MWM (Fig. 1H,I) and more arm choices in Y-maze (Fig. 2A). These observations are complementary to increased ambulation in IR and may all together reflect hyperactivity in novel environment. Isolated mice showed reduced number of alternations in Y-maze (Fig. 2B), and impairment of PPI (Fig. 2E) and spatial learning in MWM (Fig. 4.11C and 2L) (for detailed statistical analyses see Appendix A: Table 2). Upon ageing we have additionally seen increased body weight in IR mice from the 8th month of age
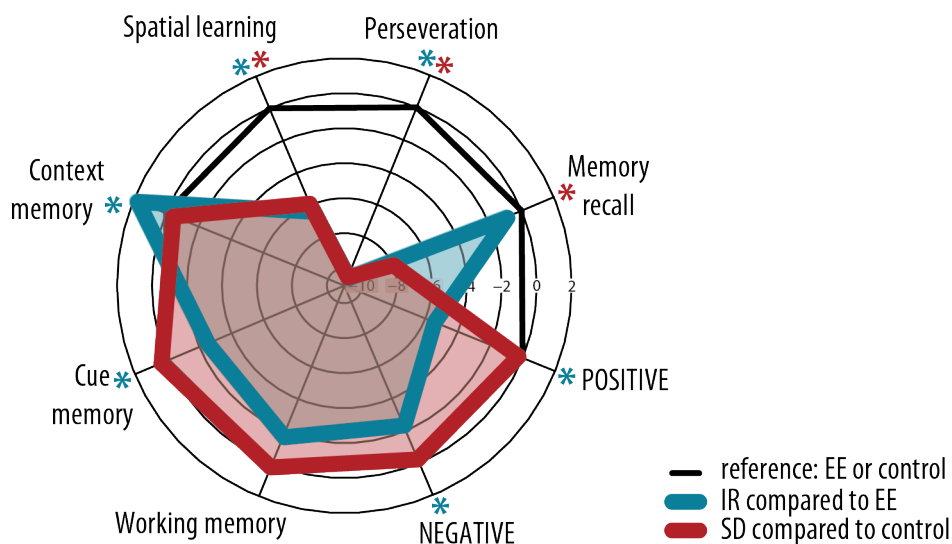
Figure 4.13: Environmental effects in the G×E cohorts. Radar charts represent effects of IR (blue) and SD (red) on cognition (domain level) and positive and negative symptoms (symptom class level), regardless of genotype. We used data from two G×E cohorts: young IR–EE and *Tcf4*tg SD–control. Lines represent performance relative to corresponding reference groups — EE or control (black). Significant effects are indicated by stars in corresponding colours. IR mice, compared to EE, showed positive, negative symptoms and in the cognitive class: impaired context and cue fear memory as well as reduced performance in MWM spatial learning and perseveration tasks. SD mice, in comparison to control condition, displayed no significant positive and negative symptoms, but showed impairments in all spatial memory tasks: memory recall, perseveration and spatial learning.

(Fig. 3A) and possibly associated with it reduction in rearing (Fig. 3E). Also anxiety in EPM was increased in 1 year old IR mice.

4.3.3 Behavioural analysis of *Tcf4*C mice

Based on our experiences with *Tcf4*tg animals, we decided to house the *Tcf4*C knockouts in IR to enhance the potential phenotype. *Tcf4*C mice showed normal context FC (Fig. 4.14A) and only mildly increased freezing in all phases of cue FC (Fig. 4.14B). However, in MWM spatial learning was dramatically impaired (Fig. 4.14C–E) and no significant difference between the groups was detected in the probe test (Fig. 4.14F). Subtle increase of anxiety was observed in OF (Fig. 5D) and reduction of alternations in Y-maze (Fig. 6C,E). Startle response to 120 dB pulse in PPI was increased in *Tcf4*C mice (Fig. 6J).
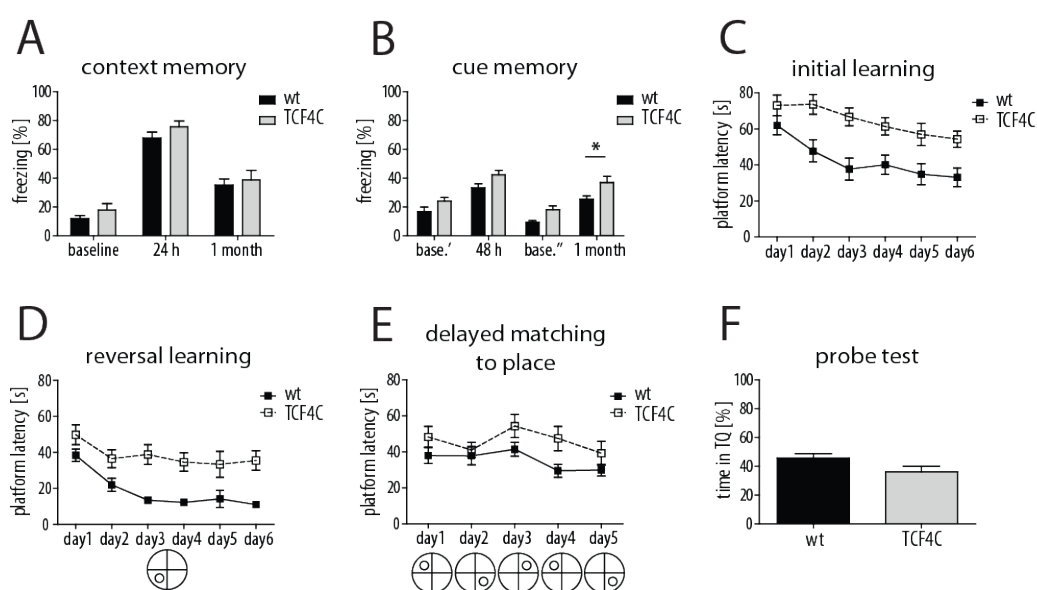
Figure 4.14: Cognition in *Tcf4*C mice. A) Context FC was not affected in *Tcf4*C animals. **B)** Cue FC was reduced in *Tcf4*C in all phases (p=0.0039, two-way ANOVA -- particularly in cue memory recall 1 month later (p<0.05, Bonferroni). C) WM, *Tcf4*C mice showed pronounced impairment of initial learning (p<0.0001, two-way RM ANOVA), **D)** reversal learning (p<0.0001, two-way RM ANOVA) **E)** and DMP (p=0.0182, two-way RM ANOVA). **F)** No significant differences in probe test were observed. Bar graph represent mean with SEM. **Abbreviations**: Fear conditioning (FC), Morris water maze (MWM), delayed matching to place (DMP).

4.3.4 Behavioural profiles of *Tcf4*tg and *Tcf4*C mice

We applied the approach described in section 4.3 and in our paper[178], to analyse behaviour of *Tcf4*tg and *Tcf4*C mice. In case of *Tcf4*tg mice, we used the data from two G×E experiments: 1) the *Tcf4*tg *Young* cohort, 2) a cohort, analysed Ananya Chowdhury in the MSc thesis[203], in which *Tcf4*tg mice were subjected to SD or control condition (individual housing with daily handling). For *Tcf4*C, the data from the cohort housed in IR, described above, were used. Detailed statistical tests are presented in Table 4.5 on domain, superdomain and symptom class level and in Table 1 in the Appendix A on measure, trait level.

  *Tcf4*tg showed no major impairments in EE, except from a mild reduction in curiosity (Fig. 4.15A). In the control condition they exhibited mild deficits in spatial learning (Fig. 4.15A) and enhanced perseveration (Fig. 4.15B). Upon IR and SD *Tcf4*tg mice displayed impairment of spatial learning (Fig. 4.15C); however, in IR it failed to reach significance after correction for multiple testing. In both IR and SD, *Tcf4*tg mice showed enhanced perseveration, and impaired spatial learning and memory recall upon SD (Fig. 4.15D). Strong disruption of spatial learning was also evident in *Tcf4*C mice, next to a mild deficit in working memory (Fig. 4.15C). Detailed analysis of the cognition symptom class in *Tcf4*tg mice revealed normal performance in EE, mild impairment in the control condition (Fig. 4.15A), strong perseveration upon IR and moderate perseveration and impairment of memory recall upon SD (Fig. 4.15B). *Tcf4*C mice, on the other hand, displayed striking impairments in all aspects of spatial learning and mildly reduced working memory (Fig. 4.15E,F).

  We have also analysed the environment effects in the two *Tcf4*tg G×E cohorts. Similarly like in the wildtype study (see: section 4.3.1), IR compared to EE, induced positive symptoms (hyperactivity), negative symptoms (pain insensitivity, reduced curiosity and motivation) and cognitive deficits (fear memory and spatial learning) (Fig. 4.13). Since SD was normalised to the control condition, we cannot compare these data to the wildtype study. In SD animals, we found cognitive impairments in memory recall, perseveration and spatial learning (Fig. 4.13). They also showed anxiety and reduced motivation, but the difference did not pass the significance threshold for negative symptom class.
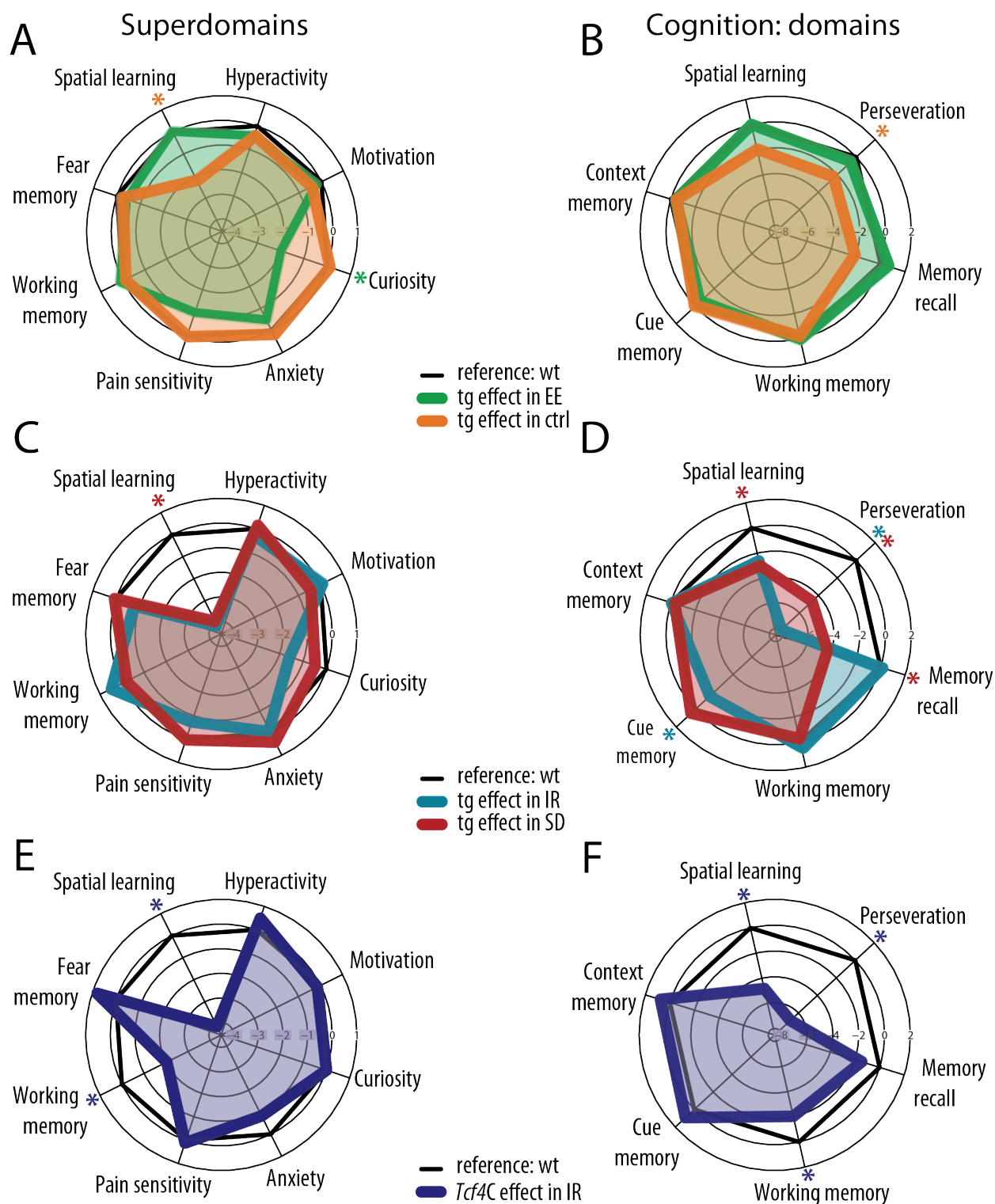
Figure 4.15: Behavioural profiles of _Tcf4_tg and _Tcf4_C mice. Radar charts represent behavioural superdomains (A,C,E) and cognitive domains (B,D,F) of young adult _Tcf4_tg (A–D) and _Tcf4_C mice (E,F), relative to the wt animals in the same condition. Significant differences are indicated by stars in corresponding colours. **A,B)** _Tcf4_tg mice in EE (green) showed no impairments, except from reduced curiosity (A). In the control condition (orange) _Tcf4_tg mice displayed moderate spatial learning deficit(A) and perseveration (B). **C)** _Tcf4_tg exhibited strong impairment of spatial learning upon SD and a tendency upon IR. **D)** _Tcf4_tg showed increased perseveration and diminished cue memory upon IR and impairments of spatial learning, perseveration and reduced memory recall upon SD. **E,F)** _Tcf4_C mice displayed a strong impairment of spatial learning (spatial learning and perseveration) and moderate deficits in working memory.

Table 4.5: Genetic main effects in *Tcf4tg* and *Tcf4C* mice in different environments: domains, superdomains, symptom classes. Significant differences are marked in bold and in stars in case of P_G. Numbers of degrees of freedom are marked for each statistic in subscript. P_G — global p-value, multivar. — multivariate, Y_altern. — alternations in Y maze.

Superdomain	Domain	Measure	P_G	EE environment tg/wt Effect	Statistic	P	IR environment tg/wt Effect	Statistic	P	SD environment tg/wt Effect	Statistic	P	IR environment ko/wt Effect	Statistic	P	G×E $P_{IR/EE}$	$P_{SD/ctrl}$
COGNITIVE SYMPTOM CLASS		multivar.	*	-0.127	$t_{80}=0.438$	0.663	-1.811	$t_{86}=-2.89$	**0.005**	-1.997	$t_{82}=-4.372$	**<0.001**	-1.632	$t_{86}=-3.723$	**<0.001**	0.019	ns
Spatial Learning		multivar.	*	0.015	$t_{76}=0.04$	0.969	-4.103	$t_{82}=-2.397$	0.019	-3.899	$t_{85}=-6.578$	**<0.001**	-4.112	$t_{82}=-6.670$	**<0.001**	0.022	0.039
	Memory recall	multivar.	*	0.645	$t_{50}=1.21$	0.232	0.002	$t_{53}=0.004$	0.997	-4.321	$t_{56}=-6.698$	**<0.001**	-1.456	$t_{26}=-1.682$	0.105	0.047	ns
	Perseveration	multivar.	*	-0.621	$t_{50}=-0.849$	0.400	-7.877	$t_{54}=-2.919$	**0.005**	-4.698	$t_{56}=-6.020$	**<0.001**	-6.862	$t_{54}=-4.632$	**<0.001**	0.014	0.046
	Spatial learning	multivar.	*	-0.093	$t_{50}=-0.128$	0.899	-2.598	$t_{54}=-1.469$	0.148	-3.035	$t_{56}=-3.378$	**0.001**	-4.834	$t_{54}=-4.815$	**<0.001**	ns	ns
	Baseline control	*multivar.*	*	*0.63*	$t_{50}=0.814$	*0.419*	*1.653*	$t_{54}=0.929$	*0.357*	*0.068*	$t_{48}=0.179$	*0.858*	*-0.791*	$t_{54}=-1.026$	*0.309*	*ns*	*ns*
Fear memory		multivar.	*	-0.413	$t_{54}=-0.939$	0.352	-0.807	$t_{58}=-2.056$	0.044	-0.318	$t_{53}=-1.129$	0.271	0.806	$t_{53}=1.433$	0.158	ns	ns
	Context memory	multivar.	*	-0.417	$t_{52}=-0.83$	0.410	-0.066	$t_{58}=-0.144$	0.886	0.453	$t_{23}=0.801$	0.431	0.763	$t_{46}=1.512$	0.137	ns	ns
	Cue memory	multivar.	*	-0.467	$t_{52}=-0.729$	0.469	-1.548	$t_{58}=-3.437$	**0.001**				0.935	$t_{54}=1.585$	0.119	ns	ns
	Social fear memory	*multivar.*	*							*1.153*	$t_{56}=2.099$	*0.040*				*ns*	*ns*
Working memory	Working memory	Y_altern.	ns	0.104	$t_{26}=0.175$	0.863	0.439	$t_{28}=0.581$	0.566	-0.218	$t_{28}=-0.300$	0.767	-2.032	$t_{28}=-2.666$	**0.013**	ns	ns
NEGATIVE SYMPTOM CLASS		multivar.	*	-0.922	$t_{110}=-3.359$	**0.001**	-0.389	$t_{121}=-0.682$	0.497	-0.159	$t_{88}=-0.537$	0.593	-0.018	$t_{118}=-0.028$	0.978	ns	ns
Pain sensitivity	Pain sensitivity	HP-pain	*	-1.032	$t_{26}=-0.935$	0.358	-0.773	$t_{28}=-0.348$	0.730	0.371	$t_{87}=0.641$	0.523	0.120	$t_{28}=0.098$	0.923	ns	ns
	Pain sensitivity	multivar.	*	-0.492	$t_{54}=-1.251$	0.216	-0.115	$t_{58}=0.49$	0.626	-0.486	$t_{57}=-0.828$	0.411	-0.829	$t_{83}=-1.271$	0.207	ns	ns
	Anxiety	multivar.	*	-1.994	$t_{54}=-2.742$	**0.008**			0.221					$F_{1.0,27.2}=0.251$	0.621	ns	ns
	Curiosity	multivar.	*	-0.246	$t_{54}=-0.403$	0.689	-1.56		0.932	-0.439	$t_{58}=-2.045$	0.045				ns	ns
	Motivation	multivar.	*	-0.418	$t_{54}=-0.824$	0.413	0.115	$t_{59}=0.086$	0.791	0.163	$t_{58}=0.560$	0.577	-0.142	$t_{53}=-0.287$	0.775	ns	ns
POSITIVE SYMPTOM CLASS		multivar.	*	0.409	$t_{110}=0.89$	0.376	-0.224	$t_{60}=-0.266$	0.360	0.776	$t_{117}=-1.205$	0.231	0.49	$t_{58}=1.07$	0.289	ns	ns
Hyperactivity	Ambulation	multivar.	*				-0.768	$t_{119}=-0.919$					0.447	$t_{13}=0.832$	0.407	ns	ns
	Speed	multivar.	*	-1.238	$t_{52}=-1.553$	0.127	-0.087	$t_{55}=-0.071$	0.944	-0.413	$t_{56}=-1.180$	0.243	0.38	$t_{56}=0.944$	0.349	ns	ns

4.4 Isolation rearing-induced hypoalgesia in wt mice

In the course of our studies we observed that IR, but not SD[178], leads to *hypoalgesia* – reduced sensitivity to pain — known to occur in isolated mice[134,135]. It affects various kinds of pain: e.g. thermal, chemical[204] and electric shocks (Fig. 2J,K, Appendix A). Pain insensitivity is also an endophenotype of schizophrenia observed in patients[205–207] and their relatives[208] – which supports the use of social isolation in rodents for modelling psychotic diseases. However, the mechanism of hypoalgesia in isolated rodents is not understood. Several mechanisms in peripheral and central nervous system could be potentially involved, e.g. changes in neuronal plasticity, neurotransmission, hormone release, endocannabinoids or endogenous opioids.

As the opioid system may be involved in IR-induced hypoalgesia[209–211], we focused on *endorphins* — analgesic peptides[212] that originate from proopiomelanocortin (POMC) in pituitary gland and hypothalamus and are released to the blood and act on opioid receptors[213]. Endorphins regulate several biological processes including analgesia, reward and cognition[214] and are involved in schizophrenia[215]. However, there is no consistent data on whether levels of β-endorphin, the most studied endorphin, are altered in the blood of schizophrenic patients [216–220]. Inconsistency may be due to several factors that can play a role e.g. diurnrhythm[221–224] or body weight[225,226].

To investigate potential mechanisms of isolation-induced hypoalgesia we analysed a cohort of C57Bl/6N mice (Charles River), subjected to IR (n=7), EE (n=6) or 3 weeks of SD (n=7) from the age of 4 weeks. At the age of 12 weeks the animals were sacrificed and blood, hypothalamic, PFC, and hippocampal tissue was isolated. Lumbar DRGs and spinal cord were prepared by Theresa Kungl[7].

We attempted to measure basal β-endorphin serum levels in IR mice and EE controls. We also analysed gene expression in hypothalamus (important for hormone release and analgesia), DRGs (the first pain information processing point in peripheral after pain receptors) and PFC (involved in top–down mechanisms pain regulation).

4.4.1 β-endorphin ELISA

The level of β-endorphin, measured in mouse serum using an ELISA kit, showed no significant difference between EE and IR animals. However, the values measured in serum were very low (just above the lower detection range of the kit). Expected concentrations were around 1000 pg/ml (Fig. 8 in Appendix C, page 108). Trials with the measured blood plasma instead of serum were not successful. Thus this result has to be taken with caution and optimally the measurement should be performed with an alternative method, e.g. mass spectrometry.

---

[7]Dept. Neurogenetics, Max-Planck-Institute of Experimental Medicine, Göttingen, Germany

4.4.2 RNAseq analysis in hypothalamus and dorsal root ganglia

Hypothalamus Differential RNA expression analysis revealed 13 genes upregulated in IR mice (Tab. 4.6), among which were *Ramp3, Oxt, Avp* and *Vgf*. We also observed downregulation of hemoglobin genes *Hba* and *Hbb*, which is contradictory to observations in rats[127], thus it may be a preparation artefact. In GSEA no gene sets passed the FDR<25% threshold. At nominal p-value<1% one gene set ("Spindle") was upregulated in hypothalamus upon IR (Tab. 4.8) and 6 gene sets were downregulated (Tab. 4.9).

Dorsal root ganglia (DRGs) 63 genes were differentially regulated in DRGs of socially isolated mice. Among them *P2ry1* was upregulated and *Vgf, Bdnf* and *Npy1r* were downregulated (Tab. 4.7). GSEA revealed 4 gene sets significantly enriched at FDR<25% and 12 at the nominal p-value<1% (Tab. 4.10. 3 gene sets were downregulated at the nominal p-value<1% (Tab. 4.11).

Table 4.6: Genes downregulated in hypothalamus upon isolation rearing. The "log2 fold change" column shows the fold change of IR (n=3) in reference to EE (n=3).

Gene	log2 fold change	p-value	q-value
Vgf	-0.551035	5.65882E-06	0.00728805
Avp	-0.700171	1.95312E-08	3.45873E-05
Oxt	-0.884047	7.10254E-11	3.35406E-07
Hbb-b1,Hbb-b2	-0.953084	1.22439E-08	0.00002478
Aldh1a2	-0.958683	4.36736E-05	0.0475942
Hba-a1,Hba-a2	-0.960583	1.05089E-09	2.48133E-06
Hba-a1,Hba-a2	-0.995811	1.95938E-10	6.93963E-07
Synpo2	-0.99893	0.000001669	0.00236447
Beta-s	-1.00092	4.75175E-14	3.36591E-10
Ptpn3	-1.06501	5.25983E-10	1.49032E-06
Ramp3	-1.24534	4.26193E-05	0.0475942
Prkcd	-1.58436	0	0
Slc17a7	-1.70666	2.71124E-08	4.26779E-05

Table 4.7: Genes regulated in DRGs upon isolation rearing. The "log2 fold change" column shows the fold change of IR (n=3) in reference to EE (n=3).

Gene	log2 fold change)	p-value	q-value
upregulated			
Myh1	5.28286	1.33855E-05	0.00449921
Myh4	5.11314	5.79981E-13	1.13615E-09
Tnnt3	4.73327	1.13685E-07	6.36871E-05
Atp2a1	4.44052	1.47011E-07	7.90623E-05
Ckm	3.98091	9.9351E-06	0.0035152
Acta1	3.19523	3.70517E-11	3.832E-08
Bub1b	1.23776	3.13201E-05	0.00877288
Ptgds	0.986996	0	0
Agtr1a	0.773642	4.50134E-07	0.000208691
H2-Ab1	0.596775	4.07763E-05	0.0109647
Thbs1	0.542664	0.000205695	0.044606
Cd74	0.520954	0.000170995	0.037689

Continued on next page

Table 4.7 – *Continued from previous page*

Gene	log2 fold change)	p-value	q-value
Col3a1	0.44349	4.1547E-08	2.53909E-05
Chrna6	0.406638	1.54371E-05	0.00506225
Lpar3	0.351372	0.00016359	0.0366578
P2ry1	0.340415	7.65321E-05	0.0190551
Dcn	0.324887	0.000154903	0.036538
Dpp10	0.307874	2.13286E-05	0.00651733
Acpp	0.30243	0.000028578	0.00835284
Col1a2	0.295389	6.70262E-05	0.0173302
downregulated			
Hsph1	-0.269234	0.000110112	0.0269173
Serpina3n	-0.279389	0.000151786	0.0364423
Calca	-0.304452	6.06486E-06	0.00226506
Itga7	-0.324319	1.11202E-05	0.00383363
Sfrp5	-0.327904	0.000162263	0.0366578
Lgmn	-0.341363	1.01553E-06	0.000440447
Pak1ip1	-0.357659	2.92483E-05	0.00836687
Gap43	-0.363329	1.13635E-06	0.000477446
Tfrc	-0.372069	2.98611E-07	0.000143387
Jun	-0.372814	7.23423E-06	0.00262876
Chl1	-0.374771	5.19592E-07	0.000232864
Ngfr	-0.384488	8.64147E-09	6.11498E-06
Plxna4	-0.436119	3.88159E-09	3.06988E-06
Nptx1	-0.459688	5.88496E-11	5.27489E-08
Ptchd2	-0.465143	2.06001E-05	0.00644112
Serpinb1a	-0.497715	6.91746E-09	5.16696E-06
Ly86	-0.50427	1.70444E-08	1.09125E-05
Adcyap1	-0.513163	2.29052E-09	1.92476E-06
Flrt3	-0.520852	0.000209712	0.0447552
Eif2s3y	-0.527505	0.000158595	0.0366578
Etv5	-0.5374	9.70157E-12	1.1858E-08
Lars2	-0.540064	9.01501E-13	1.51509E-09
Sema6a	-0.550827	0.000064524	0.0170103
Nkain1	-0.625398	1.58729E-05	0.00508121
Sox11	-0.62693	7.31773E-05	0.0185636
Rn45s	-0.663448	0	0
Angptl2	-0.679788	2.98396E-06	0.00114627
Hba-a1,Hba-a2	-0.711127	4.37299E-11	4.19963E-08
Hba-a1,Hba-a2	-0.714693	7.00462E-12	9.41771E-09
Npy1r	-0.717397	1.54751E-08	1.04032E-05
Tifa	-0.729562	2.39201E-07	0.000123695
Hbb-b1,Hbb-b2	-0.755756	5.91527E-13	1.13615E-09
Beta-s	-0.762768	0	0
Nts	-0.871439	2.90484E-06	0.00114627
Bdnf	-0.919004	5.20532E-08	3.04285E-05
Pappa	-1.04208	2.75491E-12	4.11553E-09
Vgf	-1.04544	0	0
Plaur	-1.12381	3.70315E-05	0.010161
Tmem173	-1.1371	2.51355E-05	0.00750993
Atf3	-2.01481	0	0
Gpr151	-2.07325	2.34476E-06	0.000955313
Ecel1	-2.26513	2.86617E-07	0.000142725
Sprr1a	-5.02805	2.87046E-11	3.21611E-08

Table 4.8: Gene sets upregulated in hypothalamus upon isolation rearing. GSEA revealed no gene sets significantly deregulated at FDR<25%, but "Spindle" is the top upregulated gene set at nominal p-value<1%.

NAME	SIZE	ES	NES	NOM p-val	FDR q-val	FWER p-val
SPINDLE	38	-0.6309913	-1.5952135	0.009230769	1	0.999
CELL CYCLE CHECKPOINT GO 0000075	45	-0.57641065	-1.4996719	0.026239067	1	1
TELOMERIC DNA BINDING	9	-0.7804627	-1.4428499	0.08396947	1	1

Table 4.9: Gene sets downregulated in hypothalamus upon isolation rearing. 6 gene sets associated with transmembrane transport, secretion and neurite development are downregulated upon IR at nominal p-value<1%, but not at FDR<25%.

NAME	SIZE	ES	NES	NOM p-val	FDR q-val	FWER p-val
PHOSPHATE TRANSMEMBRANE TRANSPORTER ACTIVITY	12	0.8746991	1.6164454	0	1	0.93
SECRETORY GRANULE	17	0.7633645	1.5262561	0.008169935	1	1
INORGANIC ANION TRANSPORT	17	0.7525263	1.5033239	0.025316456	1	1
ANCHORED TO MEMBRANE	11	0.8161317	1.499629	0.017350158	1	1
AMINO ACID TRANSMEMBRANE TRANSPORTER ACTIVITY	29	0.6955017	1.497823	0.020249221	1	1
NEURITE DEVELOPMENT	47	0.62744933	1.4962971	0.01433121	1	1
INORGANIC ANION TRANSMEMBRANE TRANSPORTER ACTIVITY	18	0.7388429	1.4873075	0.021276595	1	1
ANCHORED TO PLASMA MEMBRANE	11	0.8161317	1.4856927	0.032786883	1	1
MONOOXYGENASE ACTIVITY	21	0.7071364	1.4703019	0.03069467	1	1
DIGESTION	38	0.633322	1.4671487	0.030120483	1	1
SKELETAL DEVELOPMENT	95	0.56289417	1.4608468	0.011126565	1	1
ACUTE INFLAMMATORY RESPONSE	11	0.805388	1.4567382	0.03069467	1	1
GENERATION OF NEURONS	76	0.5691497	1.4501585	0.030478954	1	1
AXONOGENESIS	38	0.62605125	1.4492811	0.033280507	1	1
EXOPEPTIDASE ACTIVITY	29	0.65743476	1.4420316	0.05304212	1	1
OXIDOREDUCTASE ACTIVITY ACTING ON NADH OR NADPH	24	0.671245	1.4372844	0.048309177	1	1
REGULATION OF MUSCLE CONTRACTION	18	0.7050116	1.4246622	0.065318815	1	1
CARBOXYLIC ACID TRANSMEMBRANE TRANSPORTER ACTIVITY	43	0.60864633	1.421431	0.056574922	1	1
NEURON DEVELOPMENT	55	0.5885536	1.4203693	0.033282906	1	1
HORMONE METABOLIC PROCESS	26	0.67117655	1.419442	0.044207316	1	1
ANION CATION SYMPORTER ACTIVITY	16	0.7275763	1.4185106	0.05	1	1
PHAGOCYTOSIS	13	0.7500188	1.4153485	0.04700162	1	1
ION TRANSMEMBRANE TRANSPORTER ACTIVITY	259	0.4848874	1.4136977	0.009815951	1	1
NEGATIVE REGULATION OF MYELOID CELL DIFFERENTIATION	9	0.7938968	1.412717	0.059800666	1	1
ION CHANNEL ACTIVITY	140	0.51552075	1.4119701	0.011363637	1	1
BODY FLUID SECRETION	10	0.7882244	1.4114146	0.06935484	1	1
SYMPORTER ACTIVITY	30	0.6400289	1.411332	0.05206738	1	1
ORGANIC ACID TRANSMEMBRANE TRANSPORTER ACTIVITY	44	0.6038959	1.4098958	0.042089984	1	1
SUBSTRATE SPECIFIC TRANSMEMBRANE TRANSPORTER ACTIVITY	324	0.4754348	1.4073892	0.002350176	1	1
NEUROGENESIS	85	0.5433593	1.4070809	0.023876404	1	1
POSITIVE REGULATION OF CYTOKINE SECRETION	7	0.8249769	1.4018607	0.08094435	1	1
NEURON DIFFERENTIATION	69	0.55657935	1.3999331	0.039492242	1	1
OXIDOREDUCTASE ACTIVITY ACTING ON THE ALDEHYDE OR OXO GROUP OF DONORS	22	0.66011435	1.3980609	0.073836274	1	1
RECEPTOR MEDIATED ENDOCYTOSIS	32	0.61942405	1.391357	0.06456693	1	1
GROWTH FACTOR BINDING	29	0.64603925	1.3902059	0.052227344	1	1
OXIDOREDUCTASE ACTIVITY GO 0016705	29	0.64717835	1.3876555	0.06259781	1	1
AMINO ACID METABOLIC PROCESS	75	0.54597354	1.3866458	0.050754458	1	1
CYTOKINE AND CHEMOKINE MEDIATED SIGNALING PATHWAY	19	0.68204933	1.3807732	0.07620529	1	1
SUBSTRATE SPECIFIC TRANSPORTER ACTIVITY	366	0.4591599	1.3791789	0.005707763	1	1
EXTRACELLULAR SPACE	209	0.48399374	1.3786215	0.012562814	1	1
OXIDOREDUCTASE ACTIVITY GO 0016616	48	0.58165526	1.3758867	0.06268222	1	1

Table 4.10: Gene sets upregulated in DRGs upon isolation rearing. GSEA showed upregulation of four contractile fiber-associated gene sets at FDR<25% and upregulation several gene sets associated with response to stimuli and transcriptional activity at nominal p-value<1% in IR mice.

NAME	SIZE	ES	NES	NOM p-val	FDR q-val	FWER p-val
STRUCTURAL CONSTITUENT OF MUSCLE	32	-0.83375263	-1.8147119	0	0.012796508	0.012
CONTRACTILE FIBER	24	-0.85539	-1.7810092	0	0.01965319	0.037
CONTRACTILE FIBER PART	22	-0.8451829	-1.7275283	0	0.05542059	0.149
MYOFIBRIL	19	-0.8686934	-1.7019317	0	0.081350945	0.267
MUSCLE DEVELOPMENT	92	-0.6301342	-1.613492	0	0.39160344	0.858
ACTIN CYTOSKELETON	124	-0.5964722	-1.6131645	0.001697793	0.32829913	0.86
REGULATION OF MUSCLE CONTRACTION	18	-0.7999004	-1.5672011	0.009140768	0.5953036	0.981

Continued on next page

Table 4.10 – *Continued from previous page*

| NAME	SIZE	ES	NES	NOM p-val	FDR q-val	FWER p-val
POSITIVE REGULATION OF LYMPHOCYTE ACTIVATION	20	-0.77064747	-1.5632821	0.014842301	0.5525919	0.986
REGULATION OF BINDING	56	-0.6385182	-1.5530825	0.006980803	0.56979066	0.99
STRIATED MUSCLE DEVELOPMENT	39	-0.6750973	-1.5507587	0.015873017	0.53100055	0.992
TRANSFORMING GROWTH FACTOR BETA RECEPTOR SIGNALING PATH-WAY	35	-0.6931986	-1.5491892	0.005395684	0.49290568	0.993
RESPONSE TO LIGHT STIMULUS	45	-0.6622498	-1.5343223	0.005328597	0.5486485	0.997
REGULATION OF HEART CONTRACTION	24	-0.7321811	-1.510626	0.03125	0.6809449	1
SKELETAL MUSCLE DEVELOPMENT	30	-0.6943268	-1.506939	0.019855596	0.6605015	1
REGULATION OF MULTICELLULAR ORGANISMAL PROCESS	135	-0.55532265	-1.504274	0.003412969	0.638151	1
POSITIVE REGULATION OF TRANSCRIPTION FACTOR ACTIVITY	24	-0.7070367	-1.4663235	0.035971224	0.92684716	1
REGULATION OF DNA BINDING	45	-0.6376562	-1.4650983	0.031578947	0.88285565	1
MUSCLE CELL DIFFERENTIATION	22	-0.71898586	-1.4601359	0.042226486	0.8774138	1
MYOBLAST DIFFERENTIATION	17	-0.75436294	-1.4585813	0.059615385	0.8452153	1
POSITIVE REGULATION OF BINDING	28	-0.6861234	-1.4572084	0.032380953	0.81304485	1
REGULATION OF TRANSCRIPTION FACTOR ACTIVITY	38	-0.64849234	-1.451817	0.031034483	0.81936884	1
POSITIVE REGULATION OF DNA BINDING	26	-0.69031984	-1.4511931	0.028368793	0.7867177	1
MYOSIN COMPLEX	15	-0.7661521	-1.4367992	0.04725898	0.86807853	1
RESPONSE TO RADIATION	58	-0.59707314	-1.42647	0.026269702	0.9167564	1
CALCIUM MEDIATED SIGNALING	16	-0.74069923	-1.4194865	0.063097514	0.93962485	1
DETECTION OF STIMULUS INVOLVED IN SENSORY PERCEPTION	18	-0.71530676	-1.4192829	0.0591716	0.90500766	1
POSITIVE REGULATION OF T CELL ACTIVATION	18	-0.72044635	-1.4188728	0.06214689	0.87515736	1
CYTOSKELETAL PART	223	-0.4950115	-1.4084319	0.004761905	0.9284144	1
REGULATION OF LYMPHOCYTE ACTIVATION	31	-0.65021044	-1.405502	0.048327137	0.9199887	1

Table 4.11: Gene sets downregulated in DRGs upon isolation rearing GSEA showed downregulation of three gene sets at nominal p-value<1%.

NAME	SIZE	ES	NES	NOM p-val	FDR q-val	FWER p-val
KERATINOCYTE DIFFERENTIATION	15	0.83402413	1.6222495	0.00203666	1	0.87
HORMONE ACTIVITY	40	0.6971614	1.6105977	0	1	0.906
CELL PROJECTION PART	16	0.79349333	1.56011	0.011135858	1	0.986
REGULATION OF SECRETION	34	0.6784604	1.5398166	0.02293578	1	0.996
DEVELOPMENT OF PRIMARY SEXUAL CHARACTERISTICS	25	0.68825275	1.5004619	0.03456221	1	1
REGULATION OF PROTEIN SECRETION	17	0.75157595	1.4649369	0.039911307	1	1
CELLULAR CARBOHYDRATE CATABOLIC PROCESS	22	0.67175215	1.4365059	0.0494382	1	1
CARBOHYDRATE CATABOLIC PROCESS	23	0.6717515	1.4344515	0.06535948	1	1
GLUCOSE METABOLIC PROCESS	26	0.6462377	1.431045	0.038812786	1	1
OXIDOREDUCTASE ACTIVITY	259	0.46074706	1.422999	0	1	1
REPRODUCTIVE PROCESS	133	0.48050532	1.370164	0.02356021	1	1

4.4.3 RT-qPCR validation of RNAseq candidate genes

RT-qPCR in hypothalamus and DRGs To validate the candidate genes from RNAseq, we performed RT-qPCR on hypothalamic and DRG cDNA of 12 weeks old animals subjected to IR (n=7), SD (n=7) or EE (n=6). We confirmed downregulation of *Bdnf* and *Npyr1* in DRGs and *Vgf* in hypothalamus and DRGs. Similar downregulation was present also in the SD group. In the hypothalamus *Oxt* showed a tendency of reduced levels in IR and SD mice, and *Avp* was significantly downreagulated only in SD mice. This result may be explained by the fact that SD mice were kept in isolation for 5 weeks after the end of stress and at the moment of sacrifice they displayed also IR symptoms.

To prove that hypoalgesia is an IR-specific phenomenon, we will repeat the experiment, but sacrifice the mice at earlier age, to avoid the prolonged isolation period after the end of stress. The experiment is ongoing. First analysis of pain sensitivity in 7.5 weeks old mice showed a tendency for increased pain threshold in IR group compared to EE and SD mice (Fig. 9 Appendix C)
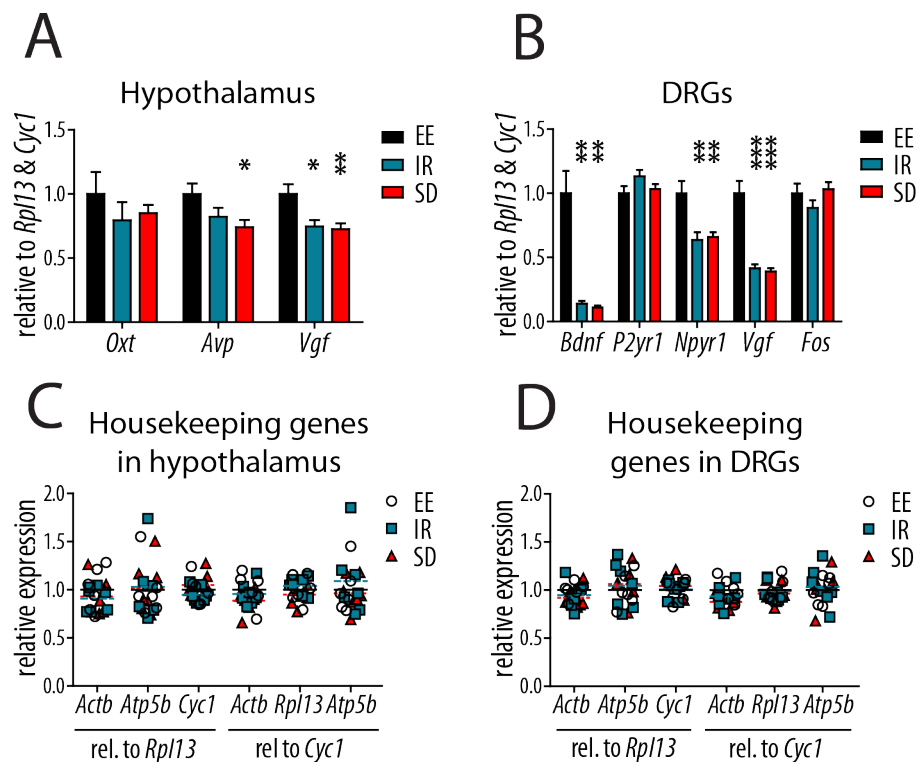
Figure 4.16: IR-induced hypoalgesia: validation of RNAseq candidates by RT-qPCR. A) In hypothalamus, oxytocin (*Oxt*) and arginine vasopressin (*Avp*) mRNAs were reduced in IR mice, but failed to reach significance due to high standard deviations. However, downregulation of *Avp* was significant in SD mice (p=0.023). *Vgf* was downregulated in IR (p=0.0138) and SD mice (p=0.0099). **B)** In DRGs IR-induced downregulation of *Bdnf* (p=0.0012, Mann Whitney test), *Npyr1* (p=0.0065), *Vgf* (p=0.0002) were confirmed. Similar changes were observed in SD mice: *Bdnf* (p=0.0022, Mann Whitney test), *Npyr1* (p=0.0078) and *Vgf* (p=0.0001). **C,D)** *Rpl13* and *Cyc1* were chosen as the reference genes due to best consistency and similar means between the experimental groups. *Actb* was slightly decreased in IR and SD mice and *Atp5b* showed higher deviations between the animals. Bar graphs represent means with SEM (n=6–7 per group). Differences were compared with unpaired t-tests, unless stated differently.

RT-qPCR in PFC   Candidate screening using RT-qPCR showed no significant deregulation of genes associated with the opioid system (*Penk, Pdyn, Oprk1*), a cannabinoid receptor gene (*Cnr1*), schizophrenia-associated genes influencing pain sensitivity (*Disc1, Comt1, Nrg1-III*[227]) nor genes associated with interneurons (*Prvlb, Gad1, Gad2*) and dopaminergic system (*Drd1a*)(Fig. 10, page 109). Only *Pomc*, encoding proopiomelanocortin — the precursor of β-endorphin — was upregulated in IR compared to EE in PFC (6, Fig. 10B) and showed a similar tendency in the hypothalamus (Fig. 10Q). However, this result is influenced by an outlier with very high *Pomc* levels.

Discussion

5.1 Behavioural profiling in mice

I N THE WILDTYPE STUDY described in our paper[178], we developed an approach to behavioural analyses, inspired by the way Van Os and Kapur[5] presented their classification of symptoms in psychotic diseases. They distinguished five domains: psychosis (positive symptoms), volition (negative symptoms), cognition, affective dysregulation and bipolar symptoms. Similar attempts to classify symptoms into domains are being made in the Research Domain Criteria (RDoC) project[39]. We adapted this stategy to study murine behaviour as syndromes, which is more clinically relevant than looking at single symptoms. Consequently, we created behavioural profiles of mouse models, based on multiple behavioural tests.

Data calibration and normalization allow to compare independent experiments. This is important, since only a limited number of animals can be tested in a single cohort and often several cohorts are needed to test different experimental conditions. In our approach, we try to overcome this problem. It can be applied to equate data from different cohorts, handled by different experimenters and even from different laboratories — provided that all cohorts contain identical calibrator groups (in our case wildtype mice in enriched environment). This way we could compare not only different housing conditions, but also mice carrying different mutations or treated with different drugs. Calibration makes it also possible to compare results expressed in different scales and units (e.g. seconds, meters). Consequently, we can include different tests that measure similar behaviours into one analysis. We could also create profiles containing not only behavioural, but also histological, electrophysiological, molecular and other kinds of data. By comparing profiles of different mouse mutants, we can evaluate their relevace to particular psychiatric diseases or their aspects. For example, in our study, social defeat (SD) induced depressive-like behaviour associated with negative symptoms, isolation rearing (IR) was more relevant for positive symptoms[178] and *Tcf4* overexpression affected specifically the cognitive domain (see page 68).

We applied multivariate statistics to merge measures of similar behaviours into higher-order categories: traits, domains superdomains and symptom classes. In this process, called dimension reduction, we reveal broader patterns of behaviour and reduce the effects of correction for multiple testing on significance thresholds. We used 15 animals per group, which is the standard *n* in behavioural studies on mice. Power analysis showed that this number is sufficient to detect only large effect sizes. Detecting smaller effects requires testing more animals or restricting the analyses to fewer domains, to reduce the influence multiple testing on significance threshold.

We present behavioural profiles in radar charts, which allows to plot huge data sets in a single figure. By overlaying them, we can also compare experimental groups to each other. Plots can be generated at every level of dimension reduction. On the trait level they show all performed tests and are useful mainly for behavioural scientists. Plots on the domain level are more interesting for clinicians, who may compare different mouse mutants to choose the one that reflects a particular class of symptoms best.

5.1.1 Comparison of IR and SD as models of psychotic diseases

Both IR and SD induced remarkable impairments in curiosity, fear conditioning and motivation, but with greater impact of SD. Stronger overall impairment in SD mice is reflected by the higher severity score. However, some behaviours impaired by IR are unaffected or barely changed upon SD. IR mice displayed typical for isolated rodents[136,139,228–230] hyperactivity in OF, which may be relevant for positive symptoms of schizophrenia[231]. Similarly, striking hypoalgesia, repeatedly reported in isolated rodents[134,135,230], is an endophenotype of schizophrenia[205–208,232]. The differences in behavioural profiles of IR and SD show that these two paradigms should be used to model different aspects of psychiatric diseases. While SD appears as relevant for negative symptoms, IR seems to be more suitable for positive symptoms.

It has to be noted, that our study focused on behavioural phenotype based on limited number of tests. For a broader symptom coverage and higher clinical relevance, the analysis should include more behavioural tests and be supplemented with other data, e.g. EEG recordings, electrophysiology, histology or gene expression.

5.1.2 G×E-dependent cognitive deficits in *Tcf4*tg mice

While environmental conditions (IR, SD or EE) strongly affected several murine behaviours, effects of *Tcf4* overexpression were mild and restricted to cognition. Both young and aged *Tcf4*tg mice displayed impaired fear conditioning and reversal learning upon IR, whereas EE rescued the phenotype. This influence of environment on manifestation of the *Tcf4*-dependent deficits proves the Gene × Environment interaction in the *Tcf4*tg mice.

Aged *Tcf4*tg mice, in comparison to young mice, showed no additional impairments upon IR except from subtly reduced rearing and increased swim speed. Reversal learning deficits were milder in the aged cohort, but were confirmed in the delayed matching to place (DMP) test. As no clear worsening of the symptoms was apparent in 12 months old *Tcf4*tg mice, we conclude that the *Tcf4* phenotype is independent of ageing.

*Tcf4*tg mice upon IR and SD, displayed impaired reversal learning in MWM, confirmed by disrupted delayed matching to place. Decline in reversal learning is a measure of behavioural rigidity, or perseveration — a psychological term describing *overall, perseverance in doing something to an awesome level or past an adequate point; (...) improper repeating of actions which are frequently correlated with injury to the brain's frontal lobe, incapacity (...) to switch from one*

method or process to another one[154]. Perseveration and reversal learning deficits are associated with dysfunction of the orbitofrontal cortex (OFC) and ventral striatum[18,233–235] and have been reported in schizophrenia and psychotic disorders[17,18]. In mice, reversal learning is specifically disrupted by *social* deprivation[145,236].

Comparison of behavioural profiles of *Tcf4*tg mice subjected to IR and SD[1] revealed that both IR and SD trigger cognitive impairments in the *Tcf4*tg mice. Upon IR, *Tcf4*tg mice showed impaired fear memory and typical for IR behavioural rigidity[145,236]. Upon SD they displayed milder rigidity and pronounced impairments of spatial learning and memory recall in MWM. In the control condition (individual housing with daily handling), used as reference for SD, *Tcf4*tg mice displayed similar deficits to the *Tcf4*tg IR mice (Fig. 4.15), but less severe. This is consistent with the observations in rats, that handling can diminish the effects of isolation[230]. It suggests that *Tcf4* overexpression increases vulnerability to harsh environment and the type environmental treatment determines which brain structures, and consequently, which behaviours will be affected the most.

5.1.3 Cognitive deficits and *Tcf4* expression in *Tcf4*C knockout mice

We generated the heterozygous *Tcf4* knockout mouse line *Tcf4*C. *Tcf4* exons 5–6, located directly downstream the deleted exon 4, had reduced expression in these mice and the levels subsequent exons were gradually increasing. Expression patterns of *Tcf4* exons in wt mice differed between PFC and hippocampus: exons 5–6 were highest expressed in hippocampus, but not in PFC. Exons 5–6 showed strongest downregulation in *Tcf4*C mice, which is in line with the exclusively hippocampal phenotype observed in the Morris water maze.

Several *TCF4* isoforms of various lengths and exon composition were found in humans[45,237] and in mice[200](Fig. 5.1A). Genetic analyses show that the Pitt-Hopkins syndrome is caused by deletions and nonsense mutations that occur in exons 8–20[45,80,237] (Fig. 5.1B). Transcription of this region is barely affected by the knockout, thus the *Tcf4*C mice should not be considered as a PTHS model, but rather as a tool to study functions of particular *Tcf4* isoforms.

*Tcf4*C animals showed no significant alterations in any of the analysed facial and body dimensions, even though craniofacial abnormalities and decreased body length were reported by the Sanger Institute in *Tcf4*E homozygotic females[199]. However, our method — manual measurements with a calliper – may be insufficient to detect subtle alterations in the facial features. Perhaps analysis of skull landmarks[238] or with the use of computer tomography[239] would reveal subtle dismorphisms in the *Tcf4*C mice.

5.1.4 *Tcf4*, G×E and behavioural profiling — conclusions

Behavioural experiments with *Tcf4* overexpressing and knockout mice revealed cognitive deficits in both cases — mild and environment-dependent in *Tcf4*tg mice; and strong, but restricted to spatial learning in *Tcf4*C knockouts. It appears that cognition in mice depends on *Tcf4* gene dosage in the

---

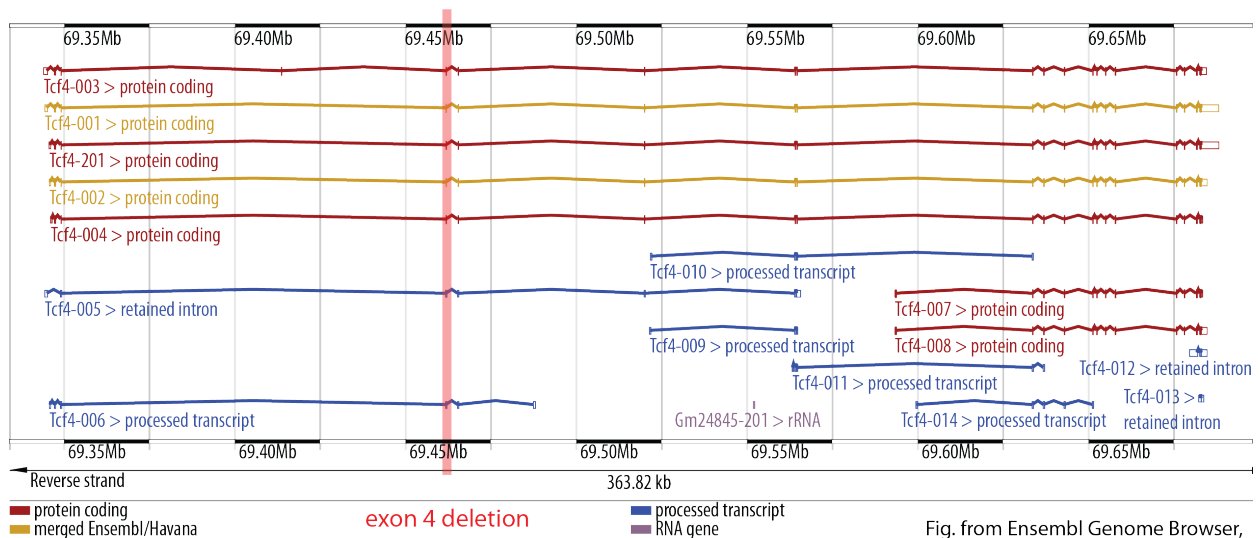[1]the *Tcf4*tg SD–ctrl data set was published in the MSc thesis of Ananya Chowdhury[203]
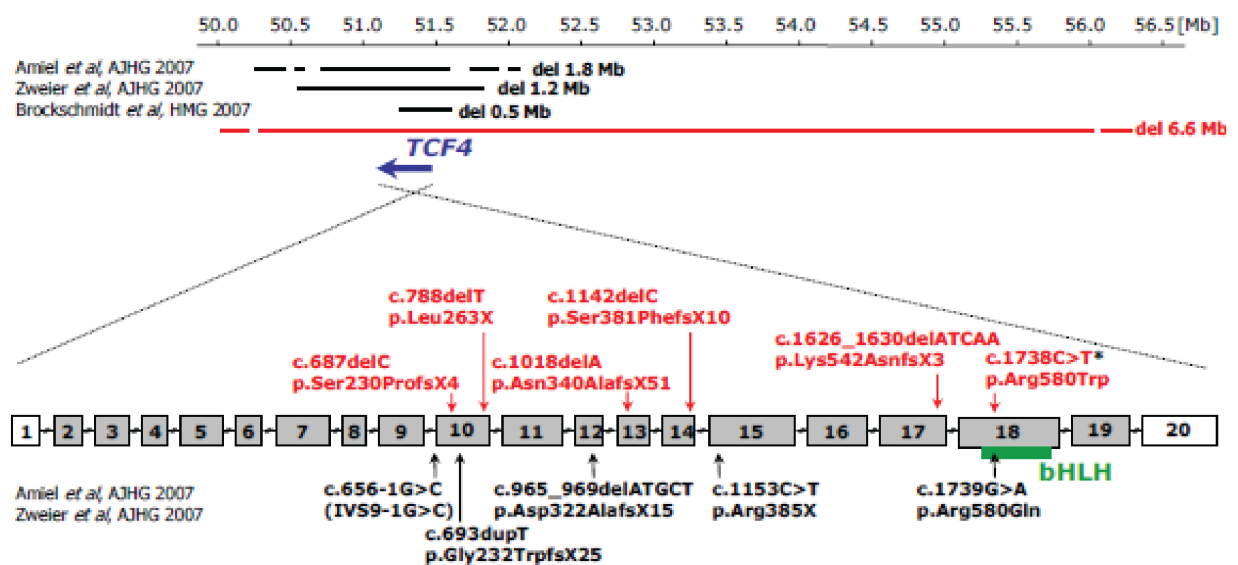
Figure 5.1: Comparison of PTHS mutations with the mutation in *Tcf4*C mice. A) Figure adapted from Ensembl Genome Browser[200]. In the *Tcf4*C line the exon 4 is deleted, which leads to frame shift and formation of non-functional *Tcf4* transcripts. Mouse *Tcf4* has numerous isoform, some of which start downstream to exon 4, e.g. short isoforms *Tcf4-007* and *Tcf4-008* located in the 3' region of the gene. These isoforms may be still functional in our knockout line. **B)** The PTHS-associated mutations are deletions and nonsense mutations in the 3' region of the human *TCF4*[45,80,237]. Therefore deleting exon 4 in the 5' region of mouse *Tcf4* may be not reflecting the situation in PTHS patients; however, is useful for studying functions of the long isoforms, e.g. *Tcf4-001* and *Tcf4-003*.

bell-shape fashion[46]. Disrupted balance, either up- or downregulation, has negative consequences (Fig. 5.2). Similar pattern has been observed for another schizophrenia risk element[240], the NRG1-ERBB4 signalling[241].

It should be noted that *Tcf4*tg mice have limited clinical relevance. *TCF4* expression may be elevated in psychotic patients[73–75] and the *Tcf4*tg mice show some schizophrenia-relevant symptoms. However, they overexpress an intron-less *Tcf4* open reading frame (overexpression of the full gene is impossible due to the huge gene size), while the schizophrenia-risk SNPs in *TCF4* are located in the introns. Therefore the *Tcf4* transgenic mice should be considered not as a clear-cut model of schizophrenia, but rather as a model for studying *Tcf4* functions in the forebrain. Similarly, *Tcf4*C knockouts are not a model of the Pitt-Hopkins syndrome, but rather a tool for studying certain *Tcf4* isoforms. Nevertheless, both mouse strains are useful for investigating the *Tcf4* functions in the brain and may help understand both diseases.
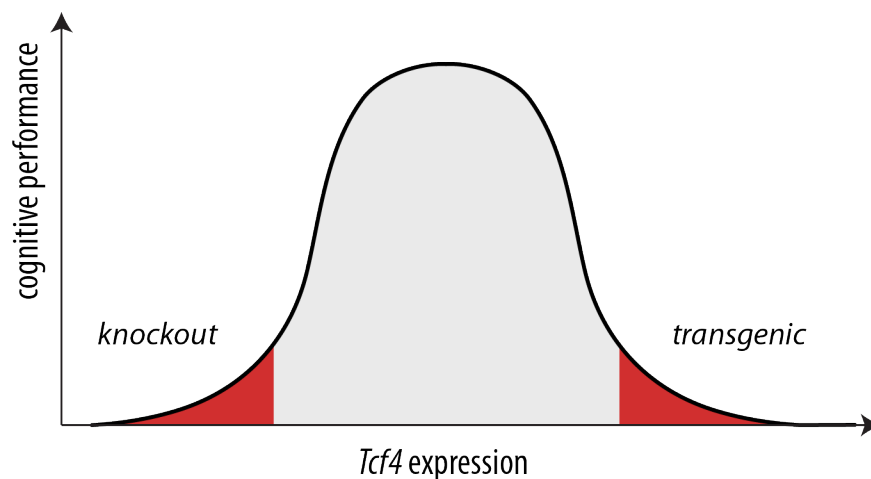
Figure 5.2: Bell-shaped relationship between *Tcf4* expression and cognition. *Tcf4* dosage influences cognitive performance — either reduced or increased levels of *Tcf4* have detrimental effect (marked in red).

5.2 Expression analyses in *Tcf4*tg mice

5.2.1 RNA sequencing

As TCF4 is a transcription factor, we expect the phenotype changes to be driven primarily by changes in gene expression on RNA level. Therefore we performed RNAseq. We found up-regulation of *Mov10* and downregulation of *Adora2a, Penk, Tac1, Drd1a, Pde10a, Pde1b* and *Foxp2* in PFC of *Tcf4*tg mice. In hippocampus, *Top3b, BC1* and *Plxna1* were up- and *Mov10* was downregulated.

Genes downregulated in PFC of *Tcf4*tg mice:

Adora2a encodes the A2A receptor of adenosine — a widespread inhibitory neuromodulator in the brain, important for fine-tuning and synchronization of neuronal activity, sleep homeostasis, hypoxia, sensorimotor gating and cognition (reviewed in[242–244]). According to the *adenosine-*

hypofunction hypothesis of schizophrenia[242], A2A receptors are proposed as a target for anty-psychotic drugs, since they have antagonistic actions to dopamine D2 receptors[244]. Adenosine receptors are blocked by caffeine[243], which in high doses has prosychotic[242,244] and anxiogenic[245] effects. *ADORA2A* is also linked to panic disorder[245] and *Adora2a*^{-/-} mice show increased anxiety[243].

Penk encodes proenkephalin A, an endogenous opioid polypeptide hormone that after proteolytic cleavage gives rise to enkephalins[246]. Enkephalins bind to δ-opioid receptors and both are involved in analgesia, reward and anxiety (reviewed in[247]). Downregulation of *Penk* in PFC has been linked to schizophrenia[248,249] and postpartum psychosis[250].

Drd1a encodes the dopamine receptor D1, which regulates AMPAR phosphorylation and trafficking to the membrane, and thus is a prominent modulator of synaptic plasticity in PFC (reviewed in[101]). Alterations in D1 activity during adolescence may have a particularly strong effect on synaptic plasticity and cortical development[101].

Tac1 encodes Protachykinin-1, a precursor of several peptides, e.g. Substance P, associated with pain perception and neuropsychiatric disorders (reviewed in[251]). *TAC1* is downregulated in the PFC of psychotic patients[252].

Pde10a and *Pde1b*, both highly expressed in striatum, encode cAMP and cAMP-inhibited cGMP 3',5'-cyclic phosphodiesterases. They regulate cAMP/PKA and cGMP/PKG signalling and inhibitors of PDE10A are proposed as drugs for schizophrenia[8,253].

Foxp2 encodes a transcription factor crucial for human speech[254], singing in birds[255] and sensorimotor integration in mice (reviewed in[256]). As one of the *TCF4* risk alleles influences verbal memory[70], *Foxp2* is a highly interesting candidate. Many targets and partners of FOXP2 have been associated with psychiatric diseases, including schizophrenia (reviewed in[256]).

Mov10 (Putative helicase MOV-10) was upregulated in PFC and downregulated in the hippocampus of tg mice. It is an element of the RNA-induced silencing complex (RISC) that silences mRNA expression, after binding microRNAs (reviewed in[257]).

Genes upregulated in the hippocampus of *Tcf4*tg mice:

BC1, Brain cytoplasmic RNA, is a small non-coding RNA. Its transcription is regulated through an E-box[258], which can be a target of TCF4. Our RNA isolation protocol captures only mRNAs, but *BC1* was detected probably due to its polyA region[259]. *BC1* represses translation predominantly in dendritic synapses[260,261]. Upon neuronal activity *BC1* inhibits activity-induced increases of Fragile X mental retardation protein 1 (FMRP) and PSD95 in mouse hippocampus[262]. *BC1*^{-/-} mice appear healthy, breed well[263] and show normal spatial learning[264]. However, they display high anxiety[264], increased γ-oscillations in EEG, neuronal hyperexcitability and startle-induced seizures[262]. *BC1* is present only in rodents, thus it has low relevance for human patients.

Top3β, encoding DNA topoisomerase 3-β-1, was upegulated in hippocampus of *Tcf4*tg mice. In humans *TOP3β* is associated with schizophrenia and cognitive impairment[265]. It is coupled to FMRP[265], a cytoplasmatic modulator of microRNA-RISC complexes[257].

Plxna1 encodes Plexin-A1, a coreceptor for class 3 semaphorins, which is expressed in neurons of hippocampal CA1–CA3 regions, sensory cortex[266] and cortical subplate[50]. It plays a role in

axon guidance[267], regeneration[268] and pruning (reviewed in[108,269]). Plexins induce changes in cytoskeletal architecture and synapse elimination[269]. Because of their developmental function, they can be involved in autims and schizophrenia[269].

Mov10 was described above in the PFC section.

5.2.2 Proteomic analysis

We analysed cytosolic and synaptosomal proteome in PFC of 4 weeks old *Tcf4*tg and wt mice. In the cytosol we observed consistent downregulation of several ribosomal proteins and GTPases and several cell growth & maintenance proteins. β-tubulins and actin-binding proteins were upregulated, which may be in line with increased frequency of synaptic spines, observed in STED microscopy. Numerous signalling proteins were upregulated in synaptosomes, mainly Ca^{2+} binding proteins, GTPases and Ser/Thr kinases (including three CaMKII subunits). Several energy metabolism proteins (oxydoreductases and phosphotransferases), few ribosomal proteins and ion channels were also upregulated. Additionally, we validated upregulation of CaMKII, HOMER1, VAMP2 in synaptosomes as well as VAMP1 and 2 in cytosol. VAMPs are Vesicle-associated membrane proteins (known also as Synaptobrevins). HOMER1 is a scaffolding protein that is upregulated during LTP and seizures. CaMKII (Calcium/calmodulin-dependent protein kinase type II) promotes LTP and LTD and formation of immature spines, by acting of actin and actin-binding proteins and CDK5 (also upregulated in *Tcf4*tg)[270,271]. It is also involved in cognition and psychiatric disorders[270].

5.2.3 Expression analyses — conclusions

There was no overlap between differentially expressed genes found by RNAseq and proteomics. This lack of coherence could be explained by deregulation of microRNAs and other non-coding RNAs (e.g. small RNAs or circRNAs). In *Tcf4*tg mice, *BC1* and *Top3b*, both involved in suppression of translation initiation, were upregulated in hippocamus. Additionally *Mov10*, associated with the RISC complex, was upregulated in PFC and downregulated in hippocampus. All three candidates closely interact with Fragile X mental retardation protein 1 (FMRP). The Fragile X syndrome is characterized by, among others, intellectual disability and distinct facial features[272]. FMRP is an RNA-binding protein that modulates microRNA-RISC complexes and is important for RNA transport and translation repression[257]. FMRP-deficiency in mice and humans leads to immature (long and thin) spine morphology and increase of dendritic spine number in the cortex, that are characteristic for early developmental stages[273,274]. Based on our RNA sequencing data, regulatory RNAs seem to be a promising candidate explaining the inconsistency between RNAseq and proteomic data. In future experiments we will adapt our protocol for microRNA and perform microRNAs sequencing.

Murine *Adora2a*, *Foxp2*, *Drd1a* and *Tac1* are highly expressed in striatum, moderately in the isocortex and low or undetectable in the hippocampal formation[50]. Downregulation of these

genes in PFC of *Tcf4 Tcf4*tg mice may be an artefact caused by striatal contamination of cortical preparation. To validate this result we need to analyse cortical samples obtained, e.g. by laser capture microdissection. The results may be also influenced by a gender bias in our sample. Unfortunately, our attempt to validate the candidate genes by RT-qPCR was unsuccessful due to the low number of replicates.

Upregulation of synaptic proteins that promote plasticity, e.g. HOMER1 and CaMKII, may be in line with enhanced LTP in the *Tcf4*tg mice and increased levels of cytosolic β-tubulins and actin-binding proteins could reflect increase of synaptic spine frequency observed in STED microscopy.

5.3 Spine frequency and synapse morphology

*Tcf4*tg mice showed increased spine frequency in PFC at the age of 4 weeks. Elevated synapse number[109] and consequent thickening of cortical gray matter lead to poorer cognitive performance[101]. Schizophrenic patients display reduced spine numbers[105,106] and excessive pruning in the cortex[101,107]. At 12 weeks of age, *Tcf4*tg mice showed no changes in spine number neither in control conditions nor after social defeat. It suggests that cognitive impairments of *Tcf4*tg mice do not result directly from the spine excess. Possibly, abnormal spine numbers during the critical period affect establishment of connectivity between PFC and other brain structures and represent a potential mechanism of schizophrenia[107].

Electron microscopy analysis showed no differences in synapse structure and quantity between *Tcf4*tg and wt mice, which does not support the STED data. Perhaps the change in spine frequency is too subtle to be detected in electron microscopy. Number of myelinated axons and myelin thickness were also not changed, which is inconsistent with the RNAseq results showing deregulation of myelin genes in the cortex. However, since myelination is unequal in different cortical layers[275], analysis of cortical transverse sections may not fully reflect overall myelin condition in PFC.

5.4 Electrophysiology

In *Tcf4*tg mice, early LTP (e-LTP) was normal and LTD was enhanced in hippocampal CA1 slices. It suggests abnormal LTD-related receptor trafficking in postsynapses. During the first 15 min after stimulation e-LTP was also enhanced in *Tcf4*tg mice, but then it came back to wt level. Presumably, after the initial 15 min some compensatory mechanisms are activated, potentially associated with LTP-LTD interaction. These phenomena are not understood and it is difficult to draw conclusions. e-LTP (first 40 min) depends on synaptic release and receptor trafficking. Late LTP (L-LTP, up to 2 h after stimulation), depends on protein synthesis. If indeed *Bc1* and *Top3b*-dependent synaptic translation is altered in *Tcf4*tg mice, we could expect changes in L-LTP. We also plan to do a depotentiation experiment (LTP followed by LTD), which may help us understand physiological changes related to the sequence of learning and relearning in the Morris water maze reversal task.

Similar enhancement of LTD in CA1 was observed in *Pde4d* knockout mice, which displayed impairments of fear memory and reversal learning in MWM[276]. However, blocking LTD was found to reduce reversal learning in Morris water maze[277]. Thus, the relationship between LTD and reversal learning remains unclear. Nevertheless, excessive LTD may be relevant to schizophrenia, since drugs promoting LTD are propsychotic whereas drugs promoting LTP are antipsychotic[21]

Enhanced LTD may be in line with downregulation of *Adora2a*, that we observed in RNA sequencing of PFC. In corticostriatal synapses, activation adenosine receptor A2A, encoded by *Adora2a*, suppresses LTD and promotes LTP. This machinery is to some degree similar in other brain structures, but has not been well studied. In CA1 region, antagonists of A2A receptors reduce LTP, with unknown effects on LTD[278]. According to Morrison and Murray[21], delusions originate from disturbed striatal LTP-LTD balance. *Tcf4*tg mice do not overexpress *Tcf4* in striatum, thus we should not expect a "delusional" phenotype. However, disturbance of LTP–LTD balance in the cortex and hippocampus would have consequences for learning and memory.

5.5 Isolation-induced hypoalgesia

In our publication[178], we demostrated that hypoalgesia in mice is induced by IR, but not by SD. As hypoalgesia is also observed in schizophrenic patients[205–207,232] and their relatives[208], we believe that IR is a suitable model of some aspects of schizophrenia.

RNA sequencing of IR and EE revealed no changes in expression of the opioid system genes in hypothalamus nor in DRGs; however, a slight upregulation of *Pomc* – the β-endorphin precursor – was found in PFC of IR mice. In order to exclude or confirm the role of endogenous opioids, such as endorphins, it is necessary to monitor their levels in the blood before and after a pain stimulus.

RNAseq analysis of IR and EE animals revealed changes in gene expression in DRGs and hypothalamus, presented in Fig. 5.3. We validated downregulation of *Vgf* (Neurosecretory protein VGF), *Npy1r* (Neuropeptide Y receptor type 1) and *Bdnf* (Brain derived neurotrophic factor) in DRGs upon IR. These genes encode pronociceptive peptides, that are increased in DRGs during hyperalgesia[279–283]. However, in the RT-qPCR experiment, the same genes were downregulated also in DRGs of SD animals, that showed normal pain sensitivity. This is most likely caused by a 5 weeks of social isolation that followed the stress period, before the SD mice were sacrificed. To control for this, we are going to perform another experiment, in which the mice will be sacrificed soon after the last stress session. If SD mice develop IR-symptoms on top of the SD-symptoms, it would mean that hypoalgesia is independent of the developmental aspect. Our preliminary data seem to confirm this hypothesis.

Our results suggest that gene expression changes in primary sensory neurons of DRGs contribute to IR-induced hypoalgesia. This is in contrast to the study by Horiguchi *et al.*[204] claiming that isolation-induced hypoalgesia is due to changes in the central nervous system and not in the periphery. However, our data do not rule out a potential involvement of cortical mechanisms.

RNAseq of hypothalamus showed downregulation of several genes potentially relevant for pain
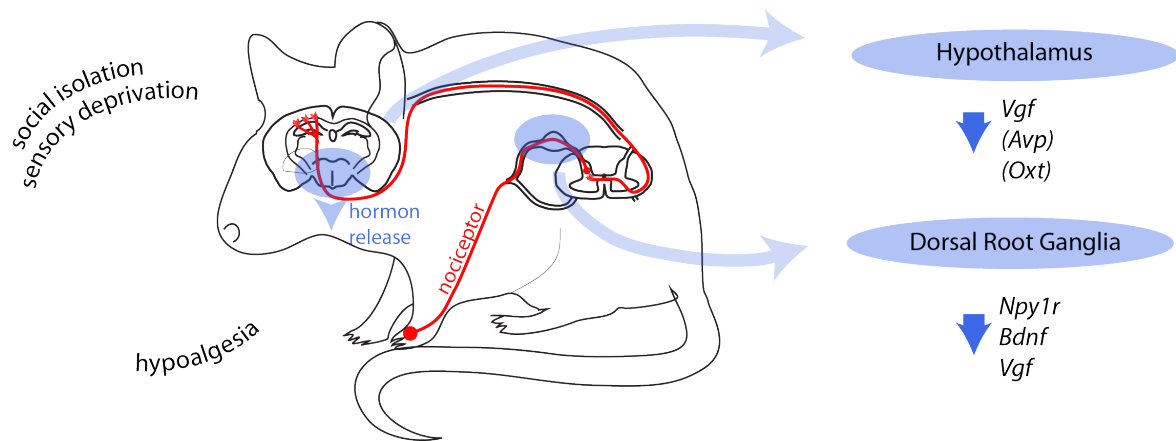
Figure 5.3: Isolation rearing-induced changes in DRGs and hypothalamus. Social isolation rearing and associated with it sensory deprivation lead to a decrease in basal expression levels of several pronociceptive genes. In dorsal root ganglions (DRGs), expression of *Npy1r* (neuropeptide Y receptor type 1), *Bdnf* (brain derived neurotrophic factor) and *Vgf* (Neurosecretory protein VGF) are downregulated. In hypothalamus, *Vgf*, *Avp* (arginine vasopressin) and *Oxt* (oxytocin) levels are reduced (in case of *Oxt* and *Avp* only a tendency in RT-qPCR), which may also play a role hypoalgesia. Additionally disturbed balance between oxytocin and arginine vasopressin (oxytocin show stronger downregulation) may contribute to aggressiveness, typical for isolated mice.

perception: *Vgf, Ramp3, Oxt* and *Avp*. *Vgf* reduction (validated by RT-qPCR) was not as prominent as in DRGs, but still significant. There is no evidence of contribution of *Ramp3* in pain, but *Ramp1*, a member of the same protein class, plays a role in migraine[284]. Downregulation of haemoglobin genes may indicate reduced vascularisation, but we cannot rule out that it could be a preparation artefact.

We observed reduction of oxytocin (*Oxt*) and arginine vasopressin (*Avp*) in RNAseq and strong tendencies in RT-qPCR — two hypothalamic peptides that regulate pain perception[285], social behaviour[88,286–288] and cognition[288]. Oxytocin is famous of its prosocial effects[287–289] while vasopressin contributes to aggression[287,290]. In IR mice both peptides were downregulated in hypothalamus, but oxytocin reduction was stronger (*Oxt* -0.884047 and *Avp* -0.700171 fold change). Misbalance between "prosocial" oxytocin and "antisocial" vasopressin[291] could explain the aggressive behaviour characteristic of isolation syndrome.

In humans, childhood abuse alters oxytocin levels in adulthood (reviewed in[287,288]). Oxytocin and vasopressin seem to be involved in psychiatric diseases, including schizophrenia[88,287,292]. Administration of oxytocin in animal models of schizophrenia has antypsychotic-like effects (reviewed in[288]), improves social performance in humans and is being tested as a medication for schizophrenia and other mental illnesses[288].

Interestingly, mRNAs encoding *Oxt* and *Avp*, similarly to *BC1*, were found in axons of magnocellular hypothalamic neurons of rats, even though axonal transport of mRNA is a rare case[293]. These *Oxt* and *Avp* mRNA levels can dramatically increase in response to environmental stimuli[293]. Possibly, *BC1* may regulate local their translation. In *Tcf4*tg mice levels of *Oxt* and *Avp* mRNAs were normal in PFC and hippocampus. It is unlikely that these animals would show altered oxytocin or vasopressin blood levels, as *Tcf4* is not overexpressed in hypothalamus. However, in patients

with *TCF4* risk alleles altered *BC1* abundance could contribute to hormonal deregulations.

In summary, we demonstrate that expression of pronociceptive *Vgf, Npy1r* and *Bdnf* are reduced in dorsal root ganglions upon isolation rearing. We also show reduction of *Vgf*, oxytocin and arginine vasopressin RNA levels in hypothalami of isolated mice. Potential disturbance of the oxytocin–vasopressin balance may explain the aggressiveness of IR mice. We found no clear evidence for involvement of the endogenous opioid system and our data suggest that not only central, but also peripheral mechanisms contribute to reduced pain sensitivity upon IR.

Summary

I N THIS STUDY, we aimed at understanding Gene × Environment interaction in mouse models of psychiatric diseases. To address this question, we first focused on studying the influence of environmental factors on behaviour of wildtype C57Bl/6N mice. In a battery of behavioural experiments we analysed behaviour of mice subjected to two paradigms inducing psychopathologies in mice — Social Isolation Rearing (IR) and Social Defeat (SD) —, calibrated them to Enriched Environment (EE) (used as a control) and compared to each other. We developed an approach to analysing huge behavioural data sets and visualising them as behavioural profiles in a single, comprehensive figure[178]. By applying multivariate statistics, we grouped tests that measure similar behaviours and merged them into higher-order categories (e.g. anxiety, curiosity, etc.) — to which we refer as *dimension reduction*. IR mice exhibited reduced curiosity, motivation and pain sensitivity, cognitive impairments and hyperactivity. SD mice displayed strong cognitive impairments, as well as anxiety and reduced motivation. We conclude that IR is better to model positive symptoms and SD is more appropriate for negative symptoms of psychotic diseases. Such a holistic view on murine behaviour has more relevance to human psychiatric syndromes than looking at single behavioural measures. The advantages of our approach are that it allows comparing independent mouse cohorts and possibly including also other data types, e.g. from histological experiments, to create a fuller profile of disease-relevant symptoms.

We adapted this approach for studying Gene × Environment and ageing interaction in a transgenic mouse model overexpressing a schizophrenia susceptibility gene *Tcf4*. Brzózka *et al.*[57] have earlier shown mild cognitive impairments in these mice in standard group housing. Here, we analysed two cohorts of *Tcf4* transgenic and wildtype mice housed in IR or EE and tested them in early adulthood or aged. We show that manifestation of the phenotype of the *Tcf4* transgenic mice depends on environmental factors — IR and SD enhance the deficits and EE rescues the phenotype. Additionally, we demonstrate that these deficits are restricted to cognitive functions and no other aspects of behaviour.

To understand *Tcf4* functions, we supplemented behavioural testing with analyses on cellular and molecular level. We found that the *Tcf4* transgenic mice displayed an increased number of dendritic spines in prefrontal cortex and enhanced LTD in hippocampus. In proteomic analyses, we observed upregulation of synaptic proteins HOMER1 and synaptobrevins, as well as of CamKII, a kinase involved in synaptic plasticity, and β-tubulins. RNA sequencing data suggest that TCF4 may regulate genes involved in regulation of translation by microRNAs, e.g. *Top3b, Mov10* and microRNA *BC1*.

To have a broader view of *Tcf4* functions, we analysed also heterozygotic *Tcf4* knockouts (*Tcf4*C mice). In humans, disruption of one of the *TCF4* alleles causes the Pitt-Hopkins syndrome (PTHS), a neurodevelopmental disease with mental retardation. *Tcf4* knockout mice show a dramatic of impairment hippocampus-dependent spatial learning, but no other PTHS-like features. The specific disruption of hippocampal function can be explained by the fact that the knockout affects mRNA levels of only the *Tcf4* exons that are particularly highly expressed in hippocampus. The isoforms that are typically mutated in PTHS patients are almost unaffected in these mice.

We conclude that *Tcf4* regulates specifically learning and memory in mice and either *Tcf4* overexpression or depletion leads to cognitive impairments. In case of *Tcf4* overexpressors, manifestation of these impairments depends also on environmental factors during puberty. The influence of environment on the *Tcf4* knockout phenotype has not been studied yet and should be assessed in the future.

In a side project, we investigated the mechanisms of IR-induced pain insensitivity in wildtype mice, which we observed repeatedly in our behavioural studies. Transcriptome analysis of hypothalami and dorsal root ganglia of IR mice revealed strong downregulation of pronociceptive genes *Vgf, Bdnf* and *Npyr1*. We also observed tendencies for downregulation of mRNAs encoding hypothalamic peptides oxytocin and arginine vasopressin — which may contribute not only to diminished pain sensitivity, but also to abnormally aggressive behaviour of isolated mice.

Bibliography

1. McGrath, J. *et al.* A systematic review of the incidence of schizophrenia: the distribution of rates and the influence of sex, urbanicity, migrant status and methodology. *BMC medicine* **2**, 13 (2004).

2. Insel, T. R. Rethinking schizophrenia. *Nature* **468**, 187–193 (2010).

3. Laursen, T. M. Life expectancy among persons with schizophrenia or bipolar affective disorder. *Schizophrenia research* **131**, 101–104 (2011).

4. Saha, S., Chant, D. & McGrath, J. A systematic review of mortality in schizophrenia: is the differential mortality gap worsening over time? *Archives of general psychiatry* **64**, 1123–1131 (2007).

5. Jim van Os, S. K. Schizophrenia. *Lancet* **374**, 635–45 (2009).

6. Andreasen, N. C. The evolving concept of schizophrenia: from Kraepelin to the present and future. *Schizophrenia research* **28**, 105–109 (1997).

7. Tandon, R. *et al.* Definition and description of schizophrenia in the DSM-5. *Schizophrenia research* **150**, 3–10 (2013).

8. Millan, M. J. *et al.* Cognitive dysfunction in psychiatric disorders: characteristics, causes and the quest for improved therapy. *Nature reviews Drug discovery* **11**, 141–168 (2012).

9. Tost, H. & Meyer-Lindenberg, A. Puzzling over schizophrenia: schizophrenia, social environment and the brain. *Nature medicine* **18**, 211–213 (2012).

10. Maurer, K., Riecher-R, A. *et al.* The influence of age and sex on the onset and early course of schizophrenia. *The British journal of psychiatry* **162**, 80–86 (1993).

11. Schultz, S. K. *et al.* The life course of schizophrenia: age and symptom dimensions. *Schizophrenia Research* **23**, 15–23 (1997).

12. Paus, T., Keshavan, M. & Giedd, J. N. Why do many psychiatric disorders emerge during adolescence? *Nature Reviews Neuroscience* **9**, 947–957 (2008).

13. Gottesman, I. I. & Gould, T. D. The endophenotype concept in psychiatry: etymology and strategic intentions. *American Journal of Psychiatry* **160**, 636–645 (2003).

14. Allen, A. J., Griss, M. E., Folley, B. S., Hawkins, K. A. & Pearlson, G. D. Endophenotypes in schizophrenia: a selective review. *Schizophrenia research* **109**, 24–37 (2009).

15. Uhlhaas, P. J. & Singer, W. Abnormal neural oscillations and synchrony in schizophrenia. *Nature Reviews Neuroscience* **11**, 100–113 (2010).

16. Barch, D. M. & Ceaser, A. Cognition in schizophrenia: core psychological and neural mechanisms. *Trends in cognitive sciences* **16**, 27–34 (2012).

17. Crider, A. Perseveration in schizophrenia. *Schizophrenia bulletin* **23**, 63 (1997).

18. Murray, G. *et al.* Reinforcement and reversal learning in first-episode psychosis. *Schizophrenia bulletin* **34**, 848–855 (2008).

19. Millan, M. J. & Bales, K. L. Towards improved animal models for evaluating social cognition and its disruption in schizophrenia: The CNTRICS initiative. *Neuroscience & Biobehavioral Reviews* **37**, 2166–2180 (2013).

20. Brisch, R. *et al.* The role of dopamine in schizophrenia from a neurobiological and evolutionary perspective: old fashioned, but still in vogue. *Frontiers in Psychiatry* **5** (2014).

21. Morrison, P. D. & Murray, R. From real-world events to psychosis: the emerging neuropharmacology of delusions. *Schizophrenia bulletin* **35**, 668–674 (2009).

22. Kapur, S. & Mamo, D. Half a century of antipsychotics and still a central role for dopamine D2 receptors. *Progress in Neuro-Psychopharmacology and Biological Psychiatry* **27**, 1081–1090 (2003).

23. Lieberman, J. A. *et al.* Effectiveness of antipsychotic drugs in patients with chronic schizophrenia. *New England Journal of Medicine* **353**, 1209–1223 (2005).

24. Sullivan, P. F. Puzzling over schizophrenia: schizophrenia as a pathway disease. *Nature medicine* **18**, 210–211 (2012).

25. Maher, B. The case of the missing heritability. *Nature* **456**, 18–21 (2008).

26. Stefansson, H. *et al.* Common variants conferring risk of schizophrenia. *Nature* **460**, 744–747 (2009).

27. Li, T. *et al.* Common variants in major histocompatibility complex region and *TCF4* gene are significantly associated with schizophrenia in han chinese. *Biological psychiatry* **68**, 671–673 (2010).

28. Schizophrenia Psychiatric Genome-Wide Association Study (GWAS) Consortium *et al.* Genome-wide association study identifies five new schizophrenia loci. *Nature genetics* **43**, 969–976 (2011).

29. Steinberg, S. *et al.* Common variants at *VRK2* and *TCF4* conferring risk of schizophrenia. *Human molecular genetics* **20**, 4076–4081 (2011).

30. Cross-Disorder Group of the Psychiatric Genomics Consortium *et al.* Identification of risk loci with shared effects on five major psychiatric disorders: a genome-wide analysis. *Lancet* **381**, 1371 (2013).

31. Ripke, S., Schizophrenia Working Group of the Psychiatric Genomics Consortium *et al.* Biological insights from 108 schizophrenia-associated genetic loci. *Nature* (2014).

32. Doherty, J. L. & Owen, M. J. Genomic insights into the overlap between psychiatric disorders: implications for research and clinical practice. *Genome Medicine* **6**, 29 (2014).

33. Bergen, S. E. & Petryshen, T. L. Genome-wide association studies (GWAS) of schizophrenia: does bigger lead to better results? *Current opinion in psychiatry* **25**, 76 (2012).

34. Kwon, E., Wang, W. & Tsai, L. Validation of schizophrenia-associated genes *CSMD1*, *C10orf26*, *CACNA1C* and *TCF4* as *miR-137* targets. *Molecular psychiatry* **18**, 11–12 (2011).

35. Van Os, J., Linscott, R. J., Myin-Germeys, I., Delespaul, P. & Krabbendam, L. A systematic review and meta-analysis of the psychosis continuum: evidence for a psychosis proneness–persistence–impairment model of psychotic disorder. *Psychological medicine* **39**, 179–195 (2009).

36. Eysenck, H. & Eysenck, S. Psychoticism as a dimension of personality. *Crane, Russak & Company, New York* (1976).

37. Purcell, S. M. *et al.* Common polygenic variation contributes to risk of schizophrenia and bipolar disorder. *Nature* **460**, 748–752 (2009).

38. Insel, T. *et al.* Research domain criteria (RDoC): toward a new classification framework for research on mental disorders. *American Journal of Psychiatry* **167**, 748–751 (2010).

39. Cuthbert, B. N. & Insel, T. R. Toward new approaches to psychotic disorders: the NIMH Research Domain Criteria project. *Schizophrenia bulletin* **36**, 1061–1062 (2010).

40. Navarrete, K. *et al.* TCF4 (*E2-2, ITF2*) A schizophrenia-associated gene with pleiotropic effects on human disease. *American Journal of Medical Genetics Part B: Neuropsychiatric Genetics* **162**, 1–16 (2013).

41. Sweatt, J. D. Pitt-Hopkins syndrome: intellectual disability due to loss of TCF4-regulated gene transcription. *Experimental & molecular medicine* **45**, e21 (2013).

42. Amiel, J. *et al.* Mutations in *TCF4* encoding a class I basic helix-loop-helix transcription factor, are responsible for Pitt-Hopkins syndrome, a severe epileptic encephalopathy associated with autonomic dysfunction. *The American Journal of Human Genetics* **80**, 988–993 (2007).

43. Ephrussi, A., Church, G. M., Tonegawa, S. & Gilbert, W. B lineage–specific interactions of an immunoglobulin enhancer with cellular factors *in vivo*. *Science* **227**, 134–140 (1985).

44. Ellenberger, T., Fass, D., Arnaud, M. & Harrison, S. C. Crystal structure of transcription factor E47: E-box recognition by a basic region helix-loop-helix dimer. *Genes & development* **8**, 970–980 (1994).

45. Sepp, M., Pruunsild, P. & Timmusk, T. Pitt-Hopkins syndrome-associated mutations in *TCF4* lead to variable impairment of the transcription factor function ranging from hypomorphic to dominant-negative effects. *Human molecular genetics* **21**, 2873–2888 (2012).

46. Quednow, B. B., Brzózka, M. M. & Rossner, M. J. Transcription factor 4 (*TCF4*) and schizophrenia: integrating the animal and the human perspective. *Cellular and Molecular Life Sciences* 1–21 (2014).

47. Flora, A., Garcia, J. J., Thaller, C. & Zoghbi, H. Y. The E-protein TCF4 interacts with MATH1 to regulate differentiation of a specific subset of neuronal progenitors. *Proceedings of the National Academy of Sciences* **104**, 15382–15387 (2007).

48. Sepp, M., Kannike, K., Eesmaa, A., Urb, M. & Timmusk, T. Functional diversity of human basic helix-loop-helix transcription factor *TCF4* isoforms generated by alternative 5' exon usage and splicing. *PloS one* **6**, e22138 (2011).

49. Wu, C. *et al.* BioGPS: an extensible and customizable portal for querying and organizing gene annotation resources. *Genome Biol* **10**, R130 (2009).

50. ©2014 Allen Institute for Brain Science. Allen Mouse Brain Atlas @ONLINE. `http://mouse.brain-map.org/` (2014).

51. Bergqvist, I. *et al.* The basic helix-loop-helix transcription factor E2–2 is involved in t lymphocyte development. *European journal of immunology* **30**, 2857–2863 (2000).

52. Zhuang, Y., Cheng, P. & Weintraub, H. B-lymphocyte development is regulated by the combined dosage of three basic helix-loop-helix genes, *E2A, E2-2*, and *HEB*. *Molecular and cellular biology* **16**, 2898–2905 (1996).

53. Forrest, M. P., Waite, A. J., Martin-Rendon, E. & Blake, D. J. Knockdown of human *TCF4* affects multiple signaling pathways involved in cell survival, epithelial to mesenchymal transition and neuronal differentiation. *PloS one* **8**, e73169 (2013).

54. Daniel, G. Tcf4 *is a target gene of the imprinted gene* Zac1 *during mouse neurogenesis*. Ph.D. thesis, Ludwig-Maximilians-Universität München (2012).

55. NCBI. Human *TCF4*, gene ID: 6925 @ONLINE. `http://www.ncbi.nlm.nih.gov/` (2014).

56. Ensembl Genome Browser. *TCF4* ENSG00000196628, human (GRCh37) @ONLINE. `http://www.ensembl.org/` (2014).

57. Brzózka, M. M., Radyushkin, K., Wichert, S. P., Ehrenreich, H. & Rossner, M. J. Cognitive and sensorimotor gating impairments in transgenic mice overexpressing the schizophrenia susceptibility gene *Tcf4* in the brain. *Biological psychiatry* **68**, 33–40 (2010).

58. Chiaramello, A., Soosaar, A., Neuman, T. & Zuber, M. X. Differential expression and distinct DNA-binding specificity of ME1a and ME2 suggest a unique role during differentiation and neuronal plasticity. *Molecular brain research* **29**, 107–118 (1995).

59. Dörflinger, U. *et al.* Activation of somatostatin receptor II expression by transcription factors MIBP1 and SEF-2 in the murine brain. *Molecular and cellular biology* **19**, 3736–3747 (1999).

60. Yoon, S. O. & Chikaraishi, D. M. Isolation of two E-box binding factors that interact with the rat tyrosine hydroxylase enhancer. *Journal of Biological Chemistry* **269**, 18453–18462 (1994).

61. Saarikettu, J., Sveshnikova, N. & Grundström, T. Calcium/calmodulin inhibition of transcriptional activity of E-proteins by prevention of their binding to DNA. *Journal of Biological Chemistry* **279**, 41004–41011 (2004).

62. Larsson, G. *et al.* A novel target recognition revealed by calmodulin in complex with the basic helix–loop–helix transcription factor SEF2-1/E2-2. *Protein Science* **10**, 169–186 (2001).

63. Quednow, B. B. *et al.* Schizophrenia risk polymorphisms in the *TCF4* gene interact with smoking in the modulation of auditory sensory gating. *Proceedings of the National Academy of Sciences* **109**, 6271–6276 (2012).

64. Ripke, S. Broad Institute, Ricopili @ONLINE. `http://www.broadinstitute.org/mpg/ricopili/` (2014).

65. Forrest, M. P., Hill, M. J., Quantock, A. J., Martin-Rendon, E. & Blake, D. J. The emerging roles of *TCF4* in disease and development. *Trends in molecular medicine* (2014).

66. Breschel, T. *et al.* A novel, heritable, expanding CTG repeat in an intron of the *SEF2-1* gene on chromosome 18q21. 1. *Human molecular genetics* **6**, 1855–1863 (1997).

67. Quednow, B. B. *et al.* The schizophrenia risk allele C of the *TCF4* rs9960767 polymorphism disrupts sensorimotor gating in schizophrenia spectrum and healthy volunteers. *The Journal of Neuroscience* **31**, 6684–6691 (2011).

68. Hall, M.-H. *et al.* Neurophysiologic effect of GWAS derived schizophrenia and bipolar risk variants. *American Journal of Medical Genetics Part B: Neuropsychiatric Genetics* **165**, 9–18 (2014).

69. Sieradzka, D. *et al.* Are genetic risk factors for psychosis also associated with dimension-specific psychotic experiences in adolescence? *PloS one* **9**, e94398 (2014).

70. Lennertz, L. *et al.* Novel schizophrenia risk gene *TCF4* influences verbal learning and memory functioning in schizophrenia patients. *Neuropsychobiology* **63**, 131–136 (2011).

71. Zhu, X. *et al.* Associations between *TCF4* gene polymorphism and cognitive functions in schizophrenia patients and healthy controls. *Neuropsychopharmacology* **38**, 683–689 (2012).

72. Wirgenes, K. *et al. TCF4* sequence variants and mRNA levels are associated with neurodevelopmental characteristics in psychotic disorders. *Translational psychiatry* **2**, e112 (2012).

73. Mudge, J. *et al.* Genomic convergence analysis of schizophrenia: mrna sequencing reveals altered synaptic vesicular transport in post-mortem cerebellum. *PloS one* **3**, e3625 (2008).

74. Guella, I. *et al.* Analysis of miR-137 expression and rs1625579 in dorsolateral prefrontal cortex. *Journal of psychiatric research* **47**, 1215–1221 (2013).

75. Umeda-Yano, S. *et al.* Expression analysis of the genes identified in GWAS of the postmortem brain tissues from patients with schizophrenia. *Neuroscience letters* **568**, 12–16 (2014).

76. Kang, H. J. *et al.* Spatio-temporal transcriptome of the human brain. *Nature* **478**, 483–489 (2011).

77. Forrest, M. *et al.* Functional analysis of *TCF4* missense mutations that cause Pitt-Hopkins syndrome. *Human mutation* **33**, 1676–1686 (2012).

78. Li, J.-H., Liu, S., Zhou, H., Qu, L.-H. & Yang, J.-H. starBase v2. 0: decoding miRNA-ceRNA, miRNA-ncRNA and protein–RNA interaction networks from large-scale CLIP-Seq data. *Nucleic acids research* **42**, D92–D97 (2014).

79. Yang, J.-H. *et al.* starbase: a database for exploring microRNA–mRNA interaction maps from Argonaute CLIP-Seq and Degradome-Seq data. *Nucleic acids research* **39**, D202–D209 (2011).

80. Giurgea, I. *et al. TCF4* deletions in Pitt-Hopkins syndrome. *Human mutation* **29**, E242–E251 (2008).

81. Van Balkom, I. D., Vuijk, P. J., Franssens, M., Hoek, H. W. & Hennekam, R. Development, cognition, and behaviour in Pitt-Hopkins syndrome. *Developmental Medicine & Child Neurology* **54**, 925–931 (2012).

82. de Pontual, L. *et al.* Mutational, functional, and expression studies of the *TCF4* gene in Pitt-Hopkins syndrome. *Human mutation* **30**, 669–676 (2009).

83. Takano, K., Lyons, M., Moyes, C., Jones, J. & Schwartz, C. Two percent of patients suspected of having angelman syndrome have tcf4 mutations. *Clinical genetics* **78**, 282–288 (2010).

84. Zweier, C. *et al.* Haploinsufficiency of *TCF4* causes syndromal mental retardation with intermittent hyperventilation (Pitt-Hopkins syndrome). *The American Journal of Human Genetics* **80**, 994–1001 (2007).

85. Kalscheuer, V. M. *et al.* Disruption of the *TCF4* gene in a girl with mental retardation but without the classical Pitt-Hopkins syndrome. *American Journal of Medical Genetics Part A* **146**, 2053–2059 (2008).

86. van Os, J., Kenis, G. & Rutten, B. P. The environment and schizophrenia. *Nature* **468**, 203–212 (2010).

87. Bayer, T. A., Falkai, P. & Maier, W. Genetic and non-genetic vulnerability factors in schizophrenia: the basis of the two hit hypothesis. *Journal of psychiatric research* **33**, 543–548 (1999).

88. Meyer-Lindenberg, A. & Tost, H. Neural mechanisms of social risk for psychiatric disorders. *Nature neuroscience* **15**, 663–668 (2012).

89. Matheson, S., Shepherd, A. & Carr, V. How much do we know about schizophrenia and how well do we know it? evidence from the Schizophrenia Library. *Psychological Medicine* 1–19 (2014).

90. Cash-Padgett, T. & Jaaro-Peled, H. *DISC1* mouse models as a tool to decipher gene-environment interactions in psychiatric disorders. *Frontiers in behavioral neuroscience* **7** (2013).

91. Cantor-Graae, E. & Selten, J.-P. Schizophrenia and migration: a meta-analysis and review. *American Journal of Psychiatry* **162**, 12–24 (2005).

92. Bourque, F., Van der Ven, E. & Malla, A. A meta-analysis of the risk for psychotic disorders among first-and second-generation immigrants. *Psychological medicine* **41**, 897–910 (2011).

93. Pedersen, C. B. & Mortensen, P. B. Evidence of a dose-response relationship between urbanicity during upbringing and schizophrenia risk. *Archives of General Psychiatry* **58**, 1039–1046 (2001).

94. Judd, F. K. *et al.* High prevalence disorders in urban and rural communities. *Australian and New Zealand Journal of Psychiatry* **36**, 104–113 (2002).

95. Lederbogen, F. *et al.* City living and urban upbringing affect neural social stress processing in humans. *Nature* **474**, 498–501 (2011).

96. Selten, J.-P. & Cantor-Graae, E. Social defeat: risk factor for schizophrenia? *The British Journal of Psychiatry* **187**, 101–102 (2005).

97. Selten, J.-P., van der Ven, E., Rutten, B. P. & Cantor-Graae, E. The social defeat hypothesis of schizophrenia: an update. *Schizophrenia bulletin* **39**, 1180–1186 (2013).

98. McAlonan, G. M., Li, Q. & Cheung, C. The timing and specificity of prenatal immune risk factors for autism modeled in the mouse and relevance to schizophrenia. *Neurosignals* **18**, 129–139 (2010).

99. Chł odzińska, N., Gajerska, M., Bartkowska, K., Turlejski, K. & Djavadian, R. L. Lipopoly-saccharide injected to pregnant mice affects behavior of their offspring in adulthood. *Acta neurobiologiae experimentalis* **71**, 519–527 (2010).

100. Blakemore, S.-J. The social brain in adolescence. *Nature Reviews Neuroscience* **9**, 267–277 (2008).

101. Selemon, L. A role for synaptic plasticity in the adolescent development of executive function. *Translational psychiatry* **3**, e238 (2013).

102. Huttenlocher, P. R. Synapse elimination and plasticity in developing human cerebral cortex. *American journal of mental deficiency* (1984).

103. Peter, R. *et al.* Synaptic density in human frontal cortexdevelopmental changes and effects of aging. *Brain research* **163**, 195–205 (1979).

104. Sowell, E. R., Delis, D., Stiles, J. & Jernigan, T. L. Improved memory functioning and frontal lobe maturation between childhood and adolescence: a structural MRI study. *Journal of the International Neuropsychological Society* **7**, 312–322 (2001).

105. Glantz, L. A. & Lewis, D. A. Decreased dendritic spine density on prefrontal cortical pyramidal neurons in schizophrenia. *Archives of general psychiatry* **57**, 65–73 (2000).

106. Garey, L. *et al.* Reduced dendritic spine density on cerebral cortical pyramidal neurons in schizophrenia. *Journal of Neurology, Neurosurgery & Psychiatry* **65**, 446–453 (1998).

107. Dobbs, D. Schizophrenia: The making of a troubled mind. *Nature* **468**, 154–156 (2010).

108. Rosenthal, R. Of schizophrenia, pruning, and epigenetics: a hypothesis and suggestion. *Medical hypotheses* **77**, 106–108 (2011).

109. Hoffman, R. E. & McGlashan, T. H. Synaptic elimination, neurodevelopment, and the mechanism of hallucinated voices in schizophrenia. *American Journal of Psychiatry* **154**, 1683–1689 (1997).

110. Pinter, O., Beda, Z., Csaba, Z. & Gerendai, I. Differences in the onset of puberty in selected inbred mouse strains (2007).

111. Avital, A. & Richter-Levin, G. Exposure to juvenile stress exacerbates the behavioural consequences of exposure to stress in the adult rat. *The International Journal of Neuropsychopharmacology* **8**, 163–173 (2005).

112. Jones, C., Watson, D. & Fone, K. Animal models of schizophrenia. *British journal of pharmacology* **164**, 1162–1194 (2011).

113. Robinson, T. E. & Becker, J. B. Enduring changes in brain and behavior produced by chronic amphetamine administration: a review and evaluation of animal models of amphetamine psychosis. *Brain Research Reviews* **11**, 157–198 (1986).

114. Javitt, D. Negative schizophrenic symptomatology and the PCP (phencyclidine) model of schizophrenia. *The Hillside journal of clinical psychiatry* **9**, 12–35 (1986).

115. Jodo, E. The role of the hippocampo-prefrontal cortex system in phencyclidine-induced psychosis: A model for schizophrenia. *Journal of Physiology-Paris* **107**, 434–440 (2013).

116. Wiescholleck, V. & Manahan-Vaughan, D. Long-lasting changes in hippocampal synaptic plasticity and cognition in an animal model of NMDA receptor dysfunction in psychosis. *Neuropharmacology* **74**, 48–58 (2013).

117. Tseng, K. Y., Chambers, R. A. & Lipska, B. K. The neonatal ventral hippocampal lesion as a heuristic neurodevelopmental model of schizophrenia. *Behavioural brain research* **204**, 295–305 (2009).

118. Lipska, B. K. Using animal models to test a neurodevelopmental hypothesis of schizophrenia. *Journal of Psychiatry and Neuroscience* **29**, 282 (2004).

119. Meyer, U. Prenatal poly (i: C) exposure and other developmental immune activation models in rodent systems. *Biological psychiatry* **75**, 307–315 (2014).

120. Brzózka, M. M., Fischer, A., Falkai, P. & Havemann-Reinecke, U. Acute treatment with cannabinoid receptor agonist win55212. 2 improves prepulse inhibition in psychosocially stressed mice. *Behavioural brain research* **218**, 280–287 (2011).

121. Nithianantharajah, J. & Hannan, A. J. Enriched environments, experience-dependent plasticity and disorders of the nervous system. *Nature Reviews Neuroscience* **7**, 697–709 (2006).

122. Wermter, A.-K. *et al.* From nature versus nurture, via nature and nurture, to gene×environment interaction in mental disorders. *European child & adolescent psychiatry* **19**, 199–210 (2010).

123. Burrows, E. L., McOmish, C. E. & Hannan, A. J. Gene–environment interactions and construct validity in preclinical models of psychiatric disorders. *Progress in Neuro-Psychopharmacology and Biological Psychiatry* **35**, 1376–1382 (2011).

124. Hida, H., Mouri, A. & Noda, Y. Behavioral phenotypes in schizophrenic animal models with multiple combinations of genetic and environmental factors. *Journal of pharmacological sciences* **121**, 185–191 (2013).

125. Kannan, G., Sawa, A. & Pletnikov, M. V. Mouse models of gene–environment interactions in schizophrenia. *Neurobiology of disease* **57**, 5–11 (2013).

126. Karg, K. & Sen, S. Gene×environment interaction models in psychiatric genetics. In *Behavioral Neurogenetics*, 441–462 (Springer, 2012).

127. Hatch, A. *et al.* Isolation syndrome in the rat. *Toxicology and applied pharmacology* **7**, 737–745 (1965).

128. Valzelli, L. The "isolation syndrome" in mice. *Psychopharmacologia* **31**, 305–320 (1973).

129. Wilkinson, M., Stirton, C. & McConnachie, A. Behavioural observations of singly-housed grey short-tailed opossums (monodelphis domestica) in standard and enriched environments. *Laboratory animals* **44**, 364–369 (2010).

130. Maple, T. L. & Perdue, B. M. *Zoo animal welfare. Chapters:5 and 6*, vol. 14 (Springer, 2013).

131. Pietropaolo, S., Singer, P., Feldon, J. & Yee, B. K. The postweaning social isolation in C57BL/6 mice: preferential vulnerability in the male sex. *Psychopharmacology* **197**, 613–628 (2008).

132. Voikar, V., Polus, A., Vasar, E. & Rauvala, H. Long-term individual housing in C57BL/6J and DBA/2 mice: assessment of behavioral consequences. *Genes, Brain and Behavior* **4**, 240–252 (2005).

133. Gresack, J. E. *et al.* Isolation rearing-induced deficits in contextual fear learning do not require CRF$_2$ receptors. *Behavioural brain research* **209**, 80–84 (2010).

134. Coudereau, J.-P., Monier, C., Bourre, J.-M. & Frances, H. Effect of isolation on pain threshold and on different effects of morphine. *Progress in Neuro-Psychopharmacology and Biological Psychiatry* **21**, 997–1018 (1997).

135. Puglisi-Allegra, S. & Oliverio, A. Social isolation: effects on pain threshold and stress-induced analgesia. *Pharmacology Biochemistry and Behavior* **19**, 679–681 (1983).

136. Gentsch, C., Lichtsteiner, M. & Feer, H. Locomotor activity, defecation score and corticosterone levels during an openfield exposure: a comparison among individually and group-housed rats, and genetically selected rat lines. *Physiology & behavior* **27**, 183–186 (1981).

137. Gentsch, C., Lichtsteiner, M., Kraeuchi, K. & Feer, H. Different reaction patterns in individually and socially reared rats during exposures to novel environments. *Behavioural brain research* **4**, 45–54 (1982).

138. Wilkinson, L. S. *et al.* Social isolation in the rat produces developmentally specific deficits in prepulse inhibition of the acoustic startle response without disrupting latent inhibition. *Neuropsychopharmacology* **10**, 61–72 (1994).

139. Heidbreder, C. *et al.* Behavioral, neurochemical and endocrinological characterization of the early social isolation syndrome. *Neuroscience* **100**, 749–768 (2000).

140. Varty, G. B., Powell, S. B., Lehmann-Masten, V., Buell, M. R. & Geyer, M. A. Isolation rearing of mice induces deficits in prepulse inhibition of the startle response. *Behavioural brain research* **169**, 162–167 (2006).

141. Silva, C. F., Duarte, F. S., Lima, T. C. M. D. & de Oliveira, C. L. Effects of social isolation and enriched environment on behavior of adult swiss mice do not require hippocampal neurogenesis. *Behavioural brain research* **225**, 85–90 (2011).

142. Makinodan, M., Rosen, K. M., Ito, S. & Corfas, G. A critical period for social experience–dependent oligodendrocyte maturation and myelination. *Science* **337**, 1357–1360 (2012).

143. Geyer, M. A., Wilkinson, L. S., Humby, T. & Robbins, T. W. Isolation rearing of rats produces a deficit in prepulse inhibition of acoustic startle similar to that in schizophrenia. *Biological psychiatry* **34**, 361–372 (1993).

144. Buuse, M., Garner, B. & Koch, M. Neurodevelopmental animal models of schizophrenia: effects on prepulse inhibition. *Current molecular medicine* **3**, 459–471 (2003).

145. Schrijver, N. C., Pallier, P. N., Brown, V. J. & Würbel, H. Double dissociation of social and environmental stimulation on spatial learning and reversal learning in rats. *Behavioural brain research* **152**, 307–314 (2004).

146. Pietropaolo, S., Feldon, J. & Yee, B. K. Nonphysical contact between cagemates alleviates the social isolation syndrome in C57BL/6 male mice. *Behavioral neuroscience* **122**, 505 (2008).

147. Zuo, Y., Yang, G., Kwon, E. & Gan, W.-B. Long-term sensory deprivation prevents dendritic spine loss in primary somatosensory cortex. *Nature* **436**, 261–265 (2005).

148. van der Horst, F. C. P. & van der Veer, R. Loneliness in infancy: Harry harlow, john bowlby and issues of separation. *Integrative Psychological & Behavioral Science* **42**, 325–335 (2008).

149. Robertsone, J. "A two-year old goes to hospital". Scientific film @ONLINE. `http://www.robertsonfilms.info/2_year_old.htm` (1952).

150. Anderson, E. Effects of sensory deprivation. *Proc R Soc Med* **55**, 1003–1005 (1962).

151. Kenna, J. Sensory deprivation phenomena: Critical review and explanatory models. *Proc R Soc Med* **55**, 1005–1010 (1962).

152. Rosenzweig, N. Sensory deprivation and schizophrenia: some clinical and theoretical similarities. *American Journal of Psychiatry* **116**, 326–329 (1959).

153. Simon, N. Kaspar Hauser's recovery and autopsy: A perspective on neurological and sociological requirements for language development. *Journal of autism and childhood schizophrenia* **8**, 209–217 (1978).

154. Psychology Dictionary. @ONLINE. `http://psychologydictionary.org/` (2014).

155. Carr, C. P., Martins, C. M. S., Stingel, A. M., Lemgruber, V. B. & Juruena, M. F. The role of early life stress in adult psychiatric disorders: a systematic review according to childhood trauma subtypes. *The Journal of nervous and mental disease* **201**, 1007–1020 (2013).

156. Holtzman, C. *et al.* Stress and neurodevelopmental processes in the emergence of psychosis. *Neuroscience* **249**, 172–191 (2013).

157. Dobry, Y., Braquehais, M. D. & Sher, L. Bullying, psychiatric pathology and suicidal behavior. *International journal of adolescent medicine and health* **25**, 295–299 (2013).

158. Stilo, S. A. & Murray, R. M. The epidemology of schizophrenia: replacing dogma with knowledge. *Dialogues in clinical neuroscience* **12**, 305 (2010).

159. Trotta, A. *et al.* Prevalence of bullying victimisation amongst first-episode psychosis patients and unaffected controls. *Schizophrenia research* **150**, 169–175 (2013).

160. Björkqvist, K. Social defeat as a stressor in humans. *Physiology & behavior* **73**, 435–442 (2001).

161. Iñiguez, S. D. *et al.* Social defeat stress induces a depression-like phenotype in adolescent male C57BL/6 mice. *Stress* **17**, 247–255 (2014).

162. Yu, T. *et al.* Cognitive and neural correlates of depression-like behaviour in socially defeated mice: an animal model of depression with cognitive dysfunction. *The International Journal of Neuropsychopharmacology* **14**, 303–317 (2011).

163. Adamcio, B., Havemann-Reinecke, U. & Ehrenreich, H. Chronic psychosocial stress in the absence of social support induces pathological pre-pulse inhibition in mice. *Behavioural brain research* **204**, 246–249 (2009).

164. Buwalda, B. *et al.* Long-term effects of social stress on brain and behavior: a focus on hippocampal functioning. *Neuroscience & Biobehavioral Reviews* **29**, 83–97 (2005).

165. Tidey, J. W. & Miczek, K. A. Social defeat stress selectively alters mesocorticolimbic dopamine release: an in vivo microdialysis study. *Brain research* **721**, 140–149 (1996).

166. Olsson, I. A. S. & Dahlborn, K. Improving housing conditions for laboratory mice: a review of'environmental enrichment'. *Laboratory Animals* **36**, 243–270 (2002).

167. Bengoetxea, H. *et al.* Enriched and deprived sensory experience induces structural changes and rewires connectivity during the postnatal development of the brain. *Neural plasticity* **2012** (2012).

168. Rosenzweig, M. R., Bennett, E. L., Hebert, M. & Morimoto, H. Social grouping cannot account for cerebral effects of enriched environments. *Brain research* **153**, 563–576 (1978).

169. Meijer, J. H. & Robbers, Y. Wheel running in the wild. *Proceedings of the Royal Society B: Biological Sciences* **281**, 20140210 (2014).

170. Sherwin, C. Voluntary wheel running: a review and novel interpretation. *Animal Behaviour* **56**, 11–27 (1998).

171. Kohman, R. A. *et al.* Voluntary wheel running enhances contextual but not trace fear conditioning. *Behavioural brain research* **226**, 1–7 (2012).

172. Hillman, C. H., Erickson, K. I. & Kramer, A. F. Be smart, exercise your heart: exercise effects on brain and cognition. *Nature Reviews Neuroscience* **9**, 58–65 (2008).

173. Esteban-Cornejo, I., Tejero-Gonzalez, M. C., Sallis, J. F. & Veiga, O. L. Physical activity and cognition in adolescents: A systematic review. *Journal of Science and Medicine in Sport* (2014).

174. Pajonk, F.-G. *et al.* Hippocampal plasticity in response to exercise in schizophrenia. *Archives of General Psychiatry* **67**, 133–143 (2010).

175. Takuma, K., Ago, Y. & Matsuda, T. Preventive effects of an enriched environment on rodent psychiatric disorder models. *Journal of pharmacological sciences* **117**, 71–76 (2011).

176. Ilin, Y. & Richter-Levin, G. Enriched environment experience overcomes learning deficits and depressive-like behavior induced by juvenile stress. *PLoS One* **4**, e4329 (2009).

177. Kaufman, J. Stress and its consequences: An evolving story. *Biological psychiatry* **60**, 669–670 (2006).

178. Badowska, D. M., Brzózka, M. M., Chowdhury, A., Malzahn, D. & Rossner, M. J. Data calibration and reduction allows to visualize behavioural profiles of psychosocial influences in mice towards clinical domains. *European archives of psychiatry and clinical neuroscience* 1–14 (2014).

179. Urban, N. T., Willig, K. I., Hell, S. W. & Nägerl, U. V. Sted nanoscopy of actin dynamics in synapses deep inside living brain slices. *Biophysical journal* **101**, 1277–1284 (2011).

180. Wolfer, D. P. & Lipp, H.-P. Dissecting the behaviour of transgenic mice: is it the mutation, the genetic background, or the environment? *Experimental physiology* **85**, 627–634 (2000).

181. Testa, G. *et al.* A reliable lacZ expression reporter cassette for multipurpose, knockout-first alleles. *genesis* **38**, 151–158 (2004).

182. Moy, S. *et al.* Sociability and preference for social novelty in five inbred strains: an approach to assess autistic-like behavior in mice. *Genes, Brain and Behavior* **3**, 287–302 (2004).

183. Brzózka, M. M. *Untersuchungen zur Funktion des basischen Helix-Loop-Helix (bHLH)-Transkriptionsfaktors ME2 bei Lern- und Gedächtnisprozessen in der Maus*. Ph.D. thesis, Georg-August University.

184. Morris, R., Garrud, P., Rawlins, J. & O'Keefe, J. Place navigation impaired in rats with hippocampal lesions. *Nature* **297**, 681–683 (1982).

185. Morris, R., Schenk, F., Tweedie, F. & Jarrard, L. Ibotenate lesions of hippocampus and/or subiculum: dissociating components of allocentric spatial learning. *European Journal of Neuroscience* **2**, 1016–1028 (1990).

186. Schnell, C. *et al.* The multispecific thyroid hormone transporter OATP1C1 mediates cell-specific sulforhodamine 101-labeling of hippocampal astrocytes. *Brain Structure and Function* 1–11 (2013).

187. Kim, D. *et al.* TopHat2: accurate alignment of transcriptomes in the presence of insertions, deletions and gene fusions. *Genome Biol* **14**, R36 (2013).

188. Trapnell, C. *et al.* Differential analysis of gene regulation at transcript resolution with RNA-seq. *Nature biotechnology* **31**, 46–53 (2013).

189. Mootha, V. K. *et al.* PGC-1alpha-responsive genes involved in oxidative phosphorylation are coordinately downregulated in human diabetes. *Nature genetics* **34**, 267–273 (2003).

190. Subramanian, A. *et al.* Gene set enrichment analysis: a knowledge-based approach for interpreting genome-wide expression profiles. *Proceedings of the National Academy of Sciences of the United States of America* **102**, 15545–15550 (2005).

191. Reich, M. *et al.* GenePattern 2.0. *Nature genetics* **38**, 500–501 (2006).

192. Gray, E. & Whittaker, V. The isolation of nerve endings from brain: an electron microscopic study of cell fragments derived by homogenization and centrifugation. *Journal of anatomy* **96**, 79 (1962).

193. Biesemann, C. *et al.* Proteomic screening of glutamatergic mouse brain synaptosomes isolated by fluorescence activated sorting. *The EMBO journal* **33**, 157–170 (2014).

194. Maccarrone, G., Turck, C. W. & Martins-de Souza, D. Shotgun mass spectrometry workflow combining IEF and LC-MALDI-TOF/TOF. *The protein journal* **29**, 99–102 (2010).

195. Schmidt, A., Kellermann, J. & Lottspeich, F. A novel strategy for quantitative proteomics using isotope-coded protein labels. *Proteomics* **5**, 4–15 (2005).

196. Prasad, T. K. *et al.* Human protein reference database2009 update. *Nucleic acids research* **37**, D767–D772 (2009).

197. Karlsson, U. & Schultz, R. L. Fixation of the central nervous system for electron microscopy by aldehyde perfusion: I. preservation with aldehyde perfusates versus direct perfusion with osmium tetroxide with special reference to membranes and the extracellular space. *Journal of ultrastructure research* **12**, 160–186 (1965).

198. Berning, S., Willig, K. I., Steffens, H., Dibaj, P. & Hell, S. W. Nanoscopy in a living mouse brain. *Science* **335**, 551–551 (2012).

199. Welcome Trust Sanger Institute. Sanger Institute Mouse Resources Portal — line "EPD0103_3_A07" @ONLINE. `http://www.sanger.ac.uk/mouseportal/search?query=EPD0103_3_A07` (2014).

200. Ensembl Genome Browser. *Tcf4* ENSMUSG00000053477, mouse (GRCm38) @ONLINE. `http://www.ensembl.org/` (2014).

201. Einon, D., Morgan, M. & Sahakian, B. The development of intersession habituation and emergence in socially reared and isolated rats. *Developmental psychobiology* **8**, 553–559 (1975).

202. Koolhaas, J. *et al.* Stress revisited: a critical evaluation of the stress concept. *Neuroscience & Biobehavioral Reviews* **35**, 1291–1301 (2011).

203. Chowdhury, A. *Behavioural Characterization of* Tcf4 *Transgenic mice Subjected to Mild Chronic Psychosocial stress*. Master's thesis, MSc/MD/PhD Neuroscience Program.

204. Horiguchi, N. *et al.* Involvement of spinal 5-HT1A receptors in isolation rearing-induced hypoalgesia in mice. *Psychopharmacology* **227**, 251–261 (2013).

205. Dworkin, R. H. Pain insensitivity in schizophrenia. *Schizophrenia Bulletin* **20**, 235–248 (1994).

206. Fishbain, D. A. Pain insensitivity in psychosis. *Annals of emergency medicine* **11**, 630–632 (1982).

207. Rosenthal, S. H., Porter, K. A. & Coffey, B. Pain insensitivity in schizophrenia: case report and review of the literature. *General hospital psychiatry* **12**, 319–322 (1990).

208. Hooley, J. M. & Delgado, M. L. Pain insensitivity in the relatives of schizophrenia patients. *Schizophrenia research* **47**, 265–273 (2001).

209. Schenk, S., Britt, M. D. & Atalay, J. Isolation rearing decreases opiate receptor binding in rat brain. *Pharmacology Biochemistry and Behavior* **16**, 841–842 (1982).

210. Petkov, V., Konstantinova, E. & Grachovska, T. Changes in brain opiate receptors in rats with isolation syndrome. *Pharmacological research communications* **17**, 575–584 (1985).

211. Konecka, A. & Sroczyńska, I. Stressors and pain sensitivity in cfw mice. role of opioid peptides. *Archives Of Physiology And Biochemistry* **98**, 245–252 (1990).

212. Loh, H. H., Tseng, L., Wei, E. & Li, C. H. Beta-endorphin is a potent analgesic agent. *Proceedings of the National Academy of Sciences* **73**, 2895–2898 (1976).

213. Kieffer, B. L. Recent advances in molecular recognition and signal transduction of active peptides: receptors for opioid peptides. *Cellular and molecular neurobiology* **15**, 615–635 (1995).

214. Rose, S. R. & Orlowski, J. Review of research on endorphins and learning. *Journal of Developmental & Behavioral Pediatrics* **4**, 131–135 (1983).

215. Wiegant, V. M., Ronken, E., Kovacs, G. & De Wied, D. Endorphins and schizophrenia. *Progress in brain research* **93**, 433–453 (1992).

216. Espinosa-Meléndez, E., Lal, S., Nair, N. & Chang, T. M. S. Artificial organs: Thoughts & progress: Plasma β-endorphin levels in chronic schizophrenic patients and normal controls. *Artificial organs* **3**, 375–377 (1979).

217. Ross, M., Berger, P. A. & Goldstein, A. Plasma beta-endorphin immunoreactivity in schizophrenia. *Science* **205**, 1163–1164 (1979).

218. Brambilla, F., Facchinetti, F., Petraglia, F., Vanzulli, L. & Genazzani, A. Secretion pattern of endogenous opioids in chronic schizophrenia. *The American journal of psychiatry* (1984).

219. Albus, M., von Gellhorn, K., Münch, U., Naber, D. & Ackenheil, M. A double-blind study with ceruletide in chronic schizophrenic patients: biochemical and clinical results. *Psychiatry research* **19**, 1–7 (1986).

220. Mauri, M. C. *et al.* Cholecystokinin, β-endorphin and vasoactive intestinal peptide in peripheral blood mononuclear cells of drug-naive schizophrenic patients treated with haloperidol compared to healthy controls. *Psychiatry research* **78**, 45–50 (1998).

221. Berger, P. A. *et al.* β-endorphin and schizophrenia. *Archives of general psychiatry* **37**, 635–640 (1980).

222. Gil-Ad, I., Dickerman, Z., Amdursky, S. & Laron, Z. Diurnal rhythm of plasma beta endorphin, cortisol and growth hormone in schizophrenics as compared to control subjects. *Psychopharmacology* **88**, 496–499 (1986).

223. Labrecque, G. & Vanier, M.-C. Biological rhythms in pain and in the effects of opioid analgesics. *Pharmacology & therapeutics* **68**, 129–147 (1995).

224. Konecka, A. M. & Sroczynska, I. Circadian rhythm of pain in male mice. *General Pharmacology: The Vascular System* **31**, 809–810 (1998).

225. Facchinetti, F. *et al.* Hyperendorphinemia in obesity and relationships to affective state. *Physiology & behavior* **36**, 937–940 (1986).

226. Scavo, D. *et al.* Hyperendorphinemia in obesity is not related to the affective state. *Physiology & behavior* **48**, 681–683 (1990).

227. Walsh, J. *et al.* Disruption of thermal nociceptive behaviour in mice mutant for the schizophrenia-associated genes *NRG1, COMT* and *DISC1. Brain Research* **1348**, 114–119 (2010).

228. Bouet, V., Lecrux, B., Tran, G. & Freret, T. Effect of pre- versus post-weaning environmental disturbances on social behaviour in mice. *Neuroscience letters* **488**, 221–224 (2011).

229. Robbins, T., Jones, G. & Wilkinson, L. Behavioural and neurochemical effects of early social deprivation in the rat. *Journal of Psychopharmacology* **10**, 39–47 (1996).

230. Gentsch, C., Lichtsteiner, M., Frischknecht, H.-R., Feer, H. & Siegfried, B. Isolation-induced locomotor hyperactivity and hypoalgesia in rats are prevented by handling and reversed by resocialization. *Physiology & behavior* **43**, 13–16 (1988).

231. Fone, K. C. F. & Porkess, M. V. Behavioural and neurochemical effects of post-weaning social isolation in rodents-relevance to developmental neuropsychiatric disorders. *Neuroscience and Biobehavioral Reviews* **32**, 1087–1102 (2008).

232. Jochum, T. *et al.* Influence of antipsychotic medication on pain perception in schizophrenia. *Psychiatry research* **142**, 151–156 (2006).

233. McAlonan, K. & Brown, V. J. Orbital prefrontal cortex mediates reversal learning and not attentional set shifting in the rat. *Behavioural brain research* **146**, 97–103 (2003).

234. Ferry, A. T., Lu, X.-C. M. & Price, J. L. Effects of excitotoxic lesions in the ventral striatopallidal–thalamocortical pathway on odor reversal learning: inability to extinguish an incorrect response. *Experimental Brain Research* **131**, 320–335 (2000).

235. Bissonette, G. B. & Powell, E. M. Reversal learning and attentional set-shifting in mice. *Neuropharmacology* **62**, 1168–1174 (2012).

236. Jones, G., Marsden, C. & Robbins, T. Behavioural rigidity and rule-learning deficits following isolation-rearing in the rat: neurochemical correlates. *Behavioural brain research* **43**, 35–50 (1991).

237. Sepp, M. *Functions of the basic helix-loop-helix transcription factor* TCF4 *in health and disease*. Ph.D. thesis, Tallin University of Technology.

238. Richtsmeier, J. T., Baxter, L. L. & Reeves, R. H. Parallels of craniofacial maldevelopment in Down syndrome and Ts65Dn mice. *Developmental Dynamics* **217**, 137–145 (2000).

239. Viosca, J., Lopez-Atalaya, J. P., Olivares, R., Eckner, R. & Barco, A. Syndromic features and mild cognitive impairment in mice with genetic reduction on p300 activity: differential contribution of p300 and CBP to Rubinstein–Taybi syndrome etiology. *Neurobiology of disease* **37**, 186–194 (2010).

240. Agim, Z. S. *et al.* Discovery, validation and characterization of *Erbb4* and *Nrg1* haplotypes using data from three genome-wide association studies of schizophrenia. *PLoS one* **8**, e53042 (2013).

241. Agarwal, A. *et al.* Dysregulated expression of Neuregulin-1 by cortical pyramidal neurons disrupts synaptic plasticity. *Cell Reports* (2014).

242. Shen, H.-Y. & Chen, J.-F. Adenosine A2A receptors in psychopharmacology: modulators of behavior, mood and cognition. *Current neuropharmacology* **7**, 195 (2009).

243. Ribeiro, J. A. & Sebastiao, A. M. Caffeine and adenosine. *Journal of Alzheimer's Disease* **20**, 3–15 (2010).

244. Wardas, J. Potential role of adenosine A2A receptors in the treatment of schizophrenia. *Frontiers in bioscience: a journal and virtual library* **13**, 4071–4096 (2007).

245. Jacob, C., Domschke, K., Gajewska, A., Warrings, B. & Deckert, J. Genetics of panic disorder: focus on association studies and therapeutic perspectives. *Expert review of neurotherapeutics* **10**, 1273–1284 (2010).

246. Pfaff, D. W. *Hormones, Brain and Behavior. Chapter:5 (p.173)* (Elsevier, 2002).

247. Chu Sin Chung, P. & Kieffer, B. L. Delta opioid receptors in brain function and diseases. *Pharmacology & therapeutics* **140**, 112–120 (2013).

248. Mikesell, M., Sobell, J., Sommer, S. & McMurray, C. Identification of a missense mutation and several polymorphisms in the proenkephalin a gene of schizophrenic patients. *American journal of medical genetics* **67**, 459–467 (1996).

249. Volk, D. W., Radchenkova, P. V., Walker, E. M., Sengupta, E. J. & Lewis, D. A. Cortical opioid markers in schizophrenia and across postnatal development. *Cerebral Cortex* **22**, 1215–1223 (2012).

250. Eisinger, B. E., Driessen, T. M., Zhao, C. & Gammie, S. C. Medial prefrontal cortex: genes linked to bipolar disorder and schizophrenia have altered expression in the highly social maternal phenotype. *Frontiers in behavioral neuroscience* **8** (2014).

251. Chahl, L. A. Tachykinins and neuropsychiatric disorders. *Current drug targets* **7**, 993–1003 (2006).

252. Choi, K. H. *et al.* Putative psychosis genes in the prefrontal cortex: combined analysis of gene expression microarrays. *BMC psychiatry* **8**, 87 (2008).

253. Kehler, J. & Nielsen, J. PDE10A inhibitors: novel therapeutic drugs for schizophrenia. *Current pharmaceutical design* **17**, 137–150 (2011).

254. Lai, C. S., Fisher, S. E., Hurst, J. A., Vargha-Khadem, F. & Monaco, A. P. A forkhead-domain gene is mutated in a severe speech and language disorder. *Nature* **413**, 519–523 (2001).

255. Wohlgemuth, S., Adam, I. & Scharff, C. *FoxP2* in songbirds. *Current opinion in neurobiology* **28**, 86–93 (2014).

256. French, C. A. & Fisher, S. E. What can mice tell us about Foxp2 function? *Current opinion in neurobiology* **28**, 72–79 (2014).

257. Schratt, G. microRNAs at the synapse. *Nature Reviews Neuroscience* **10**, 842–849 (2009).

258. Kobayashi, S. & Anzai, K. An E-box sequence acts as a transcriptional activator for BC1 RNA expression by RNA polymerase III in the brain. *Biochemical and biophysical research communications* **245**, 59–63 (1998).

259. Muddashetty, R. S. *et al.* Poly (A)-binding protein is associated with neuronal BC1 and BC200 ribonucleoprotein particles. *Journal of molecular biology* **321**, 433–445 (2002).

260. Muslimov, I. A. *et al.* RNA transport in dendrites: a cis-acting targeting element is contained within neuronal BC1 RNA. *The Journal of neuroscience* **17**, 4722–4733 (1997).

261. Wang, H. *et al.* Dendritic BC1 RNA: functional role in regulation of translation initiation. *The Journal of neuroscience* **22**, 10232–10241 (2002).

262. Zhong, J. *et al.* BC1 regulation of metabotropic glutamate receptor-mediated neuronal excitability. *The Journal of Neuroscience* **29**, 9977–9986 (2009).

263. Skryabin, B. V. *et al.* Neuronal untranslated BC1 RNA: targeted gene elimination in mice. *Molecular and cellular biology* **23**, 6435–6441 (2003).

264. Lewejohann, L. *et al.* Role of a neuronal small non-messenger RNA: behavioural alterations in BC1 RNA-deleted mice. *Behavioural brain research* **154**, 273–289 (2004).

265. Stoll, G. *et al.* Deletion of TOP3β, a component of FMRP-containing mRNPs, contributes to neurodevelopmental disorders. *Nature neuroscience* **16**, 1228–1237 (2013).

266. Murakami, Y. *et al.* Differential expression of plexin-a subfamily members in the mouse nervous system. *Developmental Dynamics* **220**, 246–258 (2001).

267. Takahashi, T. *et al.* Plexin-neuropilin-1 complexes form functional semaphorin-3a receptors. *Cell* **99**, 59–69 (1999).

268. Spinelli, E., McPhail, L., Oschipok, L., Teh, J. & Tetzlaff, W. Class A plexin expression in axotomized rubrospinal and facial motoneurons. *Neuroscience* **144**, 1266–1277 (2007).

269. Waimey, K. E. & Cheng, H.-J. Axon pruning and synaptic development: how are they per-plexin? *The Neuroscientist* **12**, 398–409 (2006).

270. Robison, A. Emerging role of CaMKII in neuropsychiatric disease. *Trends in neurosciences* (2014).

271. Coultrap, S. J. *et al.* Autonomous CaMKII mediates both LTP and LTD using a mechanism for differential substrate site selection. *Cell reports* **6**, 431–437 (2014).

272. OMIM database. Entry: #300624: Fragile X mental retardation syndrome @ONLINE (2014).

273. Irwin, S. A. *et al.* Abnormal dendritic spine characteristics in the temporal and visual cortices of patients with fragile-X syndrome: a quantitative examination. *American journal of medical genetics* **98**, 161–167 (2001).

274. Comery, T. A. *et al.* Abnormal dendritic spines in fragile X knockout mice: maturation and pruning deficits. *Proceedings of the National Academy of Sciences* **94**, 5401–5404 (1997).

275. Tomassy, G. S. *et al.* Distinct profiles of myelin distribution along single axons of pyramidal neurons in the neocortex. *Science* **344**, 319–324 (2014).

276. Rutten, K. *et al.* Enhanced long-term depression and impaired reversal learning in phosphodiesterase 4B-knockout (*PDE4B-/-*) mice. *Neuropharmacology* **61**, 138–147 (2011).

277. Dong, Z. *et al.* Hippocampal long-term depression mediates spatial reversal learning in the Morris water maze. *Neuropharmacology* **64**, 65–73 (2013).

278. Manahan-Vaughan, D. Hippocampal long-term depression as a declarative memory mechanism. In *Synaptic Plasticity and Transsynaptic Signaling*, 305–319 (Springer, 2005).

279. Fairbanks, C. A. *et al.* The VGF-derived peptide TLQP-21 contributes to inflammatory and nerve injury-induced hypersensitivity. *Pain* **155**, 1229–1237 (2014).

280. Riedl, M. S. *et al.* Proteomic analysis uncovers novel actions of the neurosecretory protein VGF in nociceptive processing. *The Journal of Neuroscience* **29**, 13377–13388 (2009).

281. Rizzi, R. *et al.* The VGF-derived peptide TLQP-21: a new modulatory peptide for inflammatory pain. *Neuroscience letters* **441**, 129–133 (2008).

282. Brumovsky, P., Bergman, E., Liu, H.-X., Hökfelt, T. & Villar, M. Effect of a graded single constriction of the rat sciatic nerve on pain behavior and expression of immunoreactive NPY and NPY Y1 receptor in DRG neurons and spinal cord. *Brain research* **1006**, 87–99 (2004).

283. Obata, K. & Noguchi, K. BDNF in sensory neurons and chronic pain. *Neuroscience research* **55**, 1–10 (2006).

284. Summ, O., Charbit, A. R., Andreou, A. P. & Goadsby, P. J. Modulation of nocioceptive transmission with calcitonin gene-related peptide receptor antagonists in the thalamus. *Brain: A Journal of Neurology* **133**, 2540–2548 (2010).

285. Koshimizu, T.-a. & Tsujimoto, G. New topics in vasopressin receptors and approach to novel drugs: vasopressin and pain perception. *Journal of Pharmacological Sciences* **109**, 33–37 (2009).

286. Stein, D. J. Oxytocin and vasopressin: social neuropeptides. *CNS spectrums* **14**, 602–606 (2009).

287. Heinrichs, M., von Dawans, B. & Domes, G. Oxytocin, vasopressin, and human social behavior. *Frontiers in neuroendocrinology* **30**, 548–557 (2009).

288. Meyer-Lindenberg, A., Domes, G., Kirsch, P. & Heinrichs, M. Oxytocin and vasopressin in the human brain: social neuropeptides for translational medicine. *Nature Reviews Neuroscience* **12**, 524–538 (2011).

289. Anacker, A. M. J. & Beery, A. K. Life in groups: the roles of oxytocin in mammalian sociality. *Frontiers in Behavioral Neuroscience* **7**, 185 (2013).

290. Haller, J. The neurobiology of abnormal manifestations of aggression–a review of hypothalamic mechanisms in cats, rodents, and humans. *Brain Research Bulletin* **93**, 97–109 (2013).

291. Neumann, I. D. & Landgraf, R. Balance of brain oxytocin and vasopressin: implications for anxiety, depression, and social behaviors. *Trends in Neurosciences* **35**, 649–659 (2012).

292. Rubin, L. H. *et al.* Reduced levels of vasopressin and reduced behavioral modulation of oxytocin in psychotic disorders. *Schizophrenia bulletin* sbu027 (2014).

293. Tiedge, H., Bloom, F. E. & Richter, D. RNA, whither goest thou? *Science* **283**, 186–187 (1999).

Appendix A: Behaviour
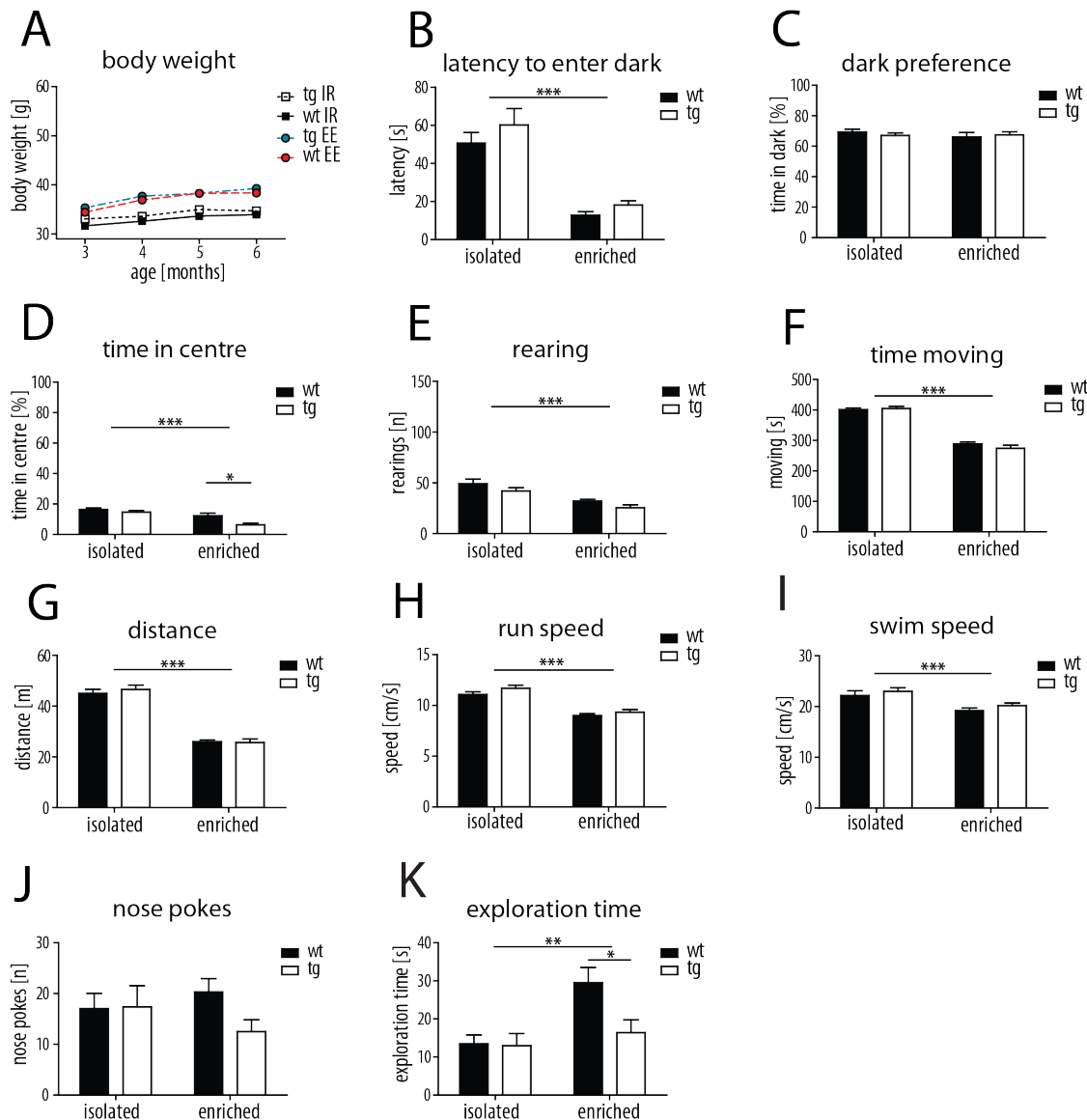
Figure 1: Basic behaviour of *Tcf4*tg mice upon IR and EE. A) Body weight was higher in EE mice (p<0.0001). **B–C)** Light-dark preference **B)** Latency to enter dark box was longer in IR than EE mice (p<0.0001). **C)** Dark preference. **D–H)** Open field. **D)** Time in the centre was reduced by EE (p<0.0001) and *Tcf4*tg (p=0.0064), particularly in EE *Tcf4*tg (p<0.01, Bonferroni). **E)** Rearing was affected by IR (p<0.0001) and *Tcf4*tg (p=0.0458). **F–H)** Time moving, distance and speed were increased by IR (p<0.0001 for all). **I)** In Water Maze IR mice swam faster (p<0.0001). **J–K)** Hole board. **J)** Nose pokes. **K)** Exploration time was increased by EE (p=0.0044) but reduced in EE *Tcf4*tg mice (p<0.05, Bonferroni, genotype effect p=0.0428). Bar graphs show means with SEM. Tests were analysed with Two-way ANOVA, unless stated differently.
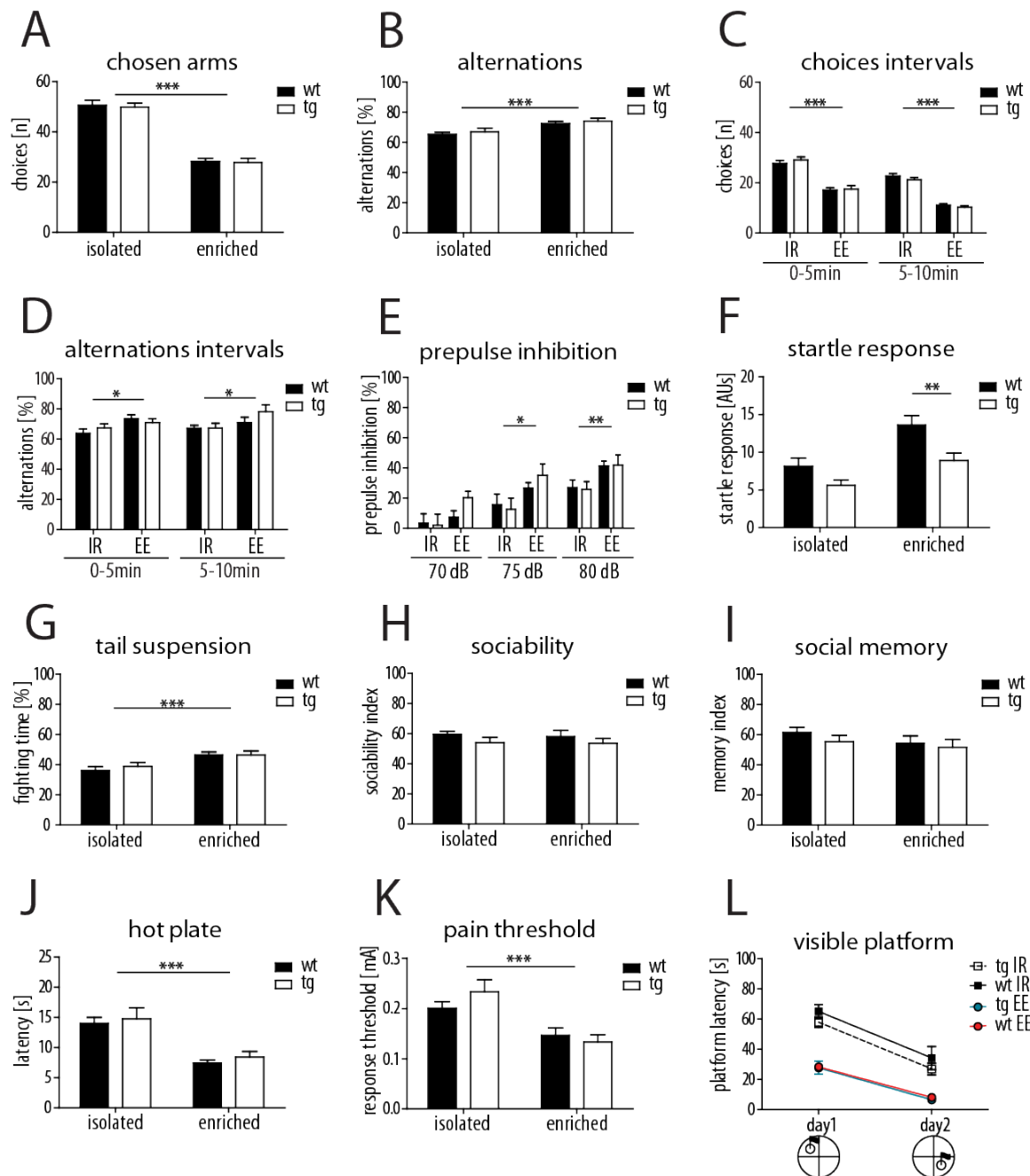
Figure 2: Basic behaviour of *Tcf4*tg mice upon IR and EE. A–D) Y-maze. **A)** Total arm exploration is increased upon IR (p<0.0001). **B)** Total number of alternations is reduced by IR (p=0.0003). **C)** IR mice explore arms of the maze more than EE in first (p<0.0001) and second interval (p<0.0001). **D)** IR mice make fewer alternations in first (p=0.0145) and second interval (p=0.0259). **E)** Prepulse inhibition is reduced by IR at 75 dB (p=0.0134) and 80 dB (p=0.0057). **F)** Startle response to 120 dB pulse is affected by housing (p<0.0001) and genotype (p=0.0013). In EE group it is reduced in *Tcf4*tg (p<0.01, Bonferroni). **G)** In tail suspension test IR mice fight less (p<0.0001) implying reduced motivation. **H–I)** Social interaction. Neither sociability nor social memory are alterations were observed. **J)** Hot plate. Thermal pain sensitivity was increased by IR (p<0.0001). **K)** Pain threshold for electric shocks is increased upon IR (p<0.0001). **L)** Water Maze, visible platform: EE mice reach the platform faster than IR mice (p<0.0001, RM ANOVA). Bar graphs represent mean with SEM. All tests were analysed using Two-way ANOVA, unless stated differently.
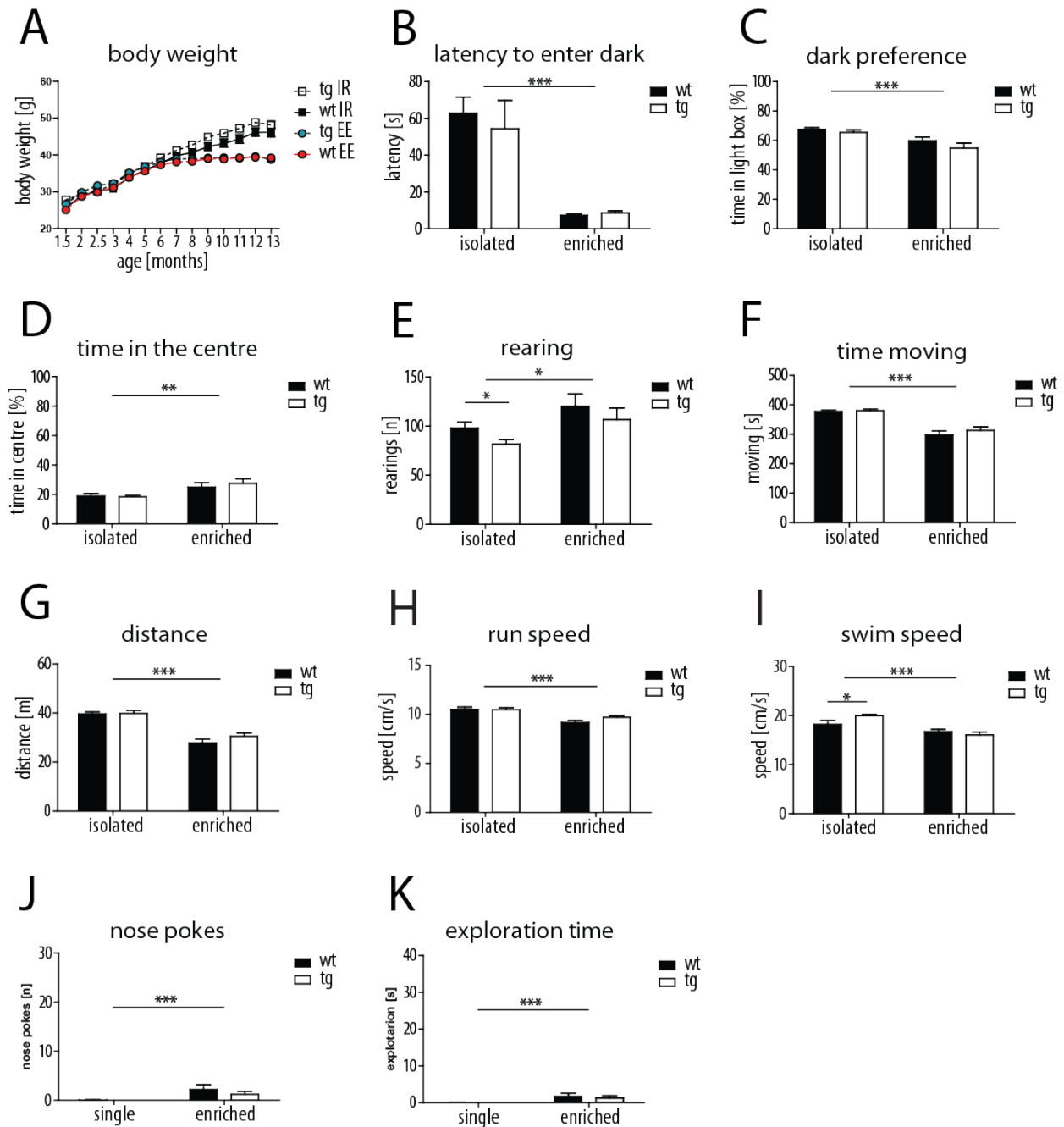
Figure 3: Basic behaviour of aged *Tcf4*tg mice upon IR and EE. A) Body weight was increased in IR mice from the age of 8 months and *Tcf4*tg mice were slightly heavier that wt in IR group. **B–C)** Light-dark preference. **B)** IR mice entered the dark compartment later than EE mice (p<0.0001). **C)** IR mice displayed higher dark preference (p<0.0001). **D–G)** Open field. **D)** IR mice spent less time in the centre (p=0.002). **E)** Rearing was reduced upon IR (p=0.0133) and particularly in *Tcf4*tg mice (p=0.0344, t-test), but without G×E. **F)** Time moving (p<0.0001), **G)** covered distance (p<0.0001) and **H)** running speed (p<0.0001) were increased upon IR. **I)** In Water Maze mean swim speed (all phases) was affected by housing (p<0.0001) and G×E (p=0.0352). In IR group *Tcf4*tg mice swam faster than wt (p<0.05, Bonferroni). **J–K)** Hole board. **J)** Number of hole nose pokes was reduced in IR (p=0.002), similarly to **K)** exploration time (p=0.0072). Bar graphs represent mean with SEM. All tests were analysed using Two-way ANOVA, unless stated differently.
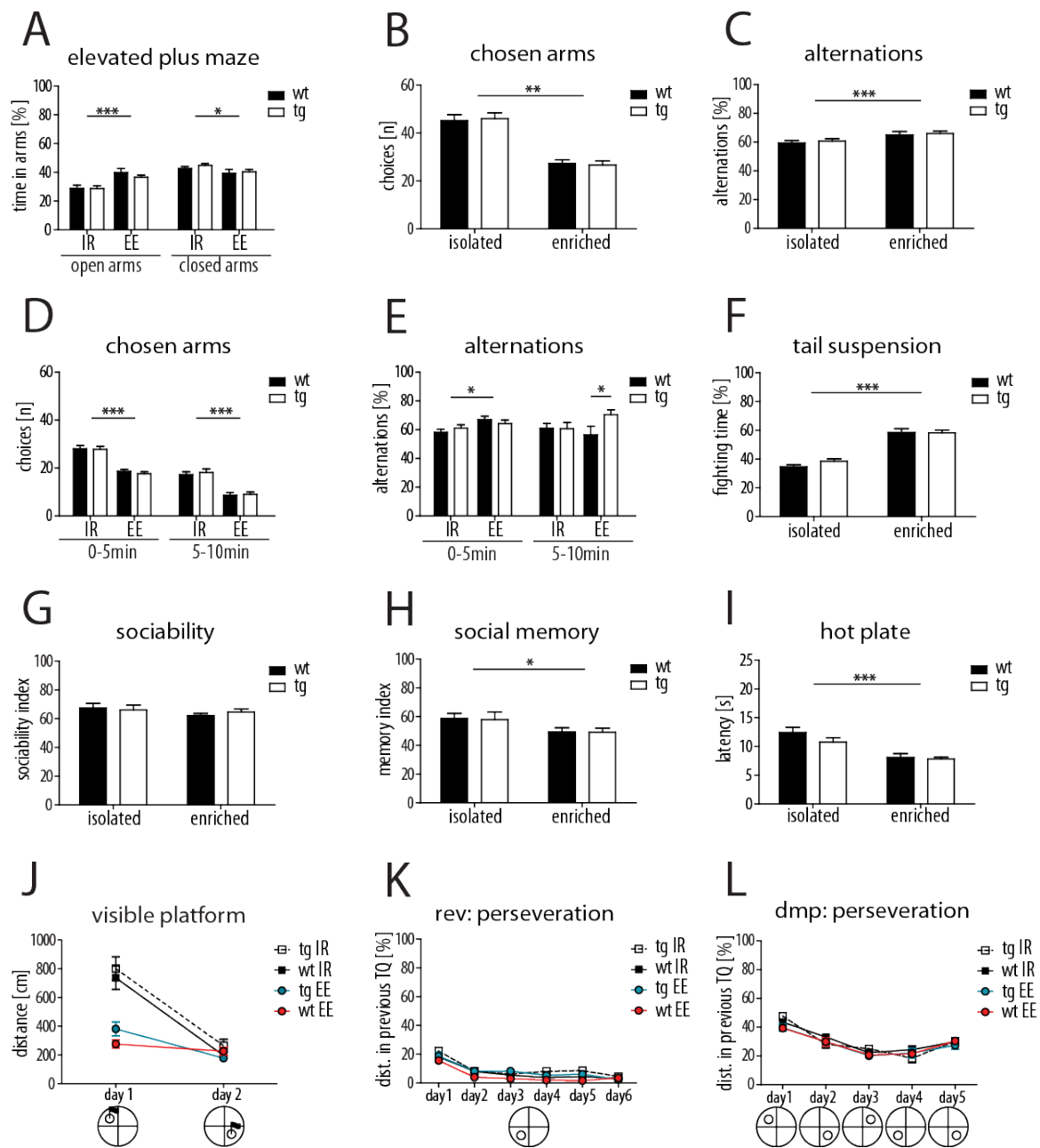
Figure 4: Basic behaviour of aged *Tcf4*tg mice upon IR and EE. A) EPM. IR mice spent less time in open (p<0.001) and more time in closed arms (p=0.0332). **B–E)** Y-maze. **B)** IR animals explored more arms in total than EE (p<0.0001). **C)** IR mice made in total fewer alternations than EE mice (p=0.0045). **D)** In both intervals IR mice made more arm choices than EE mice (both p<0.0001). **E)** IR mice made fewer alternations in first interval (p=0.0119). In the second interval effects of housing and genotype were not significant; however, in EE group *Tcf4*tg mice made more alternations than wt mice (p<0.05, Bonferroni). **F)** In TST IR mice showed reduced fighting time (p<0.0001). **G–H)** Social interaction. **G)** Sociability was not altered in any of the groups. **H)** Social memory was increased in IR mice (p=0.0203). **I)** In hot plate test pain threshold was increased upon IR (p<0.0001). **J–K)** MWM. **J)** In visible platform phase IR mice learned slower than EE mice (p<0.0001, RM ANOVA). **K–L)** Perseveration (% distance in previous target quadrant) was not altered in reversal learning nor in delayed matching to place. Bar graph represent mean with SEM. All tests were analysed using Two-way ANOVA, unless stated differently.
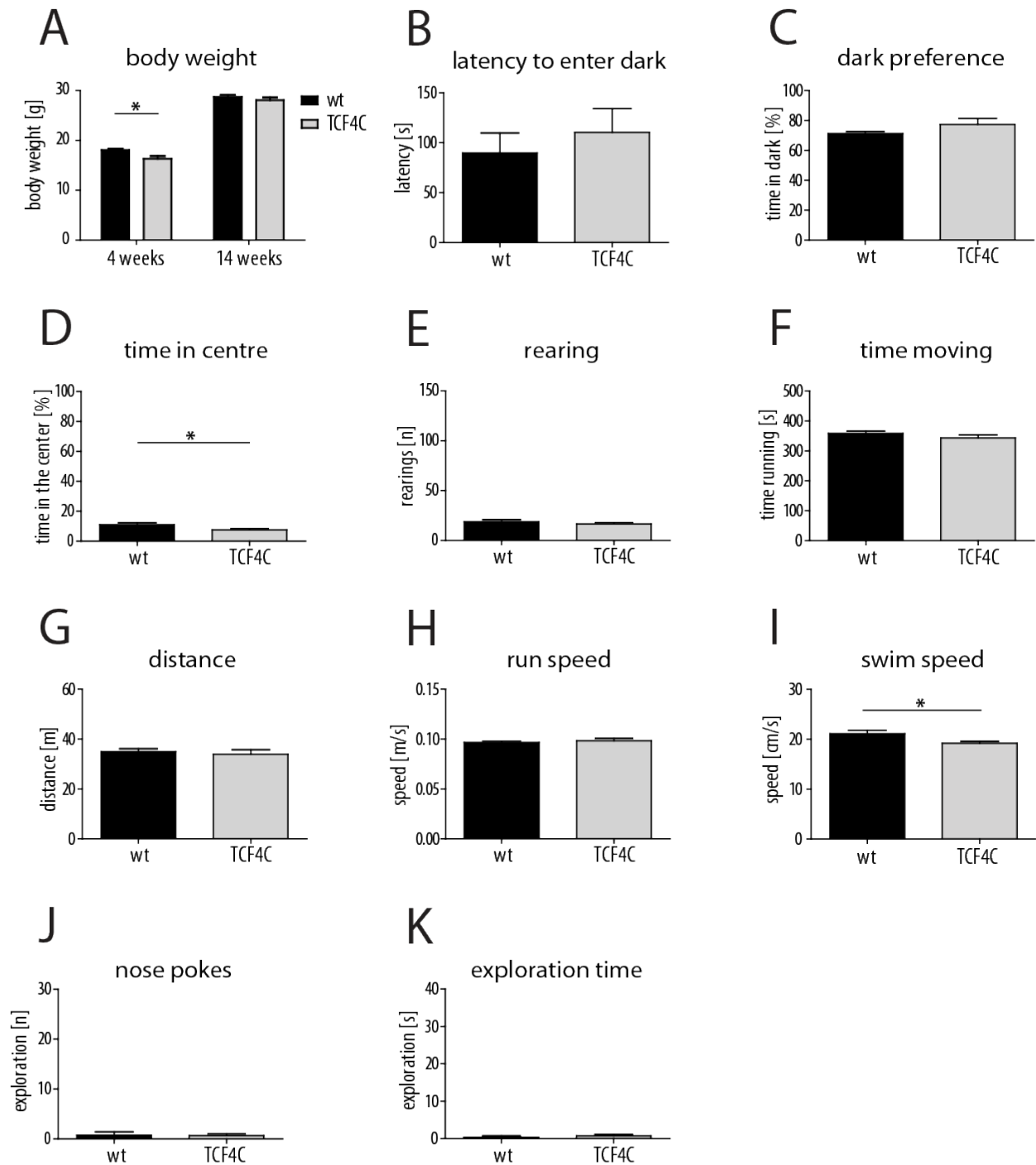
Figure 5: Basic behaviour of *Tcf4*C mice. A) Body weight was reduced in *Tcf4*C mice at the age of 4 weeks (p=0.0472, Mann Whitney test, *Tcf4*C n=23, wt n=16) but not at 14 weeks (*Tcf4*C n=16, wt n=14). **B–C)** Light-dark preference. No significant changes were detected. **D–H)** Open field. **D)** *Tcf4*C mice spent less time in the centre, which suggest mildly increased anxiety. **E–H)** Neither rearing nor locomotor activity was altered in any of the parameters. **I)** In Morris Water Maze swimming speed was reduced in *Tcf4*C mice (p=0.02229, Mann Whitney test). **J–K)** Hole board exploration was not changed in *Tcf4*C. Bar graph represent mean with SEM.
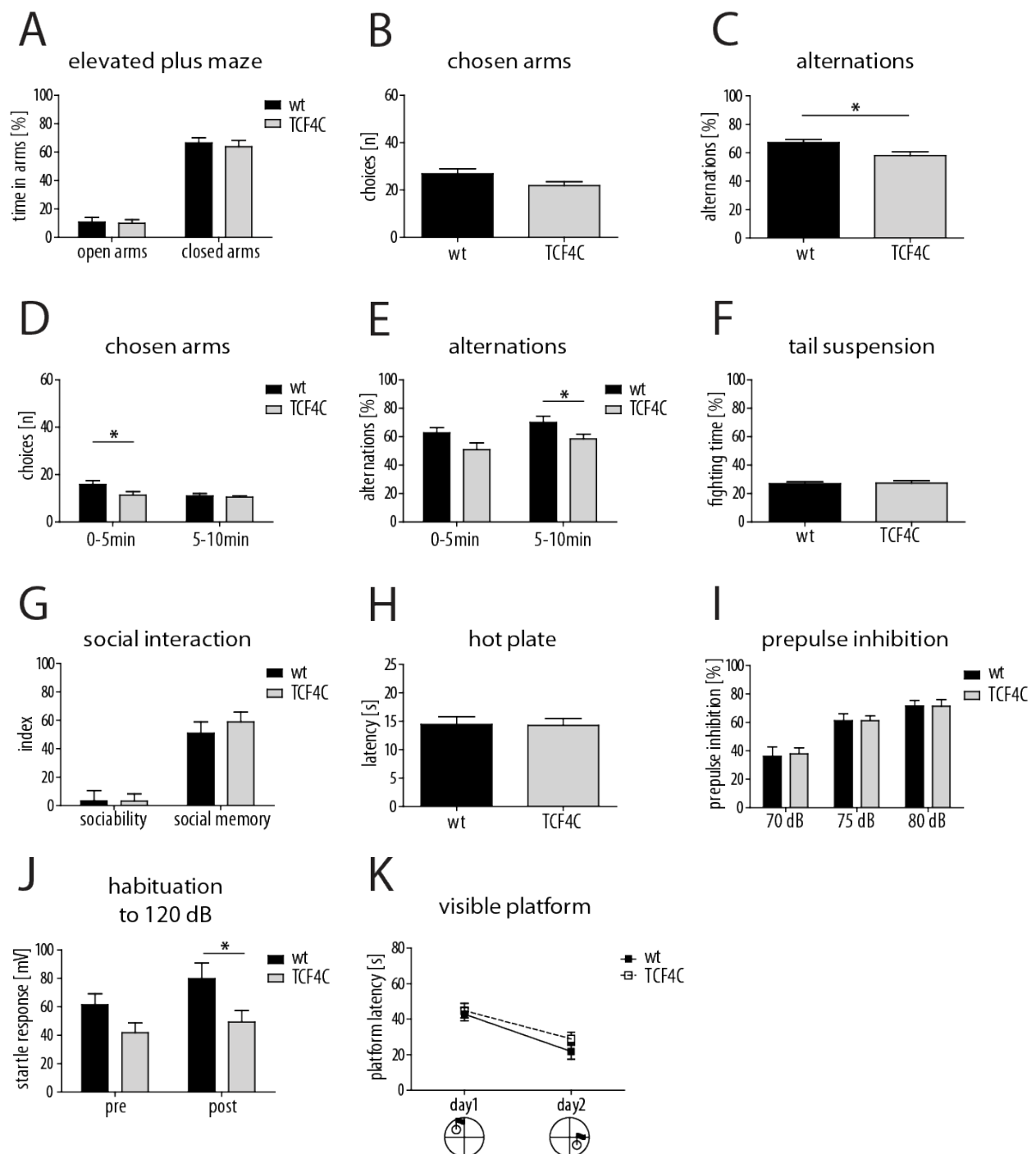
Figure 6: Basic behaviour of *Tcf4*C mice. A) Elevated plus maze. **B–E)** Y-maze. **B)** Total arm exploration was not altered in *Tcf4*C mice. **C)** Total alternation number was mildly reduced in *Tcf4*C animals (p=0.014, t-test). **D)** *Tcf4*C mice explored the arms less than wt in first (p=0.0469, t-test), but not in the second interval. **E)** Number of alternations was reduced in *Tcf4*C mice only in the second interval (p=0.0475, t-test). **G)** Sociability and social memory were normal. **H)** Pain sensitivity was unaffected in *Tcf4*C mice. **I–J)** Prepulse inhibition was normal, but startle response to 120 dB pulse was reduced in *Tcf4*C mice (p=0.0311, Two-way RM ANOVA), particularly in post-test (p<0.05, Bonferroni). **K)** In MWM visible platform *Tcf4*C mice showed no impairments. Bar graphs represent mean with SEM.

Table 1: Cognition in *Tcf4*tg and *Tcf4*C mice: domains, traits and measures. Data from the *Young Tcf4tg IR–EE* and SD–ctrl cohorts as well as from *Tcf4*C cohort housed in IR. P_G — global p-value.

Superdomain	Domain	Trait	Measure	P_G	EE env tg/wt Effect	EE Statistic	EE P	IR env tg/wt Effect	IR Statistic	IR P	SD env tg/wt Effect	SD Statistic	SD P	IR env ko/wt Effect	ko Statistic	ko P	G×E $P_{tg/wt×IR/EE}$	G×E $P_{tg/wt×SD/ctrl}$
COGNITIVE SYMPTOM CLASS			multivariate	*	-0.127	t80=-0.438	0.663	-1.811	t86=-2.89	**0.005**	-1.997	t82=4.372	**<0.001**	-1.632	t86=-3.723	**<0.001**	0.019	0.315
Spatial Learning			multivariate	*	0.015	t76=0.04	0.969	-4.103	t82=-2.397	0.019	-3.899	t85=-6.578	**<0.001**	-4.112	t82=-6.670	**<0.001**	0.022	0.039
	Memory recall		multivariate	*	0.645	t50=1.21	0.232	0.002	t53=0.004	0.997	-4.321	t56=-6.698	**<0.001**	-1.456	t26=-1.682	0.105	ns	0.047
		WM-recall	multivariate	*	1.344	t50=1.721	0.091	0.182	t54=0.193	0.848	-2.024	t56=-2.311	0.025				ns	ns
			WMt_probe1	*	1.242	t24=1.762	0.091	0.139	t26=0.257	0.799	-2.25	t27=-2.363	0.026				ns	ns
			WMd_probe1	*	1.446	t24=1.874	0.073	0.095	t26=0.131	0.897	-1.797	t27=-2.252	0.033				ns	ns
		WM-remote recall	multivariate	*	-0.055	t50=-0.078	0.938	-0.079	t52=-0.107	0.915	-6.619	t56=-5.944	**<0.001**	-1.456	t54=-1.655	0.104	ns	**<0.001**
			WMt_probe2	*	-0.044	t24=-0.072	0.943	0.0002	t25<0.001	1.000	-8.099	t27=-7.002	**<0.001**	-1.333	t26=-1.934	0.064	ns	**0.001**
			WMd_probe2	*	-0.066	t24=-0.084	0.934	-0.157	t25=-0.194	0.848	-5.139	t27=-6.644	**<0.001**	-1.579	t26=-1.509	0.143	ns	**0.001**
	Perseveration		multivariate	*	-0.621	t50=-0.849	0.400	-7.877	t54=-2.919	**0.005**	-4.698	t56=-6.020	**<0.001**	-6.862	t26=-4.555	**<0.001**	0.014	0.046
			WMt_rev_sum	*	-0.283	t24=-0.473	0.641	-8.016	t26=-2.537	0.018	-4.289	t27=-6.172	**<0.001**	-6.469	t26=-3.874	**<0.001**	0.020	0.042
			WMd_rev_sum	*	-0.959	t24=-1.070	0.295	-7.738	t26=-2.698	0.012	-5.107	t27=5.727	**<0.001**	-7.255	t26=-5.572	**<0.001**	0.028	0.040
	Spatial learning	WM initial learning	multivariate	*	-0.093	t50=-0.128	0.899	-2.598	t26=-1.469	0.148	-3.035	t56=-3.378	**0.001**	-4.834	t54=-4.815	**<0.001**	ns	ns
			WMt_hp_sum	*	0.230	t24=0.315	0.755	-2.294	t26=-1.198	0.242	-3.253	t27=-3.304	**0.003**	-7.645	t26=-5.572	**<0.001**	ns	ns
			WMd_hp_sum	*	-0.415	t24=-0.541	0.593	-2.902	t26=-1.556	0.132	-2.816	t27=3.252	**0.003**	-2.024	t26=-2.393	0.024	ns	ns
	Baseline control	WM visible platform	*multivariate*	*	*0.63*	*t50=0.814*	*0.419*	*1.653*	*t54=0.929*	*0.357*				*-0.791*	*t54=-1.026*	*0.309*	*ns*	
			WMt_vp_sum	*	*0.468*	*t24=0.565*	*0.577*	*2.273*	*t26=1.173*	*0.252*				*-0.783*	*t26=-0.988*	*0.332*	*ns*	
			WMd_vp_sum	*	*0.792*	*t24=1.198*	*0.242*	*1.033*	*t26=0.555*	*0.584*				*-0.799*	*t26=-1.036*	*0.310*	*ns*	
Fear memory	Context memory		multivariate	*	-0.413	t54=-0.939	0.352	-0.807	t58=-2.056	0.044	0.068	t48=0.179	0.858	0.806	t53=1.433	0.158	ns	ns
		Context memory	FC_context	ns	-0.417	t52=0.83	0.410	-0.066	t58=-0.144	0.886	-0.318	t23=-1.129	0.271	0.763	t46=1.512	0.137	ns	ns
		Remote context	FC_r_context	*	0.097	t26=0.149	0.882	0.093	t28=0.15	0.882	-0.318	t23=-1.129	0.271	1.126	t23=1.772	0.090	ns	ns
	Cue memory		multivariate	*	-1.034	t24=-1.593	0.124	-1.548	t58=-3.437	**0.001**				0.383	t21=0.651	0.522	ns	ns
		Cue memory	FC_cue	*	-0.467	t52=-0.729	0.469	-1.628	t28=-2.569	0.016	0.453	t23=-0.801	0.431	0.935	t54=1.585	0.119	ns	ns
		Remore cue memory	FC_r_cue	*	-0.175	t26=-0.234	0.817	-1.468	t28=-2.177	0.038	0.453	t23=-0.801	0.431	0.967	t24=1.447	0.161	ns	ns
	Social fear memory		*multivariate*	*ns*	-0.689	t24=-0.981	0.336				*1.153*	*t56=2.099*	*0.040*	1.150	t28=1.677	0.105		
		Social fear memory	*SL_soc_avoidance*	*ns*							*0.883*	*t28=1.594*	*0.122*					
		Remore social fear memory	*SL_r_soc_avoidance*	*ns*							*1.255*	*t26=1.393*	*0.175*					
Working memory			Ymaze_alternations	*	0.104	t26=0.175	0.863	0.439	t28=0.581	0.566	-0.218	t28=-0.300	0.767	-2.032	t28=-2.666	**0.013**	ns	ns

Table 2: Environmental effects in the G×E cohorts: *Tcf4tg Young IR–EE* and *Tcf4tg SD–Control.* P_G — global p-value.
(*) IR effect on superdomain anxiety is significant for the sum score (univariate test, p=0.013).

Superdomain	Domain	Measure	P_G	IR compared to EE Effect	Statistic	P	SD compared to CTRL Effect	Statistic	P
COGNITIVE SYMPTOM CLASS		**multivariate**	*	-2.745	$t_{166}=-4.703$	**<0.001**	-3.702	$t_{160}=-7.314$	**<0.001**
	Spatial Learning	multivariate	*	-5.384	$t_{158}=-4.421$	**<0.001**	-8.061	$t_{161}=-13.08$	**<0.001**
	Memory recall	multivariate	*	-0.961	$t_{103}=-1.74$	0.085	-7.948	$t_{106}=-11.53$	**<0.001**
	Perseveration	multivariate	*	-10.502	$t_{104}=-4.143$	**<0.001**	-10.466	$t_{106}=-12.75$	**<0.001**
	Spatial learning	*multivariate*	*	-6.38	$t_{104}=-4.185$	**<0.001**	-5.904	$t_{106}=-7.289$	**<0.001**
	Baseline control	*multivariate*	*	-10.15	$t_{104}=-7.378$	**<0.001**			
	Fear memory	multivariate	*	-0.329	$t_{112}=-0.694$	0.489	-0.050	$t_{126}=-0.151$	0.880
	Context memory	multivariate	*	1.821	$t_{110}=4.125$	**<0.001**	-0.451	$t_{46}=-1.433$	0.159
	Cue memory	multivariate	*	-2.479	$t_{110}=-4.16$	0.001	0.352	$t_{46}=0.703$	0.486
	Social fear memory	*multivariate*	ns	-1.69	$t_{54}=-2.248$	0.029	0.193	$t_{55}=0.203$	0.840
	Working memory	Y maze_alternations	*	-2.367	$t_{231}=-4.861$	**<0.001**	-0.235	$t_{173}=-0.89$	0.375
NEGATIVE SYMPTOM CLASS		**multivariate**	*	0.756	$t_{112}=2.303$	0.023*	-1.899	$t_{172}=-3.609$	**<0.001**
	Pain sensitivity	HP_pain	*	3.33	$t_{112}=3.476$	**0.001**	-1.087	$t_{113}=-1.596$	0.113
	Anxiety	multivariate	*	-5.245	$t_{113}=-4.597$	**<0.001**	1.446	$t_{114}=4.358$	**<0.001**
	Curiosity	multivariate	*	-5.51	$t_{114}=-7.32$	**<0.001**	-0.261	$t_{114}=-0.778$	0.438
	Motivation	multivariate	*						
POSITIVE SYMPTOM CLASS	Hyperactivity	Ambulation	multivariate	*	-7.232	$t_{229}=-10.63$	**<0.001**	0.149	$t_{231}=0.215$	0.830
		Speed	multivariate	*	-4.431	$t_{107}=-4.397$	**<0.001**	-0.608	$t_{109}=-1.44$	0.153

106

Appendix B: Proteomics

Proteome analysis of 4 weeks old *Tcf4*tg and wt male mice (line TMEBBL6).
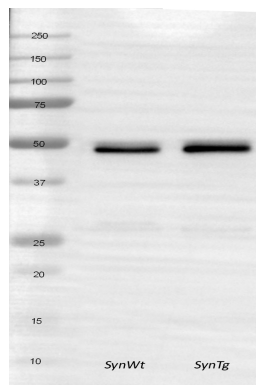
(a) CaMKIIalpha, synaptosomes
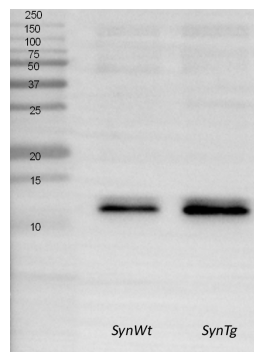
(b) HOMER1, synaptosomes
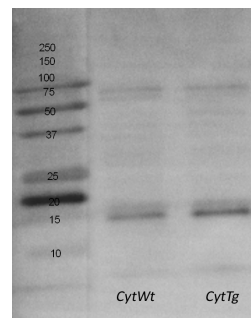
(c) VAMP1, cytoplasmatic fraction
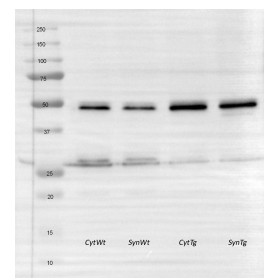
(d) VAMP2, synaptosomes and cytoplasmatic franction

Figure 7: Validation of proteomics candidates by western blotting (whole blots). Proteins from synaptosomes and cytosolic fractions of prefrontal cortices of 4 weeks old TMEBBl6 male mice. For details see Results section 4.1.5 on page 45

Appendix C: Hypoalgesia
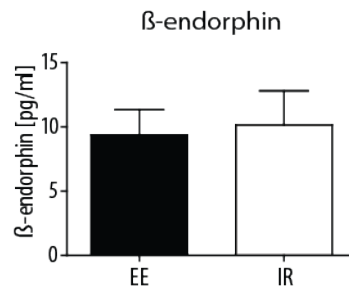
Figure 8: Serum β-endorphin levels in mice housed in IR and EE. No difference was detected between the two groups of animals. The result has to be interpreted with caution due to very low measured concentrations and high standard deviations.
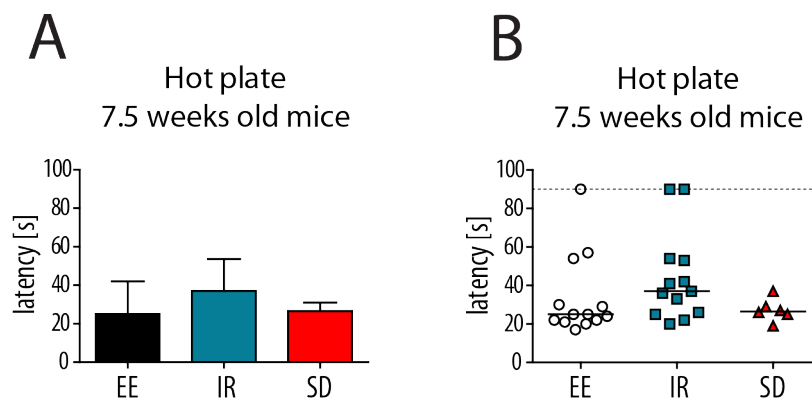
Figure 9: Pain sensitivity in 7.5 weeks old EE, IR and SD mice. To avoid the influence of prolonged isolation after the end of the stress period, we assessed whether differences in pain sensitivity apparent after 3.5 weeks of IR (n=13), SD (n=6) and EE (n=13). Hot plate test revealed no significant differences; however the median of IR latencies is higher than of EE and SD mice. Presumably, hypoalgesia in IR animals develops over time, starts to emerge already after 3 weeks of IR and would be more pronounced after longer time. The result suggests that hypoalgesia may be specific to IR and not to SD.

The cut-off value in this experiment was 90 s. Animals that failed to jump or lick their back paws within this time were assigned the value of 90 s. **A)** Bar graphs represent medians with interquartile range. **B)** Dot plots show the same data for individual animals.
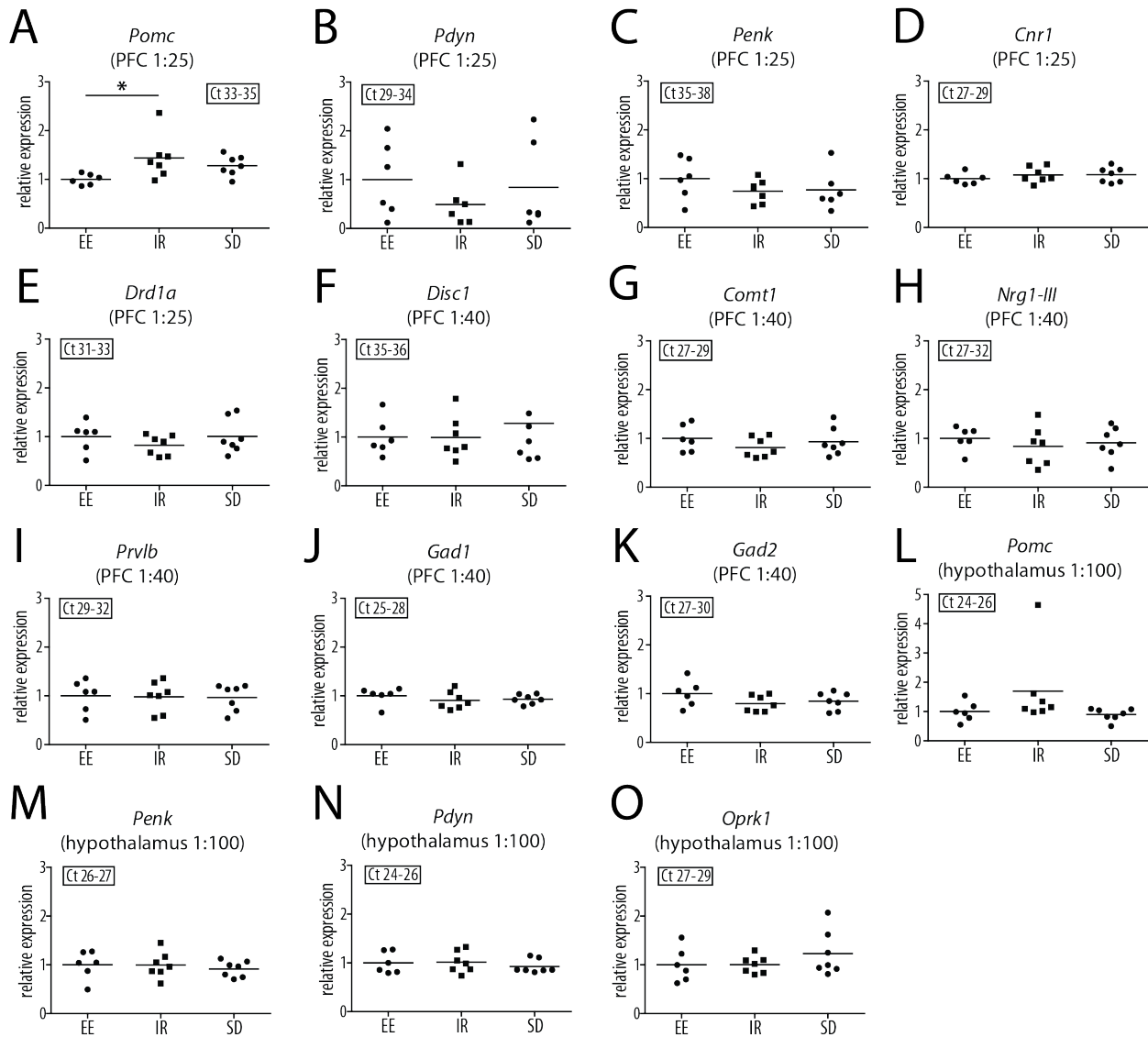
Figure 10: RT-qPCR in PFC and hypothalamus of wt EE, IR and SD mice. Genes associated with pain sensitivity or psychotic disorders were chosen. **A–E)** PFC, cDNA in dilution 1:25. **F–K)** PFC, dilution 1:40. **L–O)** Hypothalamus, dilution 1:100. **A)** *Pomc* was upregulated in IR compared to EE in PFC (p=0.0222, Kruskal-Wallis test). **C–O)** None of the other tested genes showed significant differences between the groups. Plots show single animals (dots) and group means (relative to *Actb*). Average *Ct* ranges are shown in boxes. **Genes:** *Actb* β-actin, *Pomc* proopiomelanocortin, *Pdyn* prodynorphin, *Penk* proenkephalin, *Cnr1* cannabinoid receptor 1, *Drd1a* dopamine receptor 1a, *Disc1* disrupted in schizophrenia, *Comt1* catechol-O-methyltransferase, *Nrg1-III* neuregulin 1 type III, *Prlvb* parvalbumin, *Gad1* and *Gad2* glutamate decarboxylase 1 and 2, *Oprk1* opioid kappa receptor 1. Other genes included in the screen are not shown due to low expression or high standard deviations.

List of Figures

List of Tables

Herewith I declare, that I prepared the PhD Thesis *Schizophrenia Risk Factor Tcf4 and Gene × Environment Interaction in Mice* on my own and with no other sources and aids than quoted.

Göttingen, 20th February 2015   Dorota Badowska

Curriculum Vitae

Dorota Badowska

born on 1st May 1987 in Warsaw, Poland

address: Hermann-Rein-Str. 3, 37075, Göttingen, Germany

telephone: +49 (0) 551 3899 486

e-mail: badowska@em.mpg.de

EDUCATION

2010 – present	Ph.D. candidate, Max Planck Institute for Experimental Medicine, Göttingen, Germany
2009 – 2010	MSc/PhD Neuroscience program at Georg-August Universität and Max-Planck Institutes, Göttingen, Germany
2005 - 2009	College of Inter-faculty Individual Studies in Mathematics and Natural Sciences (MISMaP), University of Warsaw, Poland. Fields of study: biotechnology (major, BSc), psychology (minor).

ACHIEVEMENTS AND SCIENTIFIC ACTIVITIES

2013	Award for the best student talk at the *Neuronus-IBRO Young Neuroscience Forum* in Cracow, Poland.
2013	Co-organizer of the *Neurizons* student conference in Göttingen, Germany
2004 – 2005	Chairman of the *Students' Society for Neuroscience (Studenckie Koło Naukowe Neurobiologii)* at the Faculty of Biology, University of Warsaw, Poland

PUBLICATIONS

Dorota M Badowska, Magdalena M Brzózka, Ananya Chowdhury, Dörthe Malzahn, Moritz J Rossner. "Data calibration and reduction allows to visualize behavioural profiles of psychosocial influences in mice towards clinical domains" *Eur Arch Psychiatry Clin Neurosci*; 2014 Oct;

Dorota Badowska, Andrea Schmitt, Peter Falkai. "Connectivity and cognition in neuropsychiatric disorders with special emphasis on Alzheimers disease and Chorea Huntington" *Eur Arch Psychiatry Clin Neurosci*; 2014 Sep;264(6):465-6